Investigation of a Suppression of Asymmetric Cell Kinetics (SACK)
Approach for *ex vivo* Expansion of Human Hematopoietic Stem Cells

by

Rouzbeh R. Taghizadeh

B.S. Chemical Engineering
University of Massachusetts, Amherst, 2000

SUBMITTED TO THE DIVISION OF BIOLOGICAL ENGINEERING IN PARTIAL
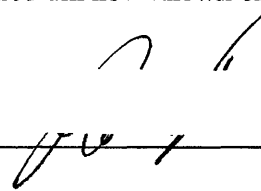FULFILLMENT OF THE REQUIREMENTS FOR THE DEGREE OF

DOCTOR OF PHILOSPHY IN STEM CELL BIOENGINEERING
AT THE
MASSACHUSETTS INSTITUTE OF TECHNOLOGY
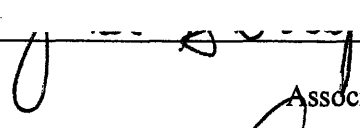
JUNE 2006

© 2006 Rouzbeh R. Taghizadeh. All Rights Reserved
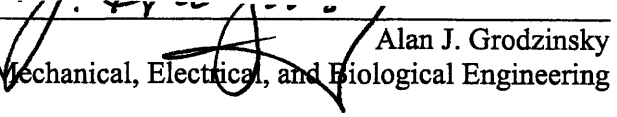
The author hereby grants to MIT permission to reproduce
and to distribute publicly paper and electronic
copies of this thesis document in whole or in part
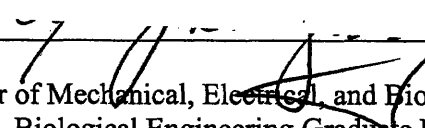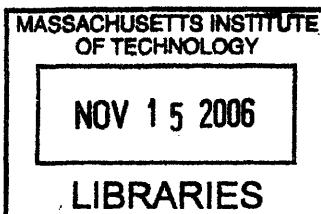in any medium now known or hereafter created

Signature of Author: _____
Rouzbeh R. Taghizadeh
Division of Biological Engineering
April 23, 2006

Certified by: _____
James L. Sherley
Associate Professor of Biological Engineering
Thesis Supervisor

Accepted by: _____
Alan J. Grodzinsky
Professor of Mechanical, Electrical, and Biological Engineering
Chair, Biological Engineering Graduate Program Committee

Investigation of a Suppression of Asymmetric Cell Kinetics (SACK)
Approach for *ex vivo* Expansion of Human Hematopoietic Stem Cells

by

Rouzbeh R. Taghizadeh

B.S. Chemical Engineering
University of Massachusetts, Amherst, 2000

SUBMITTED TO THE DIVISION OF BIOLOGICAL ENGINEERING IN PARTIAL
FULFILLMENT OF THE REQUIREMENTS FOR THE DEGREE OF

DOCTOR OF PHILOSPHY IN STEM CELL BIOENGINEERING
AT THE
MASSACHUSETTS INSTITUTE OF TECHNOLOGY

JUNE 2006

Signature of Committee Chair: _____

David B. Schauer
Professor of Biological Engineering

Signatures of Committee Members:

_____
Dan Marshak
Vice President and Chief Technology Officer, Biotechnology
Cambrex Corporation

_____
Alan J. Grodzinsky
Professor of Mechanical, Electrical, and Biological Engineering

Table of Contents

Chapter 5 – *In vivo* Characterization of SACK Effects on CD34$^+$ Mobilized
Peripheral Blood Cells in Non-Obese Diabetic/Severe Combined
Immunodeficient Mice (Phase V)

Chapter 6 – Fluorescence Tracking of Adult Stem Cells (ASCs)

Chapter 7 – Conclusion

Investigation of a Suppression of Asymmetric Cell Kinetics (SACK) Approach for *ex vivo* Expansion of Human Hematopoietic Stem Cells

by

Rouzbeh R. Taghizadeh

Submitted to the Division of Biological Engineering on May 24, 2006
in Partial Fulfillment of the Requirements for the Degree of Doctor of Philosophy in
Stem Cell Bioengineering at the Massachusetts Institute of Technology

ABSTRACT

Ex vivo expansion of hematopoietic stem cells (HSCs) is a long-standing challenge faced by both researchers and clinicians. To date, no robust, efficient method for the pure, *ex vivo* expansion of human HSCs has been demonstrated. Previous methods primarily induced the expansion of committed hematopoietic progenitor cells (HPCs), yielding even less pure populations of HSCs. This research was based on the hypothesis that, like for other adult stem cells (ASCs), the major barrier to expanding HSCs *ex vivo* is in preferentially regulating the asymmetric self-renewal of HSCs without loss in their ability to produce differentiated committed HPCs. This laboratory has shown that a p53-dependent pathway specifically controls the self-renewal pattern of several types of ASCs and thereby provides an effective means for expansion of ASCs in culture. The method, which involves the use of purine metabolites to achieve suppression of asymmetric cell kinetics, is referred to as SACK. The utility of the p53-dependent pathway was investigated for directing expansion of human HSCs. In order to support this investigation, the proliferation of HPCs in *in vitro* cultures was repressed by culturing cells without hematopoietic growth factors and cytokines. This allowed the *in vitro* detection of SACK-effects on a small sub-population of cells, predicted to include HSCs. In order to determine the self-renewal capacity and multilineage potential of SACK-cultured cells, they were transplanted into non-obese diabetic/severe combined immunodeficient (NOD/SCID) mice. *In vivo* transplantation investigations exhibited 1.9-fold to 4.5-fold increased engraftment efficiency with SACK-agents compared to SACK-free controls, suitable for clinical applications. This result suggests that SACK-culture expands a population of SCID-repopulating cells (SRCs) that yields self-renewal and multilineage engraftment in NOD/SCID mice. Accordingly, increased engraftment efficiency for successful clinical applications may be achieved after additional optimization of HSC expansion. To obtain the full therapeutic potential of expanded HSCs, development of methods for independently marking putative ASCs for future analyses and gene therapy was explored. This early success with human HSCs supports the basic hypothesis that the SACK approach may be applicable to expansion of many types of ASCs.

Thesis Supervisor: James L. Sherley
Title: Associate Professor of Biological Engineering

Chapter 1

Introduction & Background

<u>**Introduction**</u>

Hematopoietic stem cells (HSCs) are the engines that drive the maintenance and production of functional blood cells for the duration of human life. They are defined by their ability to simultaneous maintain themselves through asymmetric self-renewal cell kinetics and produce lineage committed cells that differentiate into mature, functional cells[1]. Their existence is an absolute necessity, as their continuous production of mature blood cells replaces older and expired cells. This characteristic of HSCs of lifelong regulated production of mature blood cells drives great interest in adapting HSCs for cell therapy applications, such as advanced bone marrow transplantations (BMT) and gene therapy. Currently, transplants of HSCs are part of the standard of care for the treatment of various non-hematopoietic (e.g. breast cancer[2,3]) and hematopoietic cancers and disorders[3,4]. Various sources of HSCs are used to reconstitute hematopoiesis after myeloablation, including bone marrow, umbilical cord blood (UCB) and mobilized peripheral blood (MPB)[4-6]. However, hematopoietic transplants are not always an absolute assurance of a cure for an underlying ailment. For instance, for those that are fortunate to find an allogeneic match, as much as 35% of patients receiving transplants do not survive[7]. There are several factors that play significant roles in the efficacy of hematopoietic transplants, in addition to patient morbidity and mortality, including the infused HSC dose, time to engraftment, and risk of graft-versus-host disease (GvHD)[4]. The ideal HSC source would yield decreased HSC dose and risk of GvHD, with short time to hematopoietic recovery. Currently, such an ideal source does not exist. Additionally, the transfer of genes into HSCs to repair hematopoietic disorders and cancers can be used as an important tool to overcome genetic diseases. Moreover, HSCs might be used clinically to engineer the production of functional blood cells, including erythrocytes and megakaryocytes.

For clinical fruition of these potential clinical applications, several barriers must be overcome. Such impediments include extremely low *in vivo* HSC numbers, the current lack of markers to exclusively identify HSCs, and the lack of robust technology to

expand HSCs *ex vivo* as a pure population while maintaining their primitive, undifferentiated state. This dissertation research is predicated on the proposal that regulation of HSC kinetics to promote symmetric expansion of inherently asymmetrically dividing HSCs is an overlooked means to realize the promise of *ex vivo* expanded HSCs[8,9]. Additionally, understanding the molecular and cellular mechanisms controlling symmetric HSC expansion may be the key to overcoming the current barriers in basic scientific research on HSCs and finally making the quest for new and advanced HSC replacement a reality.

The scarcity of HSCs in adult bone marrow presents a primary barrier to their use as a source for cell therapy applications. It is estimated that the frequency of HSCs in the adult bone marrow is approximately 10^{-4} to 10^{-5} [10,11]. Despite their extraordinarily low numbers, HSCs collectively have enough proliferative capacity to last several lifetimes[1,12]. It is even more remarkable that a rare population of cells has the power and memory to fuel the production of approximately 1 billion red blood cells and 100 million white blood cells per hour in the adult human[13] and a total of 6 billion cells per kilogram of body weight per day[14]. The low numbers of HSCs *in vivo* has resulted in a lack of understanding in the unique properties of these primitive cells for basic science and has represented a great obstacle for advanced therapeutic applications.

As a direct consequence of low HSC numbers *in vivo,* there has been an inability to uniquely identify and, therefore, purify HSC populations to homogeneity without contamination from differentiated and lineage-committed hematopoietic progenitor cells (HPCs). However, there are methods to enrich for HSCs using markers that are expressed on HSCs. The cell surface markers, CD34[1,15] and CD133[16,17] identify and enrich for cell populations that include HSCs. CD34 is currently the marker used as a metric to define HSC repopulation efficiency in patients receiving bone marrow transplantations (BMT)[18]. However, neither of these markers is uniquely expressed on HSCs. In addition to HSCs, CD34 and CD133 are expressed on both hematopoietic[1,15-17] and non-hematopoietic lineage-committed progenitor cells[19,20]. These markers are also selectively expressed in rare cells in other stem cell compartments, including CD34 in hair follicle[21,22]. However, neither of these markers shows exclusive expression on HSCs or any other adult stem cell (ASC)[8]. The lack of complete marker specificity for HSCs leads to an obstacle in

obtaining HSCs enriched as a pure, homogeneous population. In fact, with current enrichment methods, the estimated fraction of human HSCs in therapeutic transplant cell preparations is approximately 0.1-1.0%[8,9,11,18,23]. The remaining cells are HPCs and other differentiated cells. Moreover, lack of pure HSC populations for both research and clinical use directly correlates with the current lack of markers that uniquely identify HSCs. This is an important caveat when investigators treat these HSC-enriched populations as pure HSC populations during characterization of molecular markers for stem cell populations[24,25]. Without unique identification of HSCs, attainment of homogeneous populations of HSCs is greatly hindered; therefore, no robust, high-throughput methods can be used to investigate their properties. Existing knowledge of HSC properties is dependent on prospective studies for *in vivo* potential of human HSCs to produce long-term human myeloid and lymphoid cells in immuno-compromised animal models[10,11].

Augmenting the great challenges in the HSC field is the lack of knowledge required to regulate HSC expansion *ex vivo*. Although previous investigators have focused on extrinsic regulation of HSC expansion, this research is based on the proposal that the greatest challenge in understanding the molecular and cellular mechanisms regulating *ex vivo* expansion of HSCs lies in intrinsically manipulating the inherent property of HSCs: asymmetric self-renewal kinetics[26]. Although this property protects the exhaustion of HSCs and may limit their accumulation of mutations *in vivo*[27], it is a major obstacle to *de novo* production of *ex vivo* HSCs for use in advanced cell therapies. While it has been previously shown through time-lapse microscopy that cells from HSC-enriched populations cycle with asymmetric self-renewal kinetics are the only cells to give rise to both myeloid and lymphoid cell types *in vitro*[9,28-31], no method has been developed to regulate the cell kinetics of asymmetrically cycling HSCs to divide with symmetric cell kinetics in order to give rise to expanded HSCs. Thus far, the rationales considered for expansion efforts have been largely based on general concepts in hematopoiesis and the bone marrow microenvironment, including hematopoietic cytokines and microenvironmental factors (essential cell-to-cell or cell-to-matrices interactions). These targeted manipulations have been unsuccessful in promoting *ex vivo* expansion of human HSCs. One strategy that has not been specifically targeted and

investigated is genes that regulate asymmetric cell kinetics[9]. Manipulation of these genes could be the key to promoting symmetric expansion, as would be the case for HSCs *in vivo* as the body promotes wound healing or during growth in the development of adult tissues from juvenile tissues.

A promising method that has been used to regulate ASC kinetics in adult rat hepatocyte stem cells is based on suppressing asymmetric cell kinetics of ASCs, also referred to as SACK[8,28]. The SACK method is controlled by a p53-dependent pathway that regulates *de novo* synthesis of guanine ribonucleotides (rGNPs). Along with being a vital tumor-suppressor gene maintaining genome stability by temporarily arresting cells allowing for DNA repair and promoting apoptosis in cells with irreversible DNA damage[32], p53 regulates the production of inosine-5'-monophosphate dehydrogenase (IMPDH), the rate-limiting enzyme catalyzing the conversion of inosine monophosphate (IMP) to xanthosine monophosphate (XMP) for rGNP biosynthesis in mammalian cells[33-35]. More specifically, p53 expression was shown to cause the down-regulation of IMPDH mRNA, protein, and cellular enzymatic activity, although the exact molecular mechanism was not determined. In its role as a rate-limiting enzyme for rGNP biosynthesis, p53-dependent reduction of IMPDH decreases rGNP production and intracellular pool size. Therefore, p53 and IMPDH regulation were implicated as important factors in acquiring and controlling the asymmetric cell kinetic (ACK) state of a cell[35].

As a step to exploring how generally applicable the SACK strategy is for adult stem cells in varying tissues, HSCs were selected since hematopoietic tissues are the most extensively studied tissues for stem cell function. In principle, application of the SACK method can be utilized to regulate guanine ribonucleotide production in cells dividing with asymmetric cell kinetics (ACKs). This can be done independent of direct p53 regulation, which might perturb numerous other metabolic pathways, most notably those involved in neoplastic transformation. Salvage pathways, regulated by purine nucleotide precursors (i.e., hypoxanthine, xanthine, xanthosine) can be used to regulate asymmetric cell kinetics, with minimal effects on p53 regulation. As proof of principle, the SACK method has been used to expand and culture, for the first time, adult rat and human hepatic stem cells[28,36,37]. Since HSCs have been shown to divide with asymmetric cell

kinetics (ACKs)[31,38], conversion of HSC ACKs to symmetric cell kinetics (SCKs) by the SACK method may be the key to developing a robust method to expand HSCs.

Additionally, due to inefficient techniques to identify HSCs *in vitro*, enrichment of HSCs as a pure population is currently not possible. Contamination by HPCs and other differentiated cells may negatively regulate HSC expansion[39] and may impair *in vitro* detection of HSCs since HPCs far outnumber HSCs in these enriched populations[23]. Consequently, in addition to the SACK method, a technique was needed to deplete HPCs and other differentiated cells or suppress their growth and proliferation. This adaptation would provide increased specificity for detecting and following HSCs *in vitro*. HPC proliferation may be suppressed by starving HSC-associated populations of growth factors. This is based on precedent in our laboratory, where we have determined that SACK-derived adult liver stem cells are resistant to differentiation induced by transforming growth factor-β (TGF-β) and epidermal growth factor (EGF). Conversely, non-SACK derived adult liver progenitor and hepatocyte cells are sensitive to TGF-β and EGF induced differentiation[40]. This suggests that certain ASCs may be indifferent to growth factor induction, whereas lineage committed progenitors and differentiated cells may be more dependent on growth factors for their proliferation and/or survival.

Therefore, investigations were undertaken to evaluate the SACK method for expanding enriched populations of HSCs, in addition to increasing sensitivity for detecting HSCs and/or reducing negative regulation of HSCs by HPCs by repressing the survival and proliferation of contaminating HPCs and differentiated cells.

Background

Adult stem cells (ASCs) are a promising source for the future success of gene therapy, tissue engineering, and cell replacement therapies, since these cells have the unique potential to give rise to diverse cell lineages for the lifespan of an organism. ASCs are both the engine that drives tissue cell renewal and turnover and the memory for the tissue's cellular differentiation architecture. With recent ethical issues encompassing present and future work with embryonic stem cells (ESCs), the isolation and expansion of adult stem cells (ASCs) has become an even more attractive and, therefore, a more practical route towards stem cell therapeutic technologies.

Adult Stem Cells & Adult Stem Cell Kinetics

ASCs are defined as cells that have the unique ability to maintain themselves through asymmetric self-renewal and, additionally, to generate mature cells of a particular tissue through differentiation. ASCs are derived from committed embryonic stem cells (ESCs; Figure 1.1) and are present in most normal tissues, including hematopoietic[12,41-45], liver[28,46], intestines[47,48], muscle[49], nervous[48] and epithelia[47,50], yet are present in small numbers in these adult tissues. Furthermore, all stem cells in adult tissue share one important feature: the capacity for self-renewal by asymmetric cell kinetics[9,29,51-53].

However, the exact mathematical form of ACKs in adult mammalian tissues remains under debate[8,54-56]. On the one hand, a stochastic model suggests that multiple HSCs reside in a specified niche with each ASCs division giving rise to either zero or two ASCs in an unregulated manner. Under this model, the division of multiple ASCs per tissue unit occurs to produce different cell types to insure the life-long maintenance of ASC number (Figure 1.2A). On the other hand, a deterministic model proposes that a small number of ASCs exist in a niche and with each ASC division resulting in the production of two daughter cells that are not functionally identical. One daughter cell divides with symmetric cell kinetics to produce an abundance of progeny referred to as progenitors. These progenitors, subsequently, differentiate to form cells that comprise the cellular components of mature tissue. The other newly produced daughter cell retains the stem cell phenotype and all of the capabilities of the original mother cell in a process

referred to as self-renewal (Figure 1.2B). By this process, a dividing ASC maintains the tissue's long-term cellular differentiation architecture. In addition, the deterministic model proposes that under specific physiological conditions (e.g., adult maturation, wound repair), ASCs undergo limited symmetric cell kinetics, expanding the ASC pool and establishing new tissue units. However, under the deterministic model, ASCs can not undergo direct differentiation[9]. These newly expanded stem cells can further divide symmetrically to form more adult stem cells, or return to their inherent asymmetric self-renewal state to give rise to progenitor cells to restore the desired mature, differentiated cells (Figure 1.2B). Such kinetic shifts may be regulated by intracellular signals[31]. An example of an ASC that exhibits asymmetric self-renewal cell kinetics is the hematopoietic stem cell (HSC)[31,38,57].

Hematopoietic Stem Cells

The human body consumes an astounding 400 billion mature blood cells every day and even greater numbers when the body is under conditions of stress or trauma, such as infection, hypoxia or bleeding[58]. In order to meet this demand, a complex system of multilineage proliferation and differentiation of hematopoietic cells has evolved. The regulated production of approximately a dozen types of mature blood cells is sustained by primitive hematopoietic stem cells (HSCs), primarily residing in the bone marrow (BM) of adult humans. There are approximately a dozen major types of mature blood types that are derived from HSCs (Figure 1.3). During normal replenishment of mature blood cells, HSCs are instructed to divide asymmetrically to self-renew to maintain the HSC pool and to produce a multipotent progenitor cell that divides with symmetric cell kinetics to give rise to either of two progenitors types: common myeloid progenitors (CMP) or common lymphoid progenitors (CLP). The common myeloid progenitor will continue to divide to give rise to erythrocytes, monocyte lineage-derived cells (e.g. macrophages, osteoclasts and dendritic cells), granulocytes (e.g. neutrophils, eosinophils, basophils and mast cells), and platelets that are derived from non-circulating megakaryocytes[58]. Thymus-derived (T) lymphocytes, bone marrow-derived (B) lymphocytes, natural killer (NK), and dendritic cells constitute the lymphoid lineage (Figure 1.3). Although some lymphocytes are thought to survive for many years, cells such as erythrocytes and neutrophils have a

limited lifespan of 120 days and 8 hours, respectively[59]. As a result, hematopoiesis is a highly prolific process, which occurs throughout human life to fulfill this demand and maintain the body's hematopoietic homeostasis.

The bone marrow is the major site of effective hematopoiesis in humans, in addition to the spleen and thymus. Located in the medullary cavity of bone, the bone marrow has the capacity to produce 2.5 billion erythrocytes, 2.5 billion platelets, and 1 billion granulocytes per kilogram of body weight per day[14]. However, depending on the body's particular need, this rate of production can range from nearly zero to several fold above normal[60]. Kinetic studies suggest that marrow consists of cells with a finite functional lifespan. These cells have the capacity for limited proliferation without any capacity to self-renew. To sustain the extensive need for hematopoietic cells, pools of primitive, multipotent hematopoietic stem cells continuously self-renew to simultaneously maintain HSC numbers, in addition to producing mature, functional hematopoietic cells. HSCs give rise to downstream unilineage hematopoietic progenitor cells (HPCs) that are restricted to the production of distinct hematopoietic cells with no capacity for self-renewal. The proliferative activity of HSCs, HPCs, and mature hematopoietic cells is highly dependent on cell-to-cell interactions within the microenvironment niche of the marrow[14,39,61-66]. More specifically, the microenvironment stroma has evolved to provide a specific structural, chemical, and biological environment to support the survival, differentiation, proliferation, and continuous self-renewal of HSCs[14].

Evidence for the Existence of HSCs

The first genetic evidence that adult stem cells exist came from studies on hematopoietic stem and progenitor cells[44]. In these studies, lethally irradiated mice were injected with bone marrow (BM) cells from healthy donor mice. The hematopoietic system of mice receiving donor cells was reconstituted, whereas control mice died within a week. In the spleen of reconstituted mice, macroscopic hematopoietic colonies containing cells of the myeloid lineage were observed. Cells capable of forming colonies in the spleens of ablated recipient mice were referred to as CFU-S (spleen colony-forming unit) and although these cells were originally thought to be stem cells,

subsequent work has shown them to be myeloid-committed early progenitor cells[42,45]. As a result, the current definition of a HSC includes the ability to confer long-term *in vivo* repopulation of the myeloid and lymphoid lineages of an ablated host. This activity can be enriched for, in certain purified cell populations, supporting the hypothesis of a single multipotent stem cell[1]. Furthermore, genetic marking experiments in mice have demonstrated that long-term engraftment of both lymphoid and myeloid lineages can be achieved by the progeny of a single HSC[67,68], thereby confirming the existence of true HSCs.

To provide for the first isolation of mouse HSCs, it was necessary to develop assays for the clonal precursors of all known differentiation blood cell types, including myelo-erythroid[44], B lineage cells[69] and T lineage cells[70]. Additionally, the production of monoclonal antibodies to cell surface molecules found on bone marrow cells was essential for the first isolation of mouse HSCs, in conjunction with technology that had the capacity to sort and analyze at high-speeds cells that bared or lacked combinations of these monoclonal antibody-defined surface determinants[1,69].

Human HSC Ontogeny

Although adult hematopoiesis occurs mainly in the marrow, early embryonic hematopoietic development in humans is found at distinct anatomical sites. During embryogenesis, hematopoiesis is initiated in the yolk sac, shifts to the fetal liver, and finally localizes to the bone marrow. Hematopoiesis before the formation of the fetal liver consists mainly of nucleated erythrocytes with embryonic-type hemoglobin[71]. This stage is referred to as primitive hematopoiesis. Initially, primitive erythroblasts can be distinguished at day 18.5 of development in the yolk sac, a membrane-bound compartment in the amniotic egg which contains stored food for the developing embryo. This is the first indication that hematopoiesis has begun[72]. At day 22, the heart begins beating at which time erythroid cells are found in circulation[71,73]. Between embryonic day 24 and 34, primitive hematopoietic cells give rise to adult-type blood cells with both lymphoid and myeloid activity. This represents definitive hematopoiesis and first appears in the para-aortic splanchnopleura (P-Sp) region[74,75]. Shortly after its appearance, the P-Sp region develops into the intraembryonic aorta-gonad-mesonephros (AGM) structure,

where the first long-term repopulating HSCs can be detected[76-78]. On day 23, the liver begins developing, after which time on day 30, it is colonized by migrating primitive hematopoietic cells. Migration and colonization by primitive hematopoietic cells increases until embryonic day 42, at which time the liver is the major source of hematopoietic cells[71]. At this time, erythroid cells are the major cell type found in the embryonic liver and are located extravascularly. At the time of fetal birth, the liver essentially ceases with hematopoietic activity, although some hematopoietic production may occur. Between 6 and 8.5 weeks of gestation, the bones of the human embryo are cartilaginous, after which time chondrolysis occurs and osteoblasts, osteoclasts and perichondral precursors invade and take residence in the marrow cavity. After week 10.5, a low frequency of primitive hematopoietic cells marks the appearance of hematopoiesis in the bone marrow. By week 16, bone formation is complete and hematopoiesis continues in the marrow for the lifespan of the individual[79,80].

Understanding the development of HSCs and hematopoiesis not only indicates distinct anatomical sites for development, but also suggest that HSC numbers and activity constantly changes until full human development. During fetal development and early post-natal life, HSCs expand *in vivo*. However, subtle changes in the quality of HSCs occur throughout development and life. For instance, HSCs from murine fetal liver have greater *in vivo* proliferation potential than HSCs from post-natal BM from young and old adults[5,6].

Due to the distinct anatomical sites for hematopoiesis during human development, various sources for HSCs exist. Human HSCs have been isolated and characterized naturally from the umbilical cord blood (UCB) and bone marrow (BM). In addition, human HSCs can isolated from mobilized peripheral blood (MPB) by artificially promoting HSCs from the bone marrow to the peripheral blood in patients treated with chemotherapeutics and/or administrated cytokines. The migrated HSCs can then be readily collected using aphaeresis technology. HSCs from these sources have the distinct advantage of being reasonably well characterized and have been proven in the clinic[4-6].

Evidence that HSCs divide with deterministic asymmetric cell kinetics (ACKs)

Although other cell kinetic models such as stochastic cell kinetic model have been proposed to represent the regulation of HSCs[81-83], current *in vitro* evidence suggests that HSCs kinetically behave based on a deterministic model. It has been suggested that, inherently, HSCs divide with asymmetric self-renewal cell kinetics[31,38,57] in adult hematopoiesis in order to simultaneously produce functional blood cells and protect their exhaustion. Since the early 1970's, HSCs have been implicated, based on both biological and statistical inferences, to divide with asymmetric cell kinetics *in vivo*[56]. Although debates currently continue over the exact form of the kinetics, the existence of asymmetric cell kinetics is a well accepted precept of cell kineticists[84]. Specifically, it has been previously demonstrated by time-lapse video-microscopy that approximately 30% of CD34^{+}/CD38- enriched umbilical cord blood (UCB) cells divide with deterministic asymmetric cell kinetics[31]. Additionally, similar results have been obtained from HSC-associated populations in MPB and BM[31]. Interestingly, the addition of various cytokines and growth factors do not affect the observed asymmetric cell kinetics program[31]. Another group studied colony formation using single-sorted candidate HSCs. From their studies, they concluded that primitive hematopoietic cells from fetal liver divide with asymmetric cell kinetics in which proliferative potential and cell cycle properties are unevenly distributed among daughter cells[85]. Currently, there is no direct evidence that suggests that HSCs are stochastically regulated to give rise solely to HSCs or lineage-committed progenitor cells at a certain frequency.

Marrow Microenvironment and the Concept of the HSC Niche

Hematopoiesis in humans takes place in the extravascular spaces within marrow sinuses. This close proximity of developing blood cells to the sinuses allows for instantaneous access to the circulation, after navigating the sinus wall. The sinus wall is composed of a luminal layer of endothelial cells, which forms a complete inner lining and an abluminal coat of adventitial reticular cells, which forms an incomplete outer coat. Between these cell layers lies a thin, interrupted basement lamina[14].

Since the first concept of a niche was proposed that provides a supportive microenvironment for HSCs[86], various biological, chemical, and physical components

have been determined to be important in maintaining survival, differentiation, proliferation, and continuous self-renewal of HSCs. The marrow microenvironment is responsible for the localization of HSCs to specific anatomical regions in the bone marrow. In the bone marrow, HSCs are supported by cell-cell interactions with non-hematopoietic stem cells, including endothelial cells, fibroblast-like bone marrow stromal cells and osteoblasts. The effects of these supporting cells are mediated through specific molecular interactions, some of which have been investigated as a means to promote *ex vivo* HSC expansion. The two most important cellular components of the bone marrow microenvironment, however, are marrow stroma and osteoblasts[14].

Bone Marrow Stroma

An important cellular component of the marrow microenvironment is stromal cells which are presumably derived from fibroblasts. Stromal cells possess unique phenotypic and functional characteristics that allow them to nurture hematopoietic development in highly specialized microenvironment niches. This nurturing ability is mediated by different combinations of early acting growth factors released by stromal cells, including Flt3-ligand (fetal liver tyrosine kinase 3-ligand), stem cell factor (SCF; KIT ligand), thrombopoietin (TPO), leukemic inhibitory factor (LIF), and interleukin-6 (IL-6). Other interactions that regulate hematopoietic cell survival and development are mediated by cell-to-cell contacts through negative regulators of stromal and primitive hematopoietic cells. The pathways regulated by such interactions include transforming growth factor β (TGF-β), which downregulates c-kit expression and the Notch/Jagged pathway, which down regulates myeloid differentiation[14].

Osteoblasts

The architecture of mammalian bone marrow consists of HSCs in close proximity to the endosteal surface of the bone and differentiating cells aligned along a gradient towards the central longitudinal axis of the bone where HSCs have easy access to the central venous sinus[87,88]. As a result, it has been suggested that osteoblastic cells are important regulatory components of the HSC niche *in vivo* that influences HSC function through Notch activation[63]. Osteoblasts are derived from multipotent mesenchymal stem

cells (MSCs) and differentiate along a specified lineage to become highly specialized synthetic cells. Proliferation and differentiation of bone-forming osteoblast progenitor cells is promoted by bone morphogenetic protein-2 (BMP-2), basic fibroblast growth factor (b-FGF) and TGF-β. Osteoblasts secrete hematopoietic growth factors such as macrophage-colony stimulating factor (M-CSF), granulocyte-colony stimulating factor (G-CSF), granulocyte-macrophage-colony stimulating factor (GM-CSF), IL-1 and IL-6[66,89]. Osteoblasts also produce hematopoietic cell cycle inhibitors, such as TGF-β, which may contribute to their marked role in HSC regulation within the marrow microenvironment[90]. In keeping with their supportive role in promoting hematopoiesis, osteoblasts facilitate the engraftment of purified allogeneic HSCs when transplanted into ablated and non-ablated mice[64,91].

In addition, it has been recently shown that angiopoietin-1 mediated signaling through the Tie-2 receptor also has a role in the interaction between osteoblasts and HSCs. Tie-2 is expressed by HSCs and osteoblasts express angiopoietin-1, which binds to Tie-2, resulting in the quiescence of HSCs and their protection against apoptosis[92]. It has been found that when angioipoietin-1 expressing mouse osteoblasts localize to the bone endosteal surface, Tie-2$^+$ putative murine HSCs localize adjacent to the osteoblasts[92]. Interestingly, c-kit$^+$, Sca-1$^+$, Lin$^-$ (KSL) HSC-enriched populations that express Tie-2 show a reduction of cell division in the presence of angiopoietin-1 *in vitro*. Additionally, when bone marrow cells infected with an angiopoeitin-1 expressing retrovirus are transplanted into irradiated mice, the percentage of G_0 cells in the KSL population are significantly higher in recipient bone marrow than in mice receiving transplants of control bone marrow cells[92]. Given the importance of the quiescence of HSCs in the niche, angiopoeitin-1/Tie-2 signaling may be an important aspect of the HSCs niche.

It has also been determined that there may exist a link between Notch signaling and osteoblasts. Specifically, when bone marrow from osteoblast-specific transgenic mice is transplanted into lethally irradiated mice, the mice exhibit improved engraftment when compared to bone marrow from wildtype mice. In addition, Jagged-1 expression on osteoblastic cells is significantly upregulated in these transgenic mice and Notch-1 is activated in enriched HSC populations when compared to cells derived from control mice[63].

Regulation by stromal and osteoblast cells in the marrow niche may provide supportive roles in promoting proliferation, survival, and/or asymmetric self-renewal of HSCs *in vivo*. As a result, understanding mechanisms that control any of these may have important implications in *ex vivo* expansion of HSCs.

Previous Strategies for *Ex Vivo* Expansion of HSCs

Thus far, the rationales considered for expansion efforts have been largely based on general concepts in hematopoiesis and the bone marrow microenvironment, such as hematopoietic cytokines and microenvironmental factors, including cell-to-cell interactions. Nevertheless, investigations into these targeted manipulations have been unsuccessful in promoting *ex vivo* expansion of human HSCs. Among the various unsuccessful strategies to promote *ex vivo* expansion of HSCs are methods based on hematopoietic cytokines, homeobox gene regulation, Notch, Wnt, bone morphogenic protein (BMP), and sonic hedgehog (Shh) regulation. However, instead of promoting HSC expansion, these factors promote HSC differentiation, survival, and/or self-renewal. However, autonomous pathways of cell division regulation of HSCs may be the key to promote symmetric expansion of HSCs[9].

Hematopoietic Cytokines

Due to the complex network of hematopoietic signaling molecules that induce proliferation at various stages of hematopoietic development, the first attempts to expand HSCs focused on the use of hematopoietic cytokines and growth factors. Many of these cytokines are locally produced in the bone marrow microenvironment by stromal cells, indicating that they may be useful for promoting HSC expansion *ex vivo*. The rapid discovery of new hematopoietic growth factors and their receptors enabled researchers to test their ability to expand HSCs *ex vivo*. Much of this work was done in the context of gene therapy strategies, since to achieve efficient onco-retroviral vector integration, methods were not only required to preserve HSCs, but also to induce self-renewal divisions and HSC expansion. Through various trials, it was observed that cell populations harboring human HSCs can be induced to proliferate in cytokine cocktails including Flt3-ligand (Flt3L), thrombopoietin (TPO), stem cell factor (SCF), interleukin-

3 (IL-3) and interleukin-6 (IL-6)[40,39,93,94]. However, these cocktails have not resulted in *ex vivo* expansion of human HSCs, since growth factors permit the extensive expansion of more mature clonogenic progenitors rather than primitive HSCs[39]. Although it has been shown that these hematopoietic cytokines alone do not promote the symmetric expansion of *ex vivo* HSCs[31,38], it may be true that specific hematopoietic growth factors or cytokines promote survival of HSCs while simultaneously promoting lineage commitment and differentiation, resulting in a highly impure HSC population[23,39,95]. Although exhaustive studies of multiple cytokine and growth factor combinations have not yielded conditions that result in HSC expansion, the extensive proliferation of cells suggests that these factors may promote HSC survival and lineage-commitment, but not HSC expansion.

Homeobox genes and HOXB4

Hox genes encode a large family of transcription factors that regulate many early developmental processes, including body-part patterning along the spinal axis. They have a highly conserved DNA-binding motif known as the homeodomain. In mammals, there are four main families of Hox factors. Certain Hox family members are expressed in primitive HSC-enriched populations[96], downregulated in differentiated hematopoietic cells[96], and dysregulated in patients with acute myelogeneous leukemia (AML)[97]. Moreover, up- or down-regulation of some Hox genes affects hematopoiesis in specific lineages[98]. As a result of these observations, Hox genes may be involved in events leading to HSC specification and/or self-renewal. One particular Hox gene, HoxB4, has been extensively investigated as a potential regulator of HSC self-renewal. HoxB4 has been considered an important regulator of primitive hematopoietic cells since it is expressed in human CD34$^+$ enriched populations but it is rapidly downregulated upon differentiation[96]. It was first shown that retroviral expression of HoxB4 significantly enhanced HSC repopulation *in vivo* in primary and secondary recipients[99]. When lethally irradiated mice were reconstituted with bone marrow cells transduced with a control vector, HSC numbers only regenerated to only 5%-10% of normal levels. By contrast, when bone marrow cells transduced with a retroviral vector expressing HoxB4 were transplanted into lethally irradiated recipient mice, normal numbers of HSCs were

regenerated, suggestive of a role for HoxB4 in promoting HSC self-renewal. Attempts to increase HSC numbers did not continue after normal numbers of HSCs had been regenerated, suggesting that the homeostatic controls that regulate HSC pool size were still effective in HoxB4-overexpressing HSCs. Later studies in HoxB4-deficient mice exhibited a hematopoietic phenotype that primarily affected the HSC pool and resulted in reduced proliferative capacity of HSCs without affecting differentiation and lineage commitment[61,100]. Enforced expression of HoxB4 *in vivo* is a potent stimulus for murine HSC self-renewal and regenerative capacity after transplantation of irradiated recipients[98]. These observations suggest that HoxB4 is important in regulating the survival of HSCs, but not the expansion of primitive HSCs[99].

Notch

Notch signaling is a highly conserved pathway that controls cell fate choices in both invertebrates and vertebrates. Notch genes encode four transmembrane receptors (Notch1-4) that interact with five Notch ligands (Jagged-1 & 2, Delta-like 1, 3, & 4) in mammals. Both ligands and receptors are single-pass transmembrane glycoproteins. Notch is presented in the plasma membrane as a heterodimer after cleavage by a furin-like protease. Upon ligand-banding to the extracellular subunit of Notch, the transmembrane subunit of Notch undergoes a set of cleavages catalyzed by the ADAM (a disintegrin and metalloproteinase) family of metalloproteases and γ-secretases. The resulting intracellular domain of Notch (ICN) is released into the cytoplasm and finally translocated to the nucleus, where it binds directly to its downstream transcription factor, CSL/RBPJκ, transforming CSL/RBPJκ from repressor to activator and inducing the transcription of Notch-dependent target genes such as Hes-1, Deltex-1, pT, Meltrin-ß, and Notch receptors[101-103].

HSCs express receptors of the Notch family, which have been shown to inhibit differentiation in other systems[102,104]. The Notch-1 ligand Jagged-1 is expressed by bone marrow stromal cells, endothelial cells and osteoblasts[63,105], indicating that potentially cell-to-cell dependent signaling through Notch might have a role in the regulation of HSCs. Bone marrow from osteoblast-specific transgenic mice transplanted into lethally irradiated mice results in improved engraftment. In addition, Jagged-1 expression on

osteoblastic cells is significantly upregulated in these transgenic mice and Notch-1 is activated in enriched HSC populations when compared to cells derived from control mice[63]. Chemically inhibiting signaling through Notch-1 blocked this slight increase in HSCs, suggestive that Notch-1 signaling is required for osteoblast-mediated support[63,106].

Investigations into the potential role of Notch in the expansion of HSCs have been achieved by experimental modulation of the Notch-1 signaling pathway. Notch-1 is of potential significance for HSC regulation due to the observation that Notch-1 homozygous knockout mice show reduced definitive hematopoiesis in the P-Sp/AGM and fail to generate HSCs[107]. Due to embryonic lethality before day 11.5 for unknown reasons[108], it has not been possible to predict Notch-1 effects in adult Notch-1 knockout mice. However, in preliminary experiments by constitutively activating Notch-1, it is possible to establish multipotent hematopoietic cell lines that have long-term engraftment capacity[109]. Constitutive expression of activated Notch-1 using a retroviral vector in enriched mouse HSC populations resulted in immortalized, cytokine-dependent cell lines that could reconstitute irradiated mice[109]. Additionally, when freshly harvested murine HSC-enriched populations transduced with activated Notch-1 constructs are transplanted into irradiated recipients, a marked increase in engraftment is observed in the bone marrow. Furthermore, the observed engraftment is mediated by a relative-block in HSC differentiation[104]. Signaling through Notch-1 may inhibit differentiation of HSCs by sustaining expression of the transcription factor GATA2 (GATA-binding protein 2)[110]. A soluble form of Jagged-1 can mediate the survival of human HSCs when added to liquid cultures[105]. These observations suggest that Notch signaling may play an important role in promoting HSC survival and/or expansion by inhibiting production of differentiating progeny cells and promoting symmetric self-renewal *in vivo*[104].

The potential inhibitory effects of Notch signaling on HSC differentiation are suggestive that Notch signaling may regulate HSC expansion. The effects of soluble or cell-membrane expressed Notch ligands on the differentiation, growth, and expansion of hematopoietic stem and progenitor cells have been investigated in culture with various cytokines. It has been observed that soluble forms of Notch ligands have positive effects on human long-term severe combined immunodeficient (SCID) mice repopulating cells (LT-SRCs). HSC-enriched populations supplemented with Delta-1-Fc or Jagged-1-Fc, in

the presence of a cocktail of growth factors and cytokines, achieved higher engraftment efficiencies than control cells, when cells were transplanted into irradiated NOD/SCID mice[105,111-113]. This does not, however, provide definite evidence that *ex vivo* HSC expansion has been regulated by Notch. More fitting is the idea that Notch may be promoting survival and/or self-renewal of HSCs. Notch ligands are commonly observed to maintain cells in more primitive states as compared to untreated controls[105,109,111-115], even more indication of Notch's role as a survival factor. One big drawback discovered so far suggests that Notch-1 regulation may specifically favor lymphoid development over myeloid development[104], potentially limiting its future clinical applications. Overall, these findings reinforce interest both in the Notch pathways and in further characterization of the HSC microenvironment as a way to identify novel agents for HSC expansion.

Bone Morphogenic Proteins (BMPs)

Bone morphogenetic proteins (BMPs) are signaling molecules belonging to the transforming growth factor-β (TGF-β) superfamily that signal through binding to specific BMP receptors. BMPs have been considered potential regulators of HSC function based on critical roles in hematopoietic specification from mesoderm during early embryonic development[116]. Binding to their receptors leads to the nuclear translocation of SMAD proteins, which then regulates the transcription of specific target genes[117]. Expression of BMP receptors and known downstream signal transducers, such as the members of the SMAD family, have been documented in $CD34^+/CD38^-/Lin^-$ human umbilical cord blood (UCB) cells[118]. In Drosophila, overexpression of the BMP homolog decapentaplegic (dpp) expands the germline stem cell (GSC) niche and it leads to expansion of GSC number[119,120]. In human bone marrow, primitive hematopoietic cells express BMP type I receptors, and in culture high concentrations of BMP-4 extends the lifetime of their repopulation capability[118]. Tests of several BMPs including BMP-2, BMP-4, and BMP-7 in serum-free cultures of $CD34^+/CD38^-/Lin^-$ human UCB cells along with multiple hematopoietic cytokines revealed that in a narrow concentration range, BMP-4 was unique in its ability to extend the period in which cells with *in vivo* repopulating potential could be recovered. However, net expansion and long-term propagation of HSCs *ex vivo*

by BMP supplementation has not been convincingly demonstrated. For example, BMPs appear to act on HSCs by primarily controlling the HSC niche size in the bone marrow[106]. These studies suggest that BMP-4, at a minimum, may serve as an important survival factor for human HSCs and could be an important component for achieving enhanced HSC expansion *ex vivo.*

Wnt

The Wnt signaling pathway contributes to numerous developmental decisions in a variety of cell types and animal models. It is involved in cell fate determination, cell polarity, tissue patterning, control of cell proliferation, development of neoplasia[121,122], and potentially important for the proliferation of stem cells[123]. Wnt proteins are secreted glycoproteins with a conserved pattern of 23-24 cysteine residues. There are 19 Wnt family members in the human genome that encode for lipid-modified signaling protein that function as ligands for the Frizzled family of receptors. Downstream effects of Wnt signaling occur through different intracellular components, depending on which pathway is activated. Three pathways have been characterized: the canonical Wnt/β-catenin pathway, Wnt/Ca^{2+} pathway, and planar cell polarity[122,124].

In the absence of Wnt-mediated signaling, β-catenin is ubiquitylated and degraded by the proteosome. Wnt signaling through Frizzled inhibits the degradation of β-catenin, which results in the accumulated β-catenin forming a complex with T-cell factor (TCF)/lymphoid-enhancer binding protein (LEF)-family members to regulate the transcription of downstream genes.

Various Wnt proteins are expressed by human stromal cells in fetal bone marrow[124]. Co-culture studies with human CD34$^+$ cells and stromal cells expressing Wnt genes cause a marked expansion of myeloid progenitor cells[124]. Additionally, injection of Wnt5a into immunodeficient mice repopulated with human hematopoietic cells resulted in increased reconstitution and more primitive hematopoietic cells *in vivo*[125], suggestive that Wnt may play a role in maintaining self-renewal of HSCs. Gene expression profiling of enriched mouse HSCs confirmed expression of TCF/LEF-family[126]. Retroviral transduction investigations of HSCs with a vector expressing a constitutively expressing active β-catenin gene resulted in expanded primitive hematopoietic cells that were

relatively refractory to differentiation. Conversely, inhibition of Wnt signaling in HSCs blocked their growth and made them ineffective for bone marrow repopulation[126]. As few as 125 transduced cells were required to reconstitute irradiated recipient mice, suggestive of a 5-50-fold expansion in primitive hematopoietic cells *in vivo*[126]. Coincidently, hematopoietic cells transduced with a β-catenin-expressing vector yielded an up-regulation of HoxB4 and Notch mRNA, suggestive that the Wnt-dependent effects observed may have been mediated through these pathways[126]. This observation implicates Wnt as a potential regulator of HSC self-renewal. When soluble Wnt3a protein is directly added to enriched mouse bone marrow cells, a six-fold expansion of primitive hematopoietic cells is observed and similarly when these cells are transplanted into irradiated mice, a five-fold expansion is observed[127]. However, despite these transient effects, Wnt ligand supplementation has not proven effective for long-term propagation of HSCs. The cellular basis for this failing remains unclear. An important consideration with the manipulation of elements from the Wnt β-catenin signaling pathway is the risk of carcinogenesis[128]. Consequently, it is possible that prolonged treatment of hematopoietic cells with molecules activating the Wnt pathway will promote their neoplastic transformation. More studies focused on the long-term effects of continuous activation of the Wnt canonical pathway in HSCs will be needed for a sound assessment of whether this can be a viable approach to producing therapeutic quantities of HSCs.

Sonic Hedgehog (Shh)

The vertebrate hedgehog gene family is represented by at least three members: Desert hedgehog (Dhh), Indian hedgehog (Ihh) and Sonic hedgehog (Shh). Shh is the most extensively characterized vertebrate homolog, and it is involved in a wide variety of embryonic events. It can act as a short-range, contact-dependent factor and as a long-range, diffusible morphogen[129,130].

Human bone marrow cells enriched for primitive hematopoietic cells exhibits survival of repopulating cells after a 7-day culture period when the medium is supplemented with Shh. Moreover, the number of repopulating cells is increased approximately 2-fold in Shh-supplemented medium. Interestingly, the BMP-4 inhibitor, noggin, blocks the Shh-induced effects, suggesting that Shh acts via downstream BMP

signaling in this system[131]. However, no long term expansion of HSCs induced by HSCs has been shown.

Autonomous Pathways of Cell Division Regulation in HSCs
P21^{wafl/cipl/sdil}

The cyclin dependent kinase inhibitor (CDKI), $p21^{wafl/cipl/sdil}$ (p21) is best known functionally as a key mediator of p53-dependent checkpoint arrest in response to DNA damaging agents[132,133] (Figure 1.4A). However, recent reports suggest a possible role for p21 in homeostatic control for hematopoietic stem cell kinetics[134,135]. Bone marrow cells from p21-knockout mice exhibit a greatly reduced ability to reconstitute the hematopoietic system of lethally irradiated recipient mice. Additionally, flow cytometry analyses indicate that the HSC compartment of p21- knockout mice have a significantly reduced fraction of non-cycling cells. It was, therefore, suggested that p21-deficiency compromised the ability of HSCs to maintain a quiescent state that serves to protect the animals from toxic injury[135]. It is proposed that complete deficiency of p21 leads to increased HSC proliferation, amplifying the size of the HSC pool under homeostatic conditions in the mouse[135]. Therefore, p21 deficiency leads to the depletion of the HSC pool, since regulation to maintain HSCs in a quiescent state is defective. Furthermore, down-regulation of p21 in $CD34^+/CD38^-$ human umbilical cord blood cells resulted in an expanded stem cell number and improved stem cell function *in vivo* without affecting differentiation. This observation indicated that controlled modulation of p21 may be useful to expand HSCs *ex vivo*[136]. Consistent with the proposal that p21 is an important regulator of adult stem cell kinetics, p21-knockout mice exhibit an early cancer phenotype, although with a longer latency than p53-knockouts, with 65% of the detected tumors being hematopoietic in origin[137]. As a result, direct regulation of p21 would not be an effective strategy to expand human HSCs, especially when these expanded cells will be used for therapeutic applications.

P53

One gene demonstrated to regulate asymmetric cell kinetics in adult stem cells is the *p53* tumor-suppressor gene[9,29,30,34,35]. The *p53* gene encodes a 53-kDa phospho-

protein with several functions[138]. First, p53 is a transcription factor, increasing the rate of transcription of genes that possess p53 response elements in their regulatory regions. Examples of such genes include the growth arrest and DNA damage-inducible *gadd45* gene, the apoptogenic *bax* gene[139,140], and p21 as described above. Second, p53 inhibits the transcriptional activation of many genes that do not contain the p53-response element by binding to the TATA-binding protein[32]. Furthermore, it is believed that p53 arrests cells in the G1 phase of cell cycle in order to allow time for DNA repair resulting from replication error or DNA damage. In addition, p53 promotes apoptosis to counteract the accumulation of genetic errors and, therefore, is an important inhibitory protein in the process leading to neoplastic transformation. Furthermore, transgenic mice lacking the *p53* gene develop cancer by 6 to 9 months of age. These observations attest to the key role of the *p53* tumor suppressor gene in preventing tumor formation[32] and its possible role in regulating adult stem cell kinetics[34,35].

P53 has been implicated as an important gene for the cell-autonomous regulation of asymmetric cell kinetics in mammalian cells[34,35]. Up-regulation of p53 by less than 50% above basal endogenous wild-type p53 levels[35,141], induces a switch from symmetric cell kinetics to determined cell kinetics. This observation was made using time-lapse microscopy tracking divisions of murine embryonic fibroblasts expressing varying levels of p53[30,34,35,141]. Cells were characterized as dividing with deterministic asymmetric cell kinetics by divisions producing one continuously dividing daughter and one viable daughter arrested in G1/S of the cell cycle[141]. Furthermore, restoration of wild-type p53 to basal expression levels in p53-null murine fetal fibroblasts restores determined asymmetric cell kinetics[30]. These observations were independent of cell type as the same cell kinetic program was observed for cells in pre-senescent cultures of murine fetal and human lung fibroblasts[30,35]. Since the *p53* gene is mutated in 60% of human tumors[138], it is believed that p53 regulation plays a major role in adult stem cell-targeted cancer mechanisms.

Evidence that couples asymmetric cell kinetics and p53-dependency in HSCs is the observation that mice with a transgenic knock-out of the *p53* gene exhibit more abundant and longer lived cobblestone islands in long-term mouse bone marrow culture[142]. More notably, populations enriched for HSCs from p53 knockout mice have

greater engraftment potential, when transplanted into lethally irradiated hosts, as compared to wild-type p53 expressing mice[143,144]. The p53-dependent ASC kinetic model for *in vitro* ASC propagation and expansion predicts increased ASC number in the absence of normal p53 expression or in the presence of exogenous nucleosides that promote expansion of guanine ribonucleotide pools, as discussed later (Figure 1.4B).

An important consideration is whether these *in vitro* findings with respect to p53 are relevant to adult stem cell mechanisms *in vivo*. In several examined epithelial tissues, p53 protein expression is detected in basal cells localized in regions thought to harbor adult stem cells[145,146]. Additionally, several different lines of transgenic p53-knockout mice have been derived with consistent early development of diverse tumors[32,147-149]. This finding is consistent with well-established ideas that increased symmetric stem cell divisions induce elevated rates of carcinogenesis[150,151]. DNA damage checkpoint arrest deficiencies have been one of the rationales to account for the remarkable cancer phenotype of these mice[152]. However, consistent with the findings in these p53-knockout mice is the observation that cells cultured from diverse tissues of p53-knockout animals no longer senesce in culture[148,152]. It is anticipated, then, that p53 is a key regulator of HSC kinetics (Figure 1.4).

Inosine Monophosphate Dehydrogenase (IMPDH)

Subsequent investigations into the dependence of p53 in determined asymmetric cell kinetics led to an important piece of the mechanism by which p53 expression modulates cell kinetic symmetry. Specifically, expression of p53 causes down-regulation of inosine monophosphate dehydrogenase (IMPDH). Although the responsible molecular mechanisms have not been elucidated, p53 expression is associated with coordinate down-regulation of IMPDH mRNA, protein and cellular enzymatic activity[33,34]. IMPDH catalyzes the conversion of inosine monophosphate (IMP) to xanthosine monophosphate (XMP) for guanine nucleotide biosynthesis. This enzymatic reaction is rate-determining for the formation of the next metabolite in the pathway, guanine monophosphate (GMP), from which all other cellular guanine nucleotides are derived. One line of evidence for this mechanism of regulation of IMPDH by p53 is that nucleotide salvage compounds that promote the formation of the product of the IMPDH mechanism (i.e. xanthine

monophosphate, XMP) prevent the p53-induced switch to asymmetric cell kinetics[33-35] (Figure 1.4B). Furthermore, forced expression of an IMPDH transgene prevents p53-dependent asymmetric cell kinetics[30,153], suggesting that IMPDH is a rate-determining component of the p53-dependent pathway for asymmetric cell kinetics. This invoked a role for cellular guanine ribonucleotides in asymmetric cell kinetics control mechanisms. Initial studies suggested that the critical guanine nucleotide(s) is a ribonucleotide(s)[34,35], although the exact identity of the acting guanine ribonucleotide(s) and its target(s) have not been determined (Figure 1.4B).

There are two reported *impdh* genes (type I and type II) in both mice and humans[154]. Although the human type I *impdh* gene exhibits no growth-dependent regulation, the type II *impdh* gene exhibits elevated expression in malignancies and other highly proliferative growth states. The murine type II *impdh* gene mediates p53-dependent asymmetric cell kinetics in cultured cell models[30,33,155]. Interestingly, the type II *impdh* gene is a member of a recently defined set of genes whose expression is associated with hematopoietic stem cell-enriched populations[156-158,166]. Due to embryonic lethality, type II *impdh* transgenic knockout mice have not yielded any additional information on the possible role of IMPDH in adult stem cell kinetics[159].

Besides the type II *impdh* gene association with HSC-enriched populations[156-158,166], there has been no direct correlations between IMPDH and HSCs documented to date, although several studies indicate a role for IMPDH in hematopoiesis. In one study, the human myeloid leukemia cell line (HL-60) was induced to mature when specific inhibitors of IMPDH were administered, leading to decreased levels of guanine ribonucleotides. This finding is consistent with the concept that the regulation of myeloid cell maturation may be influenced by intracellular concentrations of guanine ribonucleotides[160]. Additionally, inhibition of IMPDH reduces the frequency of immunoglobulin producing cells, decreasing the levels of secreted immunglobulins and cytokines[161]. The level of IMPDH has been suggested to determine whether acute leukemia cells proliferate (when IMPDH activity is high) or differentiate (when IMPDH levels are low). In humans, IMPDH levels have been found to be higher in B lymphocytes and in acute leukemia blasts[162]. Accordingly, it can be presumed that IMPDH plays a critical role in the cell cycle kinetics of hematopoietic cells and, may

therefore be an important factor in HSC expansion since increased IMPDH activity is observed in hematopoietic malignancies.

Autonomous pathways of cell division regulation in HSCs may be the key factors in developing strategies to expand HSCs *ex vivo*. It is evident that p21, p53 and IMPDH are important regulators in HSC kinetics. On the one hand, p21 regulation may maintain a quiescent HSC pool, while p53 regulation promotes HSC expansion *in vivo*, by decreasing the production of IMPDH. P53 may be promoting increased expression of p21, thereby maintaining HSC pools, while downstream p53 regulation in the form of guanine ribonucleotide production may promote HSC kinetics, as needed by the body. Since malfunctions of p21 and p53 increase the frequency for neoplastic transformations, regulation of these genes is not a viable therapeutic application. One method that controls ASC kinetics, independent of direct p53 regulation is the SACK, or suppression of asymmetric cell kinetics, method[26,28,36,37,40].

Suppression of Asymmetric Cell Kinetics (SACK) Strategy for *Ex Vivo* Expansion of Adult Stem Cells

One of the methods by which adult stem cells can regulate their kinetics is through a p53-dependent pathway that regulates *de novo* guanine ribonucleotide (rGNP) production[9] (Figure 1.4B). Genes involved in regulating this pathway, namely p53 and inosine monophosphate dehydrogenase (IMPDH), were discovered in cultured cell systems that model deterministic asymmetric stem cell kinetics, which is predicted to occur *in vivo*[30,31,35,38,57,141]. The development of these cultured stem cell models has allowed the elucidation of the aforementioned genes responsible for the regulation of adult stem cell kinetics. Specifically, it has been determined that IMPDH is a rate-limiting mediator of p53-dependent asymmetric cell kinetics. Reduced IMPDH activity in response to p53 expression is obligatory for p53-dependent asymmetric cell kinetics. This experimental response is proposed to reflect a physiological response to variation in the levels of critical guanine ribonucleotides (rGNPs) required for cell regulation[33] (Figure 1.4B).

Based on these pathways, a strategy was developed for a cell kinetic method to potentially manipulate adult stem cell kinetics *ex vivo* to achieve expansion[29,30]. Since

adult stem cells divide with determined asymmetric self-renewal kinetics to simultaneously maintain the stem cell pool and to give rise to less primitive differentiated cells, this provides a major barrier to their *ex vivo* expansion. Due to the asymmetric self-renewal kinetics of ASCs, the number of ASCs during *ex vivo* culture is, at a minimum, maintained. However, due to the production of progenitor cells by ASCs, the ASC becomes diluted in the culture by the symmetrically dividing progenitor cells (Figure 1.5). Furthermore, as culture space decreases due to increased progenitor cell production, a fraction of the cells must be passaged to a new vessel to insure continued propagation of the culture. As a result though, there is a high likelihood that with every passage, ASCs will be lost since they represent a small fraction of the culture. Under normal conditions, dilution and eventual loss of ASCs through *ex vivo* and passage will result in the extinction of the culture.

In order to overcome this barrier, it is proposed that regulating the adult stem cell through intrinsic manipulation of a p53-dependent stem cell kinetic pathway to shift the adult stem cell to symmetric kinetics facilitates the desired expansion. Under physiological conditions, p53 regulates the activity of IMPDH and controls the guanine nucleotide pool in dividing cells. Salvage precursors for cellular IMPDH products (hypoxanthine, Hx; xanthosine, Xs; xanthine, Xn), convert cells dividing with asymmetric cell kinetics into cells dividing with symmetric expansion kinetics in culture[9,33,155], without interfering with wildtype p53 function. This regulation is associated with the p53-dependent metabolic pathway in the *de novo* synthesis of purines and is referred to as the suppression of asymmetric cell kinetics (SACK)[9,28].

Specifically, the SACK method has been used to derive adult rat hepatic and cholangiocyte stem cell strains[28,36,37,40]. Non-parenchyma cells taken from a perfused rat liver were cultured under control (no Xs) and Xs supplementation. Two specific Xs-derived strains, Lig-8 and Lig-13, exhibit Xs-dependent asymmetric cell kinetics and Xs-dependent expression of hepatocyte-specific differentiation markers, including α-fetoprotein (AFP), albumin, α1-antitrypsin (AAT), and cholangiocyte-specific differentiation markers, including cytokeratin 7 (CK7)[28], respectively. Currently, the SACK method has been used to explore the expansion of various ASCs, including human hepatic[163], murine pancreatic [164] and hair follicle[165] stem cells.
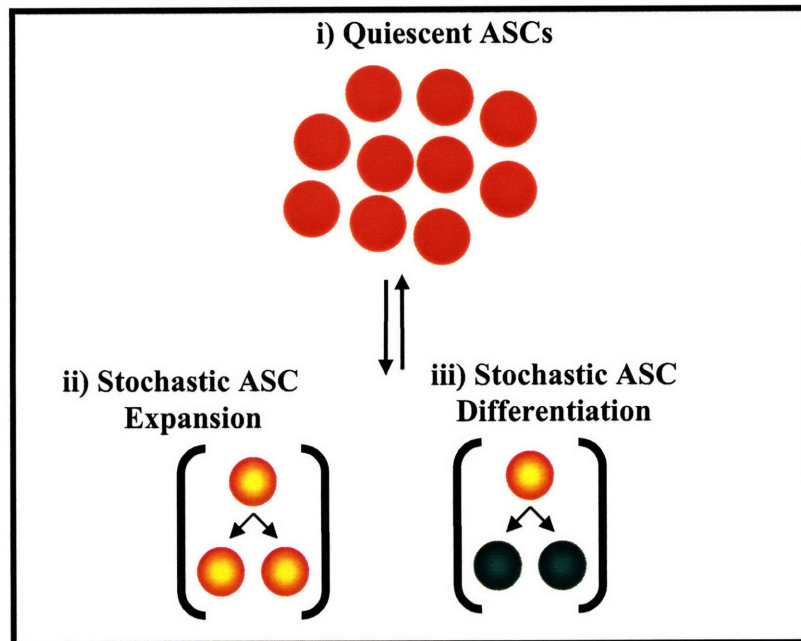
As a step to exploring whether the SACK approach can be applied to the challenge of expanding human HSCs successfully, CD34$^+$ enriched human mobilized peripheral blood (MPB) cells were explored under varying culture conditions, supplemented with purine nucleosides (Figure 1.4). If the SACK method is successful in promoting symmetric expansion of human HSCs *ex vivo*, it may be a simple solution to a longstanding challenge in the HSC field. However, it may be that other factors are needed for optimal SACK-dependent effects. Additionally, SACK regulation may be a safe, universal approach to expand other ASCs that exhibit asymmetric self-renewal kinetics since it relies on natural purine nucleosides that already exist in the cell. Furthermore, SACK-dependent manipulation of cell kinetics is reversible. Any method that aims to expand HSCs *ex vivo* must depend on a process that is reversible in order to revert HSCs back to their asymmetrically self-renewing state, thereby producing fully differentiated, functional blood cells. Selective expansion of human HSCs by SACK, or any other method, would yield increased purity of HSCs resulting in significant improvements in research to define unique properties of HSCs and to identify exclusive markers that are expressed on HSCs.
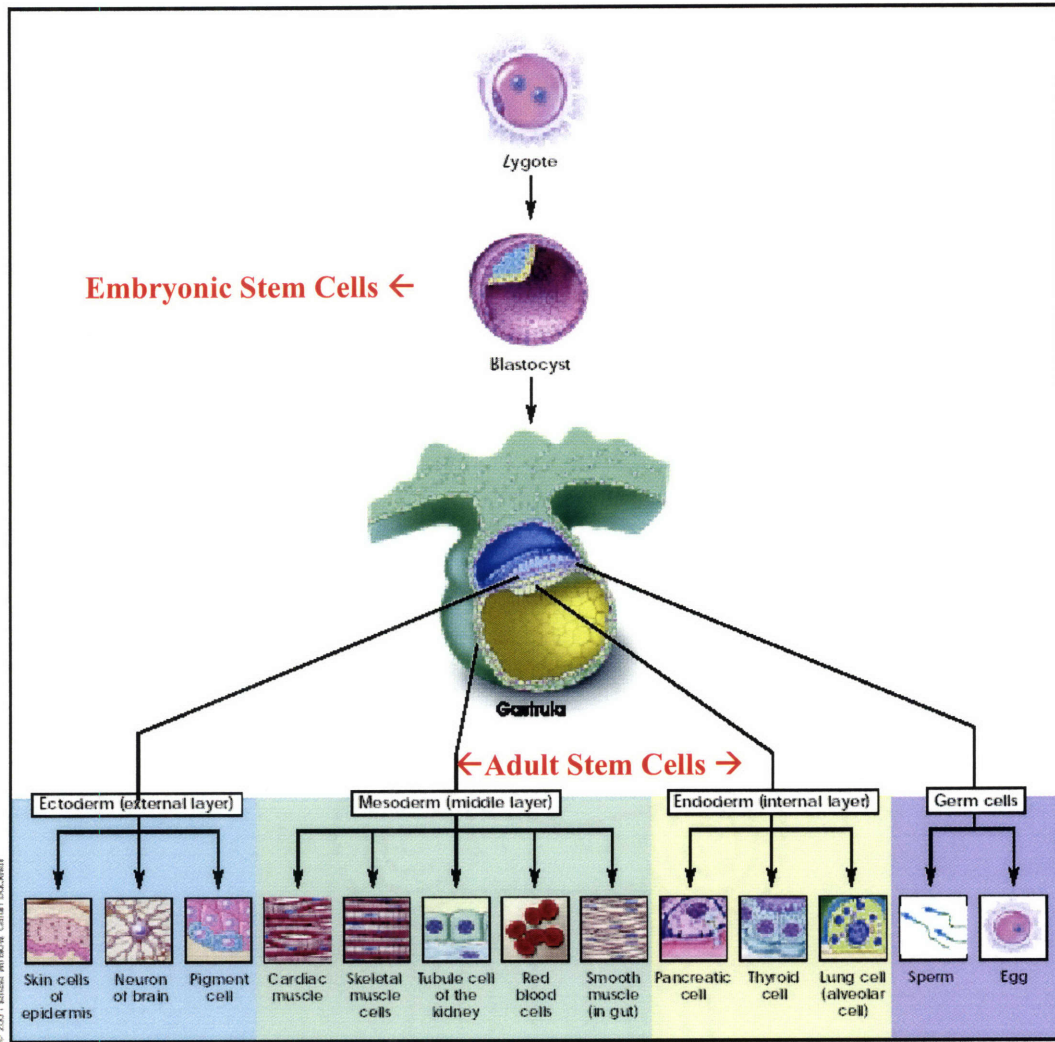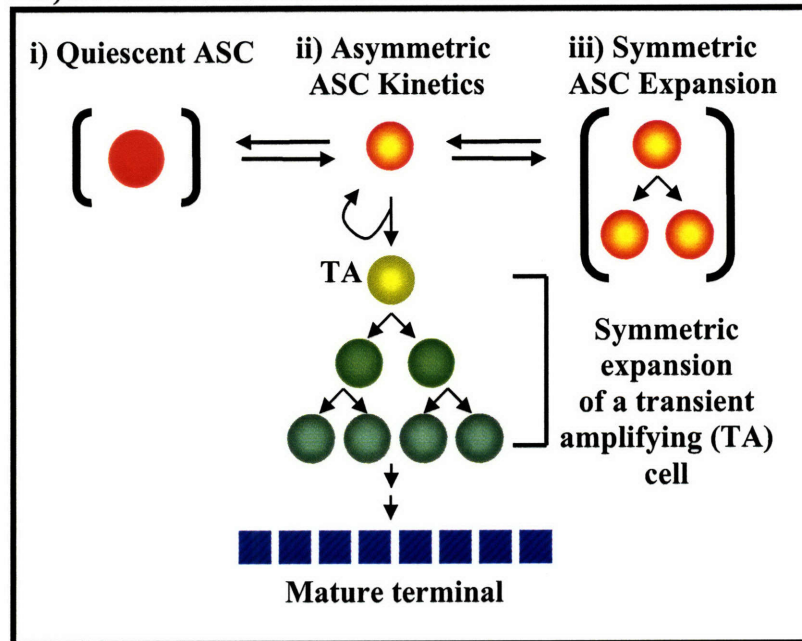
Figure 1.1 | Human Development. During human development, there are two forms of stem cells: embryonic stem cell (ESC) derived from the inner cell mass of a blastocyst and adult stem cells (ASCs) derived from various types of adult tissue. There is interest in stem cells, in general, due to their unique capability to produce differentiated, functional cells for the duration of a human's life. In order for ESCs to become specialized, functional cells, they must go through an ASC phase.

© 2001 Terese Winslow (assisted by Caitlin Duckwall)

A) STOCHASTIC CELL KINETICS

i) Quiescent ASCs

ii) Stochastic ASC Expansion

iii) Stochastic ASC Differentiation

B) DETERMINISTIC ASYMMETRIC CELL KINETICS

i) Quiescent ASC

ii) Asymmetric ASC Kinetics

iii) Symmetric ASC Expansion

TA

Symmetric expansion of a transient amplifying (TA) cell

Mature terminal

Figure 1.2 | Models for Adult Stem Cell Kinetics (ASCs) in a tissue turnover unit. Stochastic cell kinetic models invokes that Ai) a pool of quiescent ASCs can produce Aii) two or Aiii) zero ASCs with zero or two non-stem cell sisters, respectively. Deterministic cell kinetic model invokes that tissue units are derived by a Bi) small number of quiescent ASCs that can divide with Bii) determined asymmetric cell kinetics or Biii) can be regulated to divide with symmetric ASC kinetics for tissue repair and adult maturation. Depending on tissue types, a transient amplifying cell (TC) commits to a different fate.

34
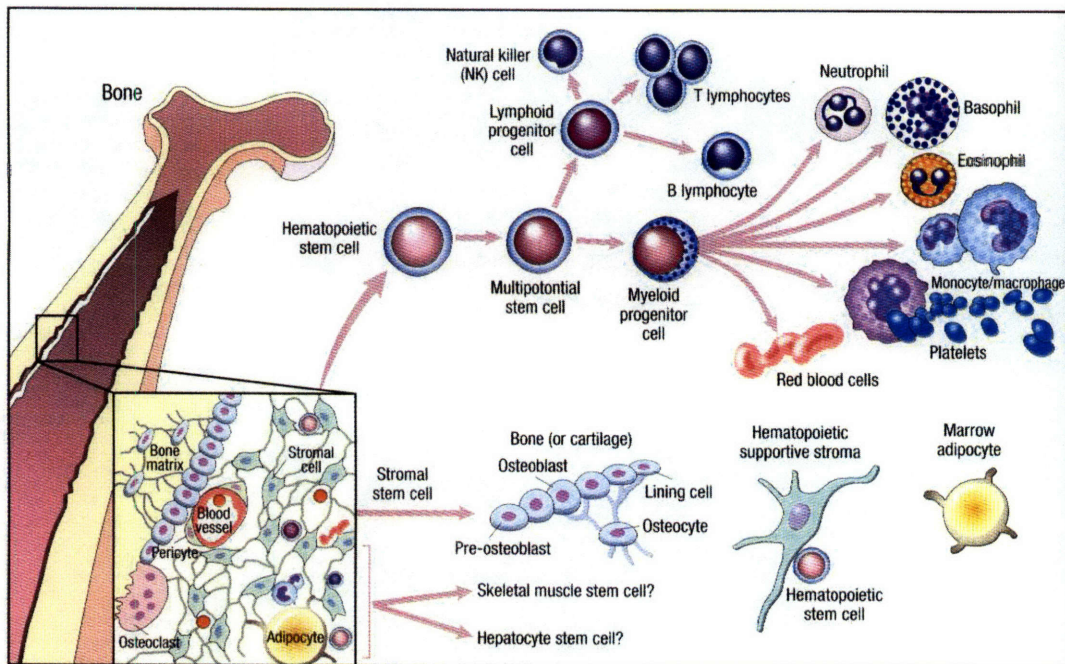
Figure 1.3 | Hematopoiesis Lineage Map. Hematopoiesis comprises the generation of mature, differentiated blood cells from long-term hematopoietic stem cells (HSCs). HSCs give rise to the common myeloid progenitor (CMP) that gives rise to erythrocytes, megakaryocytes, macrophages and various granulocytes and, in addition, HSCs give rise to the common lymphoid progenitor (CLP), from which, natural killer cells, T and B cell lymphocytes arise. Hematopoiesis, from the primitive HSC to the mature myeloid or lymphoid cell, is a highly regulated process, controlled by growth factors and cytokines.

© 2001 Terese Winslow (assisted by Lydia Kibiuk)

A

B
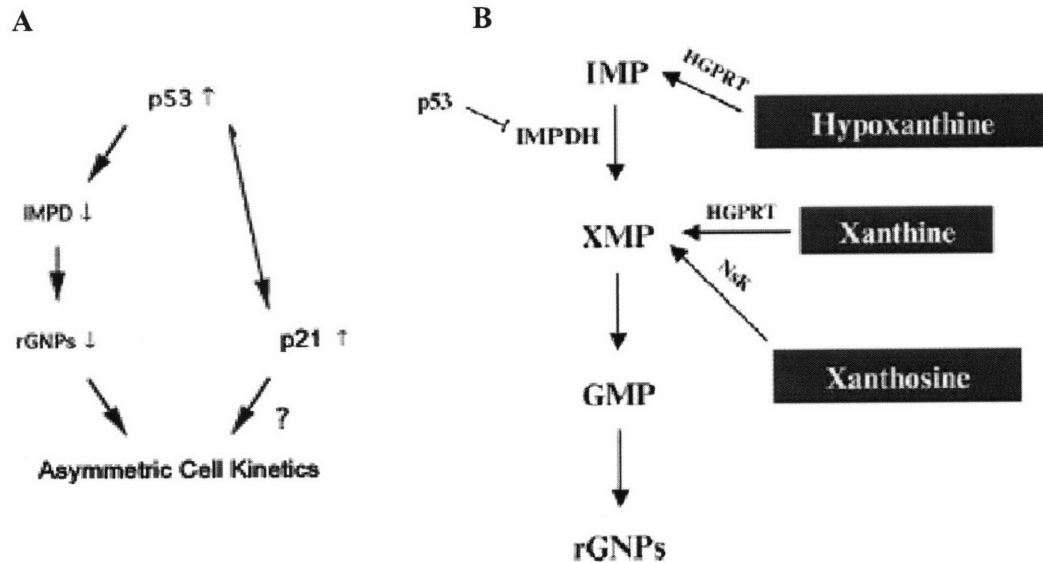
Figure 1.4 | Potential Autonomous Pathways of Cell Division Regulation in HSCs. A) Relationship between IMPDH and mediators of p53-dependent asymmetric cell kinetics. The left branch of the flow diagram depicts IMPDH in its role as a rate-determining mediator of p53-dependent growth suppression in the absence of cellular damage. Reduced IMPDH activity in response to p53 expression is obligatory for p53-dedpendent asymmetric cell kinetics. This reflects a physiological response to variation in the levels of critical guanine ribonucleotides (rGNPs) required for cell regulation. B) Suppression of asymmetric cell kinetics (SACK) is based on a p53-dependent pathway that regulates guanine ribonucleotide biosynthesis. P53 inhibits the production of inosine monophosphate dehydrogenase (IMPDH), the rate limiting enzyme in the conversion of inosine monophosphate (IMP) to xanthosine monophosphate (XMP), which regulates guanine nucleotide biosynthesis. This pathway can be modulated, independent of p53 regulation, by regulating salvage pathways induced by hypoxanthine, xanthosine, and xanthine.

Overcoming the HSC Kinetic Barrier
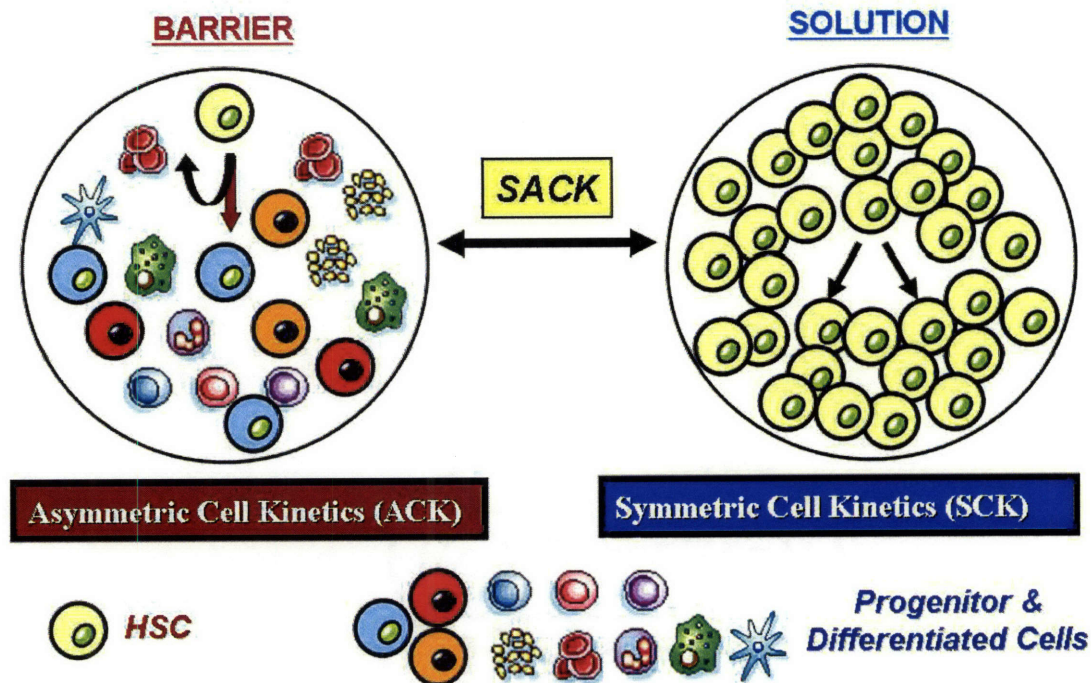
Figure 1.5 | Suppression of Asymmetric Cell Kinetics – A Solution to Overcoming the Hematopoietic Stem Cell (HSC) Kinetic Barrier. HSCs divide with asymmetric self-renewal cell kinetics to give rise to 2 daughter cells, one of which is an HSC and the other is a hematopoietic progenitor cell (HPC) The HPC divides to give rise to differentiated, functional blood cells. As the culture continues, the HSC will become diluted with increasing HPC proliferation and differentiation and, eventually lost with consequent passaging. One potential solution to overcome this kinetic barrier is to promote suppression of asymmetric cell kinetics (SACK) that would yield symmetric expansion of HSCs. In this state, the proliferation and number of HPCs would be suppressed. In order for this solution to be useful, it must reversible, so that once SACK regulation is withdrawn, the expanded HSCs can revert back to their asymmetrically cycling state to give rise to differentiated and functional blood cells.

Bibliographical References

1. Spangrude, G., Heimfeld, S, Weissman, IL. Purification and characterization of mouse hematopoietic stem cells. *Science* **241**, 58-62 (1988).

2. Ueno, N. et al. High-dose chemotherapy and autologous peripheral blood stem cell transplantation for primary breast cancer refractory to neoadjuvant chemotherapy. *Bone Marrow Transplantation* **AOP** (2006).

3. Jansen, J., Hanks, S., Thompson, J., Dugan, M. & Akard, L. Transplantation of hematopoietic stem cells from the peripheral blood. *J Cell Mol Med* **9**, 37-50 (2005).

4. Storb, R. Allogeneic hematopoietic stem cell transplantation-Yesterday, today, and tomorrow. *Experimental Hematology* **31**, 1-10 (2003).

5. Szilvassy, S. J., Meyerrose, T. E., Ragland, P. L. & Grimes, B. Differential homing and engraftment properties of hematopoietic progenitor cells from murine bone marrow, mobilized peripheral blood, and fetal liver. *Blood* **98**, 2108-2115 (2001).

6. Rebel, V., Miller, C., Eaves, C. & Lansdorp, P. The repopulation potential of fetal liver hematopoietic stem cells in mice exceeds that of their liver adult bone marrow counterparts. *Blood* **87**, 3500-3507 (1996).

7. Tyndall, A. & Gratwohl, A. Immune ablation and stem-cell therapy in autoimmune disease: Clinical experience. *Arthritis Research* **2**, 276-280 (2000).

8. Pare, J.-F. & Sherley, J. L. Biological Principles for Ex Vivo Adult Stem Cell Expansion. *Curr Top Dev Biol* **In Press** (2006).

9. Sherley, J. L. Asymmetric Cell Kinetics Genes: The Key to Expansion of Adult Stem Cells in Culture. *Stem Cells* **20**, 561-572 (2002).

10. van der Loo, J. C. M. et al. Nonobese Diabetic/Severe Combined Immunodeficiency (NOD/SCID) Mouse as a Model System to Study the Engraftment and Mobilization of Human Peripheral Blood Stem Cells. *Blood* **92**, 2556-2570 (1998).

11. Bhatia, M., Wang, J. C. Y., Kapp, U., Bonnet, D. & Dick, J. E. Purification of primitive human hematopoietic cells capable of repopulating immune-deficient mice. *PNAS* **94**, 5320-5325 (1997).

12. Boggs, D., Boggs, SS, Saxe, DF, Gress, LA, Canfield, DR. Hematopoietic stem cells with high proliferative potential. Assay of their concentration in marrow by the frequency and duration of cure of W/Wv mice. *J Clin Invest* **70**, 242-253 (1983).

13.   Sieff, C. & Nathans, D. *The anatomy and physiology of hematopoiesis* (W.B. Saunders, Philadelphia, 1993).

14.   Beutler, E., Lichtman, M. A., Coller, B. S., Kipps, T. J. & Seligsohn, U. *Williams Hematology* (McGraw Hill, New York, 2001).

15.   Sutherland, H., Eaves, CJ, Eaves, AC, Dragowska, W, Lansdorp, PM. Characterization and partial purification of human marrow cells capable of initiating long-term hematopoiesis in vitro. *Blood* **74**, 1563-1570 (1989).

16.   Gallacher, L. et al. Isolation and characterization of human CD34-Lin- and CD34$^+$Lin- hematopoietic stem cells using cell surface markers AC133 and CD7. *Blood* **95**, 2813-2820 (2000).

17.   de Wynter, E. A. et al. CD34$^+$AC133$^+$ Cells Isolated from Cord Blood are Highly Enriched in Long-Term Culture-Initiating Cells, NOD/SCID-Repopulating Cells and Dendritic Cell Progenitors. *Stem Cells* **16**, 387-396 (1998).

18.   Verfaillie, C. M. Hematopoietic stem cells for transplantation. *Nature Immunol* **3**, 314-317 (2002).

19.   Peichev, M. et al. Expression of VEGFR-2 and AC133 by circulating human CD34$^+$ cells identifies a population of functional endothelial precursors. *Blood* **95**, 952-958 (2000).

20.   Asahara, T. et al. Isolation of Putative Progenitor Endothelial Cells for Angiogenesis. *Science* **275**, 964-966 (1997).

21.   Trempus, C. S. et al. Enrichment for Living Murine Keratinocytes from the Hair Follicle Bulge with the Cell Surface Marker CD34. **120**, 501-511 (2003).

22.   Morris, R. J. et al. Capturing and profiling adult hair follicle stem cells. **22**, 411-417 (2004).

23.   Taghizadeh, R. R. & Sherley, J. L. Hematopoietic Stem Cell Therapy: Why Aren't We There Yet? *Cambrex Resource Notes*, **3**:2, 4-5 (2005).

24.   Ramalho-Santos, M., Yoon, S., Matsuzaki, Y., Mulligan, R. C. & Melton, D. A. "Stemness": Transcriptional Profiling of Embryonic and Adult Stem Cells. *Science* **298**, 597-600 (2002).

25.   Ivanova, N. B. et al. A Stem Cell Molecular Signature. *Science* **298**, 601-604 (2002).

26.   Sherley, J. L. Asymmetric Cell Kinetics Genes: The Key to Expansion of Adult Stem Cells in Culture. *Stem Cells* **20**, 561-572 (2002).

27. Merok, J. R., Lansita, J. A., Tunstead, J. R. & Sherley, J. L. Cosegregation of Chromosomes Containing Immortal DNA Strands in Cells That Cycle with Asymmetric Stem Cell Kinetics. *Cancer Res* **62**, 6791-6795 (2002).

28. Lee, H., Crane, CG, Merok, JR, Tunstead, JR, Hatch, NL, Panchalingam, K, Powers, MJ, Griffith, LG, Sherley, JL. Clonal expansion of adult rat hepatic stem cell lines by suppression of asymmetric cell kinetics (SACK). *Biotechnol Bioeng* **83**, 760-771 (2003).

29. Merok, J., Sherley, JL. Breaching the Kinetic Barrier to In Vitro Somatic Stem Cell Propagation. *J Biomed Biotechnol.* **1**, 25-27 (2001).

30. Rambhatla, L., Bohn, SA, Stadler, PB, Boyd, JT, Coss, RA, Sherley, JL. Cellular Senescence: Ex Vivo p53-Dependent Asymmetric Cell Kinetics. *J Biomed Biotechnol.* **1**, 28-37 (2001).

31. Huang, S., Law, P, Francis, K, Palsson, BO, Ho, AD. Symmetry of initial cell divisions among primitive hematopoietic progenitors is independent of ontogenic age and regulatory molecules. *Blood* **94**, 2595-604 (1999).

32. Klassen, C. *Casarett & Doull's Toxicology: The basic science of poisons* (McGraw-Hill, 1996).

33. Liu, Y., Bohn, SA, Sherley, JL. Inosine-5'-Monophosphate Dehydrogenase Is a Rate-determining Factor for p53-dependent Growth Regulation. *Mol. Biol. Cell* **9**, 15-28 (1998).

34. Sherley, J. Guanine nucleotide biosynthesis is regulated by the cellular p53 concentration. *J. Biol. Chem.* **266**, 24815-24828 (1991).

35. Sherley, J., Stadler, PB, Stadler, JS, Johnson, DR. Expression of the Wild-Type p53 Antioncogene Induces Guanine Nucleotide-Dependent Stem Cell Division Kinetics. *PNAS* **92**, 136-140 (1995).

36. Lee, H.-S. et al. EMP-1 is a junctional protein in a liver stem cell line and in the liver. *Biochemical and Biophysical Research Communications* **334**, 996-1003 (2005).

37. Semino, C., Merok, J., Crane, G., Panagiotakos, G. & Zhang S. Functional differentiation of hepatocyte-like spheroid structures from putative liver progenitor cells in three-dimensional peptide scaffolds. *Differentiation* **71**, 262-270 (2003).

38. Punzel, M. et al. The symmetry of initial divisions of human hematopoietic progenitors is altered only by the cellular microenvironment. *Experimental Hematology* **31**, 339-347 (2003).

39. Madlambayan, G. J. et al. Dynamic changes in cellular and microenvironmental composition can be controlled to elicit in vitro human hematopoietic stem cell expansion. *Experimental Hematology* **33**, 1229-1239 (2005).

40. Crane, G., Taghizadeh, R. R. & Sherley, J. L. Adult Rat Hepatic Stem Cells Exhibit Asymmetric Adifferentiation In Vitro. *Submitted* (2006).

41. Cheshier, S., Morrison, SJ, Liao, X, Weissman, IL. In vivo proliferation and cell cycle kinetics of long-term self-renewing hematopoietic stem cells. *Proc Natl Acad Sci U S A* **96**, 3120-3125 (1999).

42. Becker, A., McCulloch, E, Till, J. Cytological demonstration of the clonal nature of spleen colonies derived from transplanted mouse marrow cells. *Nature* **197**, 452-454 (1963).

43. Urist, M. Bone: formation by autoinduction. *Science* **150**, 893-899 (1965).

44. Till, J., McCulloch, E. A direct measurement of the radiation sensitivity of normal mouse bone marrow cells. *Radiat Res* **14**, 1419-1430 (1961).

45. Wu, A., Till, JE, Siminovitch, L, McCulloch, EA. Cytological evidence for a relationship between normal hemotopoietic colony-forming cells and cells of the lymphoid system. *J Exp Med* **127**, 455-464 (1968).

46. Sell, S. Liver Stem Cells. *Mod Pathol* **7**, 105-112 (1994).

47. Potten, C., Morris, RJ. Epithelial stem cells in vivo. *J Cell Sci Suppl* **10**, 45-62 (1988).

48. Potten, C., Loeffler, M. Stem cells: attributes, cycles, spirals, pitfalls and uncertainties. Lessons for and from the crypt. *Development* **110**, 1001-1020 (1990).

49. Qu-Petersen, Z. et al. Identification of a novel population of muscle stem cells in mice: potential for muscle regeneration. *J. Cell Biol.* **157**, 851-864 (2002).

50. Karam, S., Leblond, CP. Dynamics of epithelial cells in the corpus of the mouse stomach. I. Identification of proliferative cell types and pinpointing of the stem cell. *Anat Rec.* **236**, 259-279 (1993).

51. Hawkins, N., Garriga, G. Asymmetric cell division: from A to Z. *Genes Dev.* **12**, 3625-3638 (1998).

52. Lovell-Badge, R. The future for stem cell research. *Nature* **414**, 88-91 (2001).

53. Reya, T., Morrison, SJ, Clarke, MF, Weissman, IL. Stem cells, cancer, and cancer stem cells. *Nature* **414**, 105-111 (2001).

54.   Ro, S. & Rannala, B. Methylation patterns and mathematical models reveal dynamics of stem cell turnover in the human colon. *PNAS* **98**, 10519-10521 (2001).

55.   Lajtha, L. Stem cell concepts. *Differentiation* **14**, 23-34 (1979).

56.   Matioli, G., Niewisch, H, Vogel, H. Stochastic stem cell renewal. *Rev Eur Etud Clin Biol.* **15**, 20-22 (1970).

57.   Punzel, M., Zhang, T., Liu, D., Eckstein, V. & Ho, A. D. Functional analysis of initial cell divisions defines the subsequent fate of individual human CD34$^+$CD38- cells. *Experimental Hematology* **30**, 464-472 (2002).

58.   Koller, M., Master, JR, Palsson, BO. *Primary Hematopoietic Cells* (Kluwer Academic Publishers, 1999).

59.   Cronkite, E. Analytical review of structure and regulation of hemopoiesis. *Blood Cells* **14**, 313-328 (1988).

60.   Testa, N. G. & Molineaux, G. *Haemopoiesis: A Practical Approach* (IRL Press/Oxford University Press, New York, 1993).

61.   Brun, A. C. M. et al. Hoxb4-deficient mice undergo normal hematopoietic development but exhibit a mild proliferation defect in hematopoietic stem cells. *Blood* **103**, 4126-4133 (2004).

62.   An, J., Rosen, V, Cox, K, Beauchemin, N, Sullivan, AK. Recombinant human bone morphogenetic protein-2 induces a hematopoietic microenvironment in the rat that supports the growth of stem cells. *Exp Hematol* **24**, 768-775 (1996).

63.   Calvi, L. M. et al. Osteoblastic cells regulate the haematopoietic stem cell niche. **425**, 841-846 (2003).

64.   El-Badri, N., Wang, B., Cherry & Good, R. Osteoblasts promote engraftment of allogeneic hematopoietic stem cells. *Exp Hematol* **26**, 110-6 (1998).

65.   Magli, M. C., Largman, C. & Lawrence, J. H. Effects of HOX homeobox genes in blood cell differentiation. *Journal of Cellular Physiology* **173**, 168-177 (1997).

66.   Taichman, R. S. & Emerson, S. G. The Role of Osteoblasts in the Hematopoietic Microenvironment. *Stem Cells* **16**, 7-15 (1998).

67.   Osawa, M., Hanada, K, Hamada, H, Nakauchi, H. Long-term lymphohematopoietic reconstitution by a single CD34-low/negative hematopoietic stem cell. *Science* **273**, 242-245 (1996).

68. Szilvassy, S., Fraser, CC, Eaves, CJ, Lansdorp, PM, Eaves, AC, Humphries, RK. Retrovirus-mediated gene transfer to purified hemopoietic stem cells with long-term lympho-myelopoietic repopulating ability. *Proc Natl Acad Sci U S A* **86**, 8798-8802 (1989).

69. Muller-Sieburg, C., Whitlock, CA, Weissman, IL. Isolation of two early B lymphocyte progenitors from mouse marrow: a committed pre-pre-B cell and a clonogenic Thy-1-lo hematopoietic stem cell. *Cell* **44**, 653-662 (1986).

70. Ezine S, W. I., Rouse RV. Bone marrow cells give rise to distinct cell clones within the thymus. *Nature* **309**, 629-631 (1984).

71. Tavian, M., Hallais, M. & Peault, B. Emergence of intraembryonic hematopoietic precursors in the pre-liver human embryo. *Development* **126**, 793-803 (1999).

72. Bloom, W. & Bartelmez, G. Hematopoiesis in the young human embryos. *Am. J. Anat.* **67**, 21-53 (1940).

73. Tavian, M., Robin, C., Coulombel, L. & Peault, B. The Human Embryo, but Not Its Yolk Sac, Generates Lympho-Myeloid Stem Cells: Mapping Multipotent Hematopoietic Cell Fate in Intraembryonic Mesoderm. *Immunity* **15**, 487-495 (2001).

74. Godin, I., Dieterlen-Lievre, F. & Cumano, A. Emergence of Multipotent Hemopoietic Cells in the Yolk Sac and Paraaortic Splanchnopleura in Mouse Embryos, Beginning at 8.5 Day Postcoitus. *PNAS* **92**, 773-777 (1995).

75. Delassus, S. & Cumano, A. Circulation of Hematopoietic Progenitors in the Mouse Embryo. *Immunity* **4**, 97-106 (1996).

76. Medvinsky, A. & Dzierzak, E. Definitive Hematopoiesis Is Autonomously Initiated by the AGM Region. *Cell* **86**, 897-906 (1996).

77. Cumano, A., Dieterlen-Lievre, F. & Godin, I. Lymphoid Potential, Probed before Circulation in Mouse, Is Restricted to Caudal Intraembryonic Splanchnopleura. *Cell* **86**, 907-916 (1996).

78. Muller, A., Medvinsky, A., Strouboulis, J., Grosveld, F. & Dzierzak, E. Development of hematopoietic stem cell activity in the mouse embryo. *Immunity* **1**, 291-391 (1994).

79. Charbord, P., Tavian, M., Humeau, L. & Peault, B. Early ontogeny of the human marrow from long bones: an immunohistochemical study of hematopoiesis and its microenvironment. *Blood* **87**, 4109-4119 (1996).

80. Galloway, J. L. & Zon, L. I. Ontogeny of Hematopoiesis: Examining the Emergence of Hematopoietic Cells in the Vertebrate Embryo. *Curr Top Dev Biol* **53**, 139-158 (2003).

81.   Roeder, I. & Loeffler, M. A novel dynamic model of hematopoietic stem cell organization based on the concept of within-tissue plasticity. *Experimental Hematology* **30**, 853-861 (2002).

82.   Till, J., McCulloch, E. & Siminovitch, L. A Stochastic Model of Stem Cell Proliferation, Based on the Growth of Spleen Colony-Forming Cells. *PNAS* **51**, 29-36 (1963).

83.   Abkowitz, J. L., Golinelli, D., Harrison, D. E. & Guttorp, P. In vivo kinetics of murine hemopoietic stem cells. *Blood* **96**, 3399-3405 (2000).

84.   Loeffler, M. a. P., CS. (ed. Potten, C.) 1-28 (Harcourt Brace & Co., San Diego, 1997).

85.   Brummendorf, T. H., Dragowska, W., Zijlmans, J. M. J. M., Thornbury, G. & Lansdorp, P. M. Asymmetric Cell Divisions Sustain Long-Term Hematopoiesis from Single-sorted Human Fetal Liver Cells. *J. Exp. Med.* **188**, 1117-1124 (1998).

86.   Schofield, R. The relationship between the spleen colony-forming cell and the haemopoietic stem cell. *Blood Cells* **4**, 7-25 (1978).

87.   Lord, B., Testa, N. & Hendry, J. The relative spatial distributions of CFUs and CFUc in the normal mouse femur. *Blood* **46**, 65-72 (1975).

88.   Gong, J. K. Endosteal Marrow: A Rich Source of Hematopoietic Stem Cells. *Science* **199**, 1443-1445 (1978).

89.   Ahmed, N., Khokher, M. A. & Hassan, H. T. Cytokine-Induced Expansion of Human CD34$^+$ Stem/Progenitor and CD34$^+$CD41$^+$ Early Megakaryocytic Marrow Cells Cultured on Normal Osteoblasts. *Stem Cells* **17**, 92-99 (1999).

90.   Robey, P. et al. Osteoblasts synthesize and respond to transforming growth factor-type beta (TGF-beta) in vitro. *J. Cell Biol.* **105**, 457-463 (1987).

91.   Nilsson, S. K. et al. Cells Capable of Bone Production Engraft from Whole Bone Marrow Transplants in Nonablated Mice. *J. Exp. Med.* **189**, 729-734 (1999).

92.   Arai, F. et al. Tie2/Angiopoietin-1 Signaling Regulates Hematopoietic Stem Cell Quiescence in the Bone Marrow Niche. *Cell* **118**, 149-161 (2004).

93.   Petzer, A., Zandstra, P., Piret, J. & Eaves, C. Differential cytokine effects on primitive (CD34$^+$CD38-) human hematopoietic cells: novel responses to Flt3-ligand and thrombopoietin. *J. Exp. Med.* **183**, 2551-2558 (1996).

94.   Piacibello, W. et al. Negative influence of IL3 on the expansion of human cord blood in vivo long-term repopulating stem cells. *J Hematother Stem Cell Res.* **9**, 945-956 (2000).

95.   Jaroscak, J. et al. Augmentation of umbilical cord blood (UCB) transplantation with ex vivo-expanded UCB cells: results of a phase 1 trial using the AastromReplicell System. *Blood* **101**, 5061-5067 (2003).

96.   Sauvageau, G. et al. Differential Expression of Homeobox Genes in Functionally Distinct CD34$^+$ Subpopulations of Human Bone Marrow Cells. *PNAS* **91**, 12223-12227 (1994).

97.   Thorsteinsdottir, U. et al. Overexpression of HOXA10 in murine hematopoietic cells perturbs both myeloid and lymphoid differentiation and leads to acute myeloid leukemia. *Mol. Cell. Biol.* **17**, 495-505 (1997).

98.   Sauvageau, G. et al. Overexpression of HOXB4 in hematopoietic cells causes the selective expansion of more primitive populations in vitro and in vivo. *Genes Dev.* **9**, 1753-1765 (1995).

99.   Antonchuk, J., Sauvageau, G. & Humphries, R. K. HOXB4 overexpression mediates very rapid stem cell regeneration and competitive hematopoietic repopulation. *Experimental Hematology* **29**, 1125-1134 (2001).

100.   Bjornsson, J. M. et al. Reduced Proliferative Capacity of Hematopoietic Stem Cells Deficient in Hoxb3 and Hoxb4. *Mol. Cell. Biol.* **23**, 3872-3883 (2003).

101.   Deftos, M. L., Huang, E., Ojala, E. W., Forbush, K. A. & Bevan, M. J. Notch1 Signaling Promotes the Maturation of CD4 and CD8 SP Thymocytes. *Immunity* **13**, 73-84 (2000).

102.   Artavanis-Tsakonas, S., Rand, M. D. & Lake, R. J. Notch Signaling: Cell Fate Control and Signal Integration in Development. *Science* **284**, 770-776 (1999).

103.   Kojika, S. & Griffin, J. D. Notch receptors and hematopoiesis. *Experimental Hematology* **29**, 1041-1052 (2001).

104.   Stier, S., Cheng, T., Dombkowski, D., Carlesso, N. & Scadden, D. T. Notch1 activation increases hematopoietic stem cell self-renewal in vivo and favors lymphoid over myeloid lineage outcome. *Blood* **99**, 2369-2378 (2002).

105.   Karanu, F. N. et al. The Notch Ligand Jagged-1 Represents a Novel Growth Factor of Human Hematopoietic Stem Cells. *J. Exp. Med.* **192**, 1365-1372 (2000).

106.   Zhang, J. et al. Identification of the haematopoietic stem cell niche and control of the niche size. *Nature* **425**, 836-841 (2003).

107.   Kumano, K. et al. Notch1 but Not Notch2 Is Essential for Generating Hematopoietic Stem Cells from Endothelial Cells. *Immunity* **18**, 699-711 (2003).

108. Swiatek, P., Lindsell, C., del Amo, F., Weinmaster, G. & Gridley, T. Notch1 is essential for postimplantation development in mice. *Genes Dev.* **8**, 707-719 (1994).

109. Varnum-Finney, B. et al. Pluripotent, cytokine-dependent, hematopoietic stem cells are immortalized by constitutive Notch1 signaling. **6**, 1278-1281 (2000).

110. Kumano, K. et al. Notch1 inhibits differentiation of hematopoietic cells by sustaining GATA-2 expression. *Blood* **98**, 3283-3289 (2001).

111. Ohishi, K., Varnum-Finney, B. & Bernstein, I. D. Delta-1 enhances marrow and thymus repopulating ability of human CD34$^+$CD38- cord blood cells. *J. Clin. Invest.* **110**, 1165-1174 (2002).

112. Karanu, F. N. et al. Human homologues of Delta-1 and Delta-4 function as mitogenic regulators of primitive human hematopoietic cells. *Blood* **97**, 1960-1967 (2001).

113. Lauret, E. et al. Membrane-bound Delta-4 Notch ligand reduces the proliferative activity of primitive human hematopoietic CD34$^+$CD38low cells while maintaining their LTC-IC potential. *Leukemia* **18**, 788-797 (2004).

114. Varnum-Finney, B. et al. The Notch Ligand, Jagged-1, Influences the Development of Primitive Hematopoietic Precursor Cells. *Blood* **91**, 4084-4091 (1998).

115. Varnum-Finney, B., Brashem-Stein, C. & Bernstein, I. D. Combined effects of Notch signaling and cytokines induce a multiple log increase in precursors with lymphoid and myeloid reconstituting ability. *Blood* **101**, 1784-1789 (2003).

116. Marshall, C. J. & Thrasher, A. J. The embryonic origins of human haematopoiesis. *British Journal of Haematology* **112**, 838-850 (2001).

117. Balemans, W. & Van Hul, W. Extracellular Regulation of BMP Signaling in Vertebrates: A Cocktail of Modulators. *Developmental Biology* **250**, 231-250 (2002).

118. Bhatia, M. et al. Bone Morphogenetic Proteins Regulate the Developmental Program of Human Hematopoietic Stem Cells. *J. Exp. Med.* **189**, 1139-1148 (1999).

119. Xie, T. & Spradling, A. C. decapentaplegic Is Essential for the Maintenance and Division of Germline Stem Cells in the Drosophila Ovary. *Cell* **94**, 251-260 (1998).

120. Xie, T. & Spradling, A. C. A Niche Maintaining Germ Line Stem Cells in the Drosophila Ovary. *Science* **290**, 328-330 (2000).

121. Uren, A., Reichsman, F, Anest, V, Taylor, WG, Muraiso, K, Bottaro, DP, Cumberledge, S, Rubin, JS. Secreted Frizzled-related Protein-1 Binds Directly to Wingless and Is a Biphasic Modulator of Wnt Signaling. *J. Biol. Chem.* **275**, 4374-4382 (2000).

122. Cadigan, K., Nusse, R. Wnt signaling: a common theme in animal development. *Genes Dev.* **11**, 3286-3305 (1997).

123. van de Wetering, M., Sancho, E, Verweij, C, de Lau, W, Oving, I, Hurlstone, A, van der Horn, K, Batlle, E, Coudreuse, D, Haramis, AP, Tjon-Pon-Fong, M, Moerer, P, van den Born, M, Soete, G, Pals, S, Eilers, M, Medema, R, Clevers, H. The beta-catenin/TCF-4 complex imposes a crypt progenitor phenotype on colorectal cancer cells. *Cell* **111**, 241-250 (2002).

124. Van Den Berg, D. J., Sharma, A. K., Bruno, E. & Hoffman, R. Role of Members of the Wnt Gene Family in Human Hematopoiesis. *Blood* **92**, 3189-3202 (1998).

125. Murdoch, B. et al. Wnt-5A augments repopulating capacity and primitive hematopoietic development of human blood stem cells in vivo. *PNAS* **100**, 3422-3427 (2003).

126. Reya, T., Duncan, AW, Ailles, L, Domen, J, Scherer, DC, Willert, K, Hintz, L, Nusse, R, Weissman, IL. A role for Wnt signalling in self-renewal of haematopoietic stem cells. *Nature* **423**, 409-414 (2003).

127. Willert, K., Brown, JD, Danenberg, E, Duncan, AW, Weissman, IL, Reya, T, Yates, JR, Nusse, R. Wnt proteins are lipid-modified and can act as stem cell growth factors. *Nature* **423**, 448-452 (2003).

128. Reya, T. & Clevers, H. Wnt signalling in stem cells and cancer. **434**, 843-850 (2005).

129. Chuang, P., McMahon, AP. Vertebrate Hedgehog signalling modulated by induction of a Hedgehog-binding protein. *Nature* **397**, 617-621 (1999).

130. Johnson, R., Tabin, C. The long and short of hedgehog signaling. *Cell* **81**, 313-316 (1995).

131. Bhardwaj, G., Murdoch, B, Wu, D, Baker, DP, Williams, KP, Chadwick, K, Ling, LE, Karanu, FN, Bhatia, M. Sonic hedgehog induces the proliferation of primitive human hematopoietic cells via BMP regulation. *Nat Immunol.* **2**, 172-180 (2001).

132. el-Deiry, W., Tokino, T, Velculescu, VE, Levy, DB, Parsons, R, Trent, JM, Lin, D, Mercer, WE, Kinzler, KW, Vogelstein, B. WAF1, a potential mediator of p53 tumor suppression. *Cell* **75**, 817-825 (1993).

133. Sherley, J. in *Sourcebook of Asbestos Diseases* (ed. Peters, G. P. B.) 91-141 (Peters & Peters, Santa Monica, 2000).

134. Topley, G., Okuyama, R, Gonzales, JG, Conti, C, Dotto, GP. p21WAF1/Cip1 functions as a suppressor of malignant skin tumor formation and a determinant of keratinocyte stem-cell potential. *PNAS* **96**, 9089-9094 (1999).

135. Cheng, T., Rodrigues, N, Shen, H, Yang, YG, Dombkowski, D, Sykes, M, Scadden, DT. Hematopoietic Stem Cell Quiescence Maintained by p21cip1/waf1. *Science* **287**, 1804-1808 (2000).

136. Stier, S. et al. Ex vivo targeting of p21Cip1/Waf1 permits relative expansion of human hematopoietic stem cells. *Blood* **102**, 1260-1266 (2003).

137. Martin-Caballero, J., Flores, JM, Garcia-Palencia, P, & Serrano, M. Tumor Susceptibility of p21Waf1/Cip1-deficient Mice. *Cancer Res* **61**, 6234-6238 (2001).

138. Levine, A., Perry, ME, Chang, A, Silver, A, Dittmer, D, Wu, M, Welsh, D. The 1993 Walter Hubert Lecture: the role of the p53 tumour-suppressor gene in tumorigenesis. *Br J Cancer* **69**, 409-416 (1994).

139. Zhan, Q., Fan, S, Bae, I, Guillouf, C, Liebermann, DA, O'Connor, PM, Fornace, AJ. Induction of bax by genotoxic stress in human cells correlates with normal p53 status and apoptosis. *Oncogene* **9**, 3743-3751 (1994).

140. Miyashita, T., Reed, JC. Tumor suppressor p53 is a direct transcriptional activator of the human bax gene. *Cell* **80**, 293-299 (1995).

141. Sherley, J., Stadler, PB, Stadler, JS. Quantitative method for the analysis of mammalian cell proliferation in culture in terms of dividing and non-dividing cells. *Cell Prolif.* **28**, 137-144 (1995).

142. Epperly, M., Bray, JA, Carlos, TM, Prochownik, E, Greenberger, JS. Biology of marrow stromal cell lines derived from long-term bone marrow cultures of Trp53-deficient mice. *Radiat Res* **152**, 29-40 (1999).

143. TeKippe, M., Harrison, D. E. & Chen, J. Expansion of hematopoietic stem cell phenotype and activity in Trp53-null mice. *Experimental Hematology* **31**, 521-527 (2003).

144. Wlodarski, P. et al. Role of p53 in Hematopoietic Recovery After Cytotoxic Treatment. *Blood* **91**, 2998-3006 (1998).

145. Antoniades, H., Galanopoulos, T, Neville-Golden, J, Kiritsy, CP, Lynch, SE. p53 expression during normal tissue regeneration in response to acute cutaneous injury in swine. *J Clin Invest* **93**, 2206-2214 (1994).

146. Ahomadegbe, J., Barrois, M, Fogel, S, Le Bihan, ML, Douc-Rasy, S, Duvillard, P, Armand, JP, Riou, G. High incidence of p53 alterations (mutation, deletion, overexpression) in head and neck primary tumors and metastases; absence of correlation with clinical outcome. Frequent protein overexpression in normal epithelium and in early non-invasive lesions. *Oncogene* **10**, 1217-1227 (1995).

147. Purdie, C., Harrison, DJ, Peter, A, Dobbie, L, White, S, Howie, SE, Salter, DM, Bird, CC, Wyllie, AH, Hooper, ML, et al. Tumour incidence, spectrum and ploidy in mice with a large deletion in the p53 gene. *Oncogene* **9**, 603-609 (1994).

148. Tsukada, T., Tomooka, Y, Takai, S, Ueda, Y, Nishikawa, S, Yagi, T, Tokunaga, T, Takeda, N, Suda, Y, Abe, S, et al. Enhanced proliferative potential in culture of cells from p53-deficient mice. *Oncogene* **8**, 3313-3322 (1993).

149. Donehower, L., Harvey, M, Slagle, BL, McArthur, MJ, Montgomery, CA Jr, Butel, JS, Bradley, A. Mice deficient for p53 are developmentally normal but susceptible to spontaneous tumours. *Nature* **356**, 215-221 (1992).

150. Herrero-Jimenez, P., Thilly, G, Southam, PJ, Tomita-Mitchell, A, Morgenthaler, S, Furth, EE, Thilly, WG. Mutation, cell kinetics, and subpopulations at risk for colon cancer in the United States. *Mutat Res.* **400**, 553-578 (1998).

151. Cairns, J. Mutation selection and the natural history of cancer. *Nature* **255**, 197-200 (1975).

152. Harvey, M., Sands, AT, Weiss, RS, Hegi, ME, Wiseman, RW, Pantazis, P, Giovanella, BC, Tainsky, MA, Bradley, A, Donehower, LA. In vitro growth characteristics of embryo fibroblasts isolated from p53-deficient mice. *Oncogene* **8**, 2457-2467 (1993).

153. Weissman, I. Stem cells: units of development, units of regeneration, and units in evolution. *Cell* **100**, 157-168 (2000).

154. Zimmerman, A., Gu, JJ, Laliberte, J, Mitchell, BS. Inosine-5'-monophosphate dehydrogenase: regulation of expression and role in cellular proliferation and T lymphocyte activation. *Prog. Nucl. Acid Res.* **61**, 181-209 (1998).

155. Liu, Y., Riley, LB, Bohn, SA, Boice, JA, Stadler, PB, Sherley, JL. Comparison of bax, waf1, and IMP dehydrogenase regulation in response to wild-type p53 expression under normal growth conditions. *J cell Physiol* **177**, 364-376 (1998).

156. Wagner, W. et al. Molecular evidence for stem cell function of the slow-dividing fraction among human hematopoietic progenitor cells by genome-wide analysis. *Blood* **104**, 675-686 (2004).

157. Phillips, R., Ernst, RE, Brunk, B, Ivanova, N, Mahan, MA, Deanehan, JK, Moore, KA, Overton, GC, Lemischka, IR. The Genetic Program of Hematopoietic Stem Cells. *Science* **288**, 1635-1640 (2000).

158. Senda, M., Natsumeda, Y. Tissue-differential expression of two distinct genes for human IMP dehydrogenase. *Life Sci.* **54**, 1917-1926 (1994).

159. Gu, J., Stegmann, S, Gathy, K, Murray, R, Laliberte, J, Ayscue, L, Mitchell, BS. Inhibition of T lymphocyte activation in mice heterozygous for loss of the IMPDH II gene. *J. Clin. Invest.* **106**, 599-606 (2000).

160. Knight, R. et al. Inosine monophosphate dehydrogenase and myeloid cell maturation. *Blood* **69**, 634-639 (1987).

161. Jonsson, C. A. & Carlsten, H. Mycophenolic acid inhibits inosine 5'-monophosphate dehydrogenase and suppresses immunoglobulin and cytokine production of B cells. *International Immunopharmacology* **3**, 31-37 (2003).

162. Price, G., Hoffbrand, AV, Taheri, MR, Evans, JP. Inosine monophosphate dehydrogenase activity in acute leukaemia. *Leuk Res.* **11**, 525-528 (1987).

163. Panchalingam, K., et al. Unpublished. *Unpublished.*

164. Pare, J.-F., et al. Unpublished. *Unpublished.*

165. King, J., et al. Unpublished. *Unpublished.*

166. He, X., Gonzalez, V., Tsang, A., Thompson, J., Tsang, TC, Harris, DT. Differential Gene Expression Profiling of CD34$^+$ CD133$^+$ Umbilical Cord Blood Hematopoietic Stem Progenitor Cells. *Stem Cells and Development.* **14**, 188-198 (2005).

Chapter 2

Ex Vivo Culture and Characterization of SACK Effects on CD34^{+} Mobilized Peripheral Blood Cells Supplemented with Conventional Growth Factor Cocktail
(Phase I)

<u>Rationale</u>

The first attempts to expand HSCs *ex vivo* by others focused on the use of varied cocktails of hematopoietic growth factors and cytokines. Many of these cytokines are produced locally in the bone marrow microenvironment by stromal cells, suggesting that they may be useful for promoting HSC expansion *ex vivo*. Through many trials, it was found that populations harboring human HSCs (i.e. CD34^{+}) are induced to proliferate in cytokine cocktails including Flt3 ligand (Flt3L), thrombopoietin (TPO), stem cell factor (SCF), interleukin-3 (IL-3) and interleukin-6 (IL-6)[1-3]. However, it has been shown that these hematopoietic cytokines single-handedly do not promote the symmetric expansion of *ex vivo* HSCs[4,5]. While it may be true that specific hematopoietic growth factors or cytokines promote survival of HSCs, they appear more active in promoting lineage commitment and differentiation than HSC expansion. As a result, *ex vivo* cultured hematopoietic cells supplemented with growth factors results in a highly impure HSC population[3,6,7], risking eventual loss of HSCs. Figure 2.1 provides a theoretical model of the outcomes predicted for these different type of cytokine specificity for HSCs and HPCs. If on the other hand, both HSC and HPC expansion were induced, then the fraction of HSCs in the population would not change, relative to HPCs in the culture (Figure 2.1B). Although both HSC and HPC expansion would be advantageous for therapeutic applications, due to the contamination of HPCs in the culture, *in vitro* characterization and detection of HSCs would remain difficult. Moreover, if only HSC expansion were promoted, then the fraction of HSCs would increase exponentially as a function of generation time (GT; Figure 2.1C). Although exhaustive studies of multiple cytokine and growth factor combinations have not yielded conditions that result in HSC-specific expansion, the extensive proliferation of cells suggests that these factors may promote HPC proliferation and differentiation, but not HSC expansion.

The first attempts in this research to investigate specific SACK-effects in the culturing of CD34$^+$ enriched mobilized peripheral blood (MPB) cells were attempted under medium supplementation with the following growth factor (GF) cocktail: Flt3 ligand, TPO, SCF, IL-3, and IL-6. MPB was used as a source due to its availability and clinical advantages, including rapid hematological recovery and relative ease in recovering cells for autologous or allogeneic transplants[8]. CD34$^+$ and CD133$^+$ were used as *in vitro* metrics of HSCs, since HSCs express both CD34 and CD133. CD34 is a 110 kDa (kiloDalton) heavily glycosylated, single chain transmembrane glycoprotein that is expressed on hematopoietic stem cells[9]. CD133 is a 120 kDa, glycosylated protein containing five transmembrane domains which recognizes a subset of CD34$^+$ human HSCs[10,11]. CD133 provides an alternative to CD34 for HSC selection and *ex vivo* expansion[12]. Although both CD34 and CD133 are expressed on HSCs, they are expressed on both hematopoietic[13-16] and non-hematopoietic lineage-committed progenitor cells[17,18]. The lack of specificity of CD34 and CD133 for HSCs represents one of the shortcomings in the HSC field. Despite the specificity, most clinical and experimental protocols including *ex vivo* culture, gene therapy, and HSC transplantation are currently designed for cell populations enriched for CD34$^+$ or CD133$^+$ cells[8,16,19-22].

If SACK regulation promotes symmetric expansion of HSCs, then it would be expected that there would be a net production of SACK-dependent CD34$^+$ and CD133$^+$ (as modeled in Figure 2.1C). SACK studies were performed using the following purine nucleotides (i.e. SACK-agents): hypoxanthine (Hx), xanthine (Xn), xanthosine (Xs), and XHX (an equal mixture of Xn, Hx, and Xs). XHX was studied in order to determine whether enhancement of guanine ribonucleotide production would result in SACK-dependent production of *de novo* CD34$^+$ and CD133$^+$ cells.

Material & Methods

Experimental Design

Figure 2.2 diagrams the general strategy applied for Phase I studies.

Collection of Human CD34$^+$ Mobilized Peripheral Blood Cells (MPBs)

Human CD34$^+$ mobilized peripheral blood (MPB) cells were obtained from Cambrex Biosciences (Walkersville, MD). Briefly, donors are recruited and screened by Cambrex using IRB approved procedures. The donors are evaluated for good health by trained medical personnel and administered G-CSF (granulocyte-colony stimulating factor, Neupogen®) at a medical facility. The dose of Neupogen® was 7.5μg/kg body weight/day injected subcutaneously. Neupogen® was administered daily for four consecutive days, followed by apheresis on day 5. Mobilized peripheral blood (MPB) mononuclear cells (MNCs) were collected by a single apheresis using a Cobe® Spectra™ apheresis machine (Gambro BCT, Inc, Lakewood, CO). Mononuclear cells were obtained through Ficoll-Paque density gradient fractionation (GE Healthcare, Piscataway, NJ) and immuno-magnetically selected using MACS® (Miltenyi Biotech, Auburn, CA) for CD34$^+$ cells. CD34$^+$ MPB cells were frozen at a concentration of 10^6 cells per vial. All ampules were maintained in liquid nitrogen until used for experiments. Although donors were tested free of HIV, Hepatitis B and C, cells were treated as potentially infectious, per supplier's recommendations.

Preparation of Cytokines and Growth Factors

Recombinant human thrombopoietin (TPO), stem cell factor (SCF), fetal liver tyrosine kinase ligand (Flt3 Ligand), interleukin-3 (IL-3), and interleukin-6 (IL-6) were all purchased from R&D Systems (Minneapolis, MN). Each individual lyophilized factor was suspended in 1% human serum albumin in phosphate buffered saline (1% HSA/PBS) and stored as aliquots for not more than 6 months at -80°C.

Culture of Human CD34$^+$ Mobilized Peripheral Blood Cells (MPBs)

Cell vials taken from liquid nitrogen were thawed per manufacturer's instructions. Briefly, warm HPGM (Hematopoietic Progenitor Growth Medium; Cambrex

Biosciences, Walkersville, MD) was added drop wise to cells to slowly diffuse out intracellular dimethylsulfoxide (DMSO). After two rounds of HPGM washes and centrifugations, post-thaw viability and cell count was determined using trypan blue exclusion dye on a hemacytometer. At least 10% of the sample volume was counted using a standard hemacytometer (Hausser Scientific, Horsham, PA) and diluted with the same volume of trypan blue (0.04% in PBS; Sigma, St Louis, MO). Cell concentrations were calculated by taking the average from each $1mm^2$ areas counted and multiplying it by the dilution factor and 10^4. Accordingly, 10^5 viable cells per ml were plated into each well of a 24-well plate and cultured in serum-free HPGM supplemented with cytokines and growth factors (50ng/ml TPO; 25ng/ml SCF; 50ng/ml Flt3 Ligand; 20ng/ml IL-3; 20ng/ml IL-6). Furthermore, cultures were supplemented with SACK-agents xanthine (Xn, Sigma, St. Louis, MO) hypoxanthine (Hx, , Sigma, St. Louis, MO), xanthosine (Xs, Sigma, St. Louis, MO) and an equal mixture of Xn, Hx, and Xs (XHX) at varying concentrations from 0µM to 10µM. SACK-agents were prepared as 20mM stock concentrations, suspended in 10mls of 125mM sodium hydroxide (NaOH). SACK-free, negative controls were dosed with the exact volume of NaOH, as that of each respective SACK-treated condition.

Flow Cytometry

Cultured and uncultured cells were analyzed for human HSC-associated markers, CD34 (BD Biosciences, Franklin Lakes, NJ) and CD133 (Miltenyi Biotech, Auburn, CA). All samples were analyzed using one or two-color flow cytometry with non-specific mouse IgG proteins (Caltag, Burlingame, CA) as negative controls. For each flow cytometry evaluation, a minimum of 10^5 cells were stained and at least 10,000 events were collected and analyzed. Cells were collected and blocked using FACS (fluorescent activated cell sorting) Buffer (1X phosphate buffered saline; PBS, 3% fetal bovine serum, 0.1% sodium azide). After centrifugation and decanting of the buffer, 5µg of each phycoerythrin (PE)-conjugated antibody was added to cells in 100µl FACS Buffer, followed by incubation for 30 minute at 4° C in the dark. After incubation, FACS buffer was again added to bind free, unbound antibody in the solution. After another centrifugation and decanting, the cells were placed in fixative (2% paraformaldehyde,

PFA) to cross-link specifically plasma membrane glycoproteins. After 24 hours incubation in the dark at 4° C, flow cytometry analysis was performed using a FACSCalibur™ flow cytometer (Becton, Dickinson and Company, BD, Mountain View, CA). Data were analyzed using FlowJo software (Tree Star, Inc., San Carlos, CA).

Cell Kinetic Evaluation

All cultured cells were analyzed for cell number and percent viability using a hemacytometer. At least 10% of the sample volume was counted, diluted 1:1 with the same volume of trypan blue to account for viable and dead cells. Percent viability was determined by taking the ratio of the viable cells counted and the total cells counted. SACK-dependent $CD34^+$ and $CD133^+$ cell production were calculated by taking the product of the viable cells and the fraction of viable cells that express each respective marker.

Statistical Analyses

Individual assays (i.e., wells) were averaged across 1-10 experiments. Statistical evaluations of differences between SACK-dependent and control cultures were performed using one-group Student t-test (Statview, SAS Institute Cary, NC), or otherwise noted. Differences were considered statistically significant at $p < 0.05$.

<u>**Results**</u>

$CD34^+$ MPB cells were stained for CD34 and CD133 marker expression and analyzed using flow cytometry for all experiments. A representative FACS profile exhibits the post-thaw expression of CD34 and CD133 to be ~99% (Figure 2.3 blue line) and ~86% (Figure 2.3 red line), respectively, when the cells are gated from the live, lymphocyte gate (R1; Figure 2.3A). After 5 days of culture in GF cocktail, a representative flow diagram for control (R2), 1mM Hx (R3), and 1mM XHX (R4) conditions shows that the cells have higher side scatter (SSC; Figure 2.3B-D). Additionally, cells gated from each respective scatter profile show that 70%-80% of the cells remain $CD34^+$ for control (Figure 2.3B), 1mM Hx (Figure 2.3C) and 1mM XHX (Figure 2.3D). However, after 5 days of culture, the fraction of cells expressing CD133

falls to ~10% in control conditions (Figure 2.3B, red line), but ~20% in 1mM Hx and 1mM XHX conditions (Figure 2.3C-D).

In order to investigate the possible effects of SACK-agents in increasing the number of $CD34^+$ and $CD133^+$ cells produced, Hx, Xn, Xs and XHX were all investigated at varying concentrations. Representative FACS profiles are shown for control, 1mM Hx, and 1mM XHX conditions (Figure 2.3B-D). With GF cocktail supplementation, a range of concentrations from 1mM – 10mM for Hx were investigated, along with 1mM concentrations of Xn, Xs, and XHX. $CD34^+$ MPB cells cultured under these conditions at varying SACK-agent doses exhibited toxicity at the 3mM and 10mM concentrations of Hx, as percent viability was reduced by 14% and 21%, respectively, relative to SACK-free controls (Figure 2.4A). However, the 1mM concentrations of Hx, Xn, Xs, and XHX exhibited no toxicity. These same conditions exhibited a 41% and 51% reduction in viable cells (relative to controls) with 1mM Hx and 1mM XHX , respectively (p<0.0001 and   p=0.0012, respectively; Figure 2.4B). The observed reduction is not due to detectable toxicity-induced effects (Figure 2.4A). Additionally, cells in 1mM Xs conditions give rise to a reduction in viable cells. However, the confidence for this effect is low (p=0.06; Figure 2.4C).

Culture of $CD34^+$ MPB cells in 1mM Hx-supplemented medium, resulted in a 1.5-fold increase in the frequency of cells that express CD133 (p<0.0001; figure 2.4C). Cells cultured with 1mM XHX exhibit a 1.7-fold increase in the frequency of $CD133^+$ cells (p=0.04; Figure 2.4C). No statistically significant effects were observed for $CD34^+$ cells (Figure 2.4C). With respect to the total number of $CD34^+$ and $CD133^+$ cells that are estimated, no significant changes due to purine supplementation were observed (Figure 2.4D).

Since 1mM Hx and 1mM XHX cultured cells gave rise to a statistically significant reduction in viable cells and, simultaneously, yielded an increase in the fraction of cells that expressed CD133, titrations were performed from a concentration range of 0mM – 2mM Hx, to determine an optimum dose to detect significant SACK-dependent increases in $CD34^+$ and/or $CD133^+$ cell populations. The range of 0mM – 2mM Hx was investigated, since it was evident that 3mM Hx was already at a toxic level for $CD34^+$ MPB cells (Figure 2.4A). Indeed, this range of concentrations did not show

toxicity (Figure 2.5A). It was evident that there existed a dose-dependent reduction in viable cells with increasing Hx concentration that was not due to cell death (Figure 2.5B). Additionally, with increasing Hx concentration, a dose-dependent increase in the fraction of cells that express CD133 was observed, whereas there was no dependence observed with respect to $CD34^+$ cells (Figure 2.5C). Yet again, with respect to untreated controls, no detectable changes in the absolute number of Hx-dependent $CD34^+$ or $CD133^+$ cells was observed. However, the absolute numbers of $CD34^+$ cells decreased with increasing Hx concentration (Figure 2.5D).

Discussion

$CD34^+$ MPB cells supplemented with a GF cocktail and cultured for 5 days with SACK-agents Hx, Xs, Xn, and XHX under varying concentrations results in specific effects on both cell kinetic parameters and the population fraction of cells expressing CD34 and CD133. From initial examination, it is evident that after 5 days of culture, the size and surface granularity of all studied cells increased as determined from the side scatter and the forward scatter properties, respectively (compare Figure 2.3B-D to Figure 2.3A). Additionally, control cells cultured for 5 days showed a 10- to 15-fold increase in viable cell number (see Chapter 3, Figure 3.4B). These changes indicate the appearance of differentiated hematopoietic cells. During this period of culture, for both untreated and treated (1mM Hx and 1mM XHX), frequency of $CD34^+$ cells are reduced to ~70%, a marked reduction from the starting population expressing ~99% (Figure 2.3A-D). However, no Hx- or XHX-effects were observed with respect to the frequency and absolute number of $CD34^+$ cells.

On the other hand, culturing of untreated $CD34^+$ MPB cells resulted in a significant reduction in the frequency of $CD133^+$ cells from ~86% to ~10% (Figure 2.3A, B). The presence of Hx and the combination XHX resulted in a similar overall reduction (Figure 2.3C, D). However, compared to untreated controls, a significant increase of 1.5-fold and 1.7-fold was observed in the frequency of $CD133^+$ cell cultured in Hx and XHX-supplemented conditions, respectively (Figure 2.3C, D; Figure 2.4C; Figure 2.5C). However, no significant effects were detected in the absolute number of $CD133^+$ cells with Hx and XHX culture (Figure 2.4D; Figure 2.5D).

Although CD34 and CD133 have both been implicated to be expressed on HSCs[12,23], they exhibit contradicting effects once CD34^{+} MPB cells are cultured. On the one hand, the frequency of CD34^{+} remains high after being cultured, whereas the frequency of CD133^{+} cells declines significantly. The observed difference in their expression is consistent with the fact that they are not exclusively expressed on HSCs, but are found to be expressed on HPCs, as well[13-16]. Due to the extensive promotion of proliferation and differentiation of HPCs induced by hematopoietic growth factors and cytokines (i.e. GF cocktail)[3], the majority of cells after 5 days of culture are differentiated progenitor cells. The increase in cell size observed in Figure 2.3 (A vs. B) is consistent that HPC differentiation has occurred, since hematopoietic cells increase in size as they differentiate. Although both CD34 and CD133 are not uniquely expressed on HSCs, it is evident that CD133 is a more specific marker for HSCs than CD34, since the frequency of cells expressing CD133 declines 4- to 8-fold compared with 1.2- to 1.4-fold decrease in cells expressing CD34 (Figure 2.3). Consequently, since CD34 and CD133 are expressed at high and low levels, respectively, in cell populations consisting of differentiating HPCs, it is consistent with the observation that CD133 is a more specific marker for HSCs than CD34[12,15,23,24].

1mM concentrations of Hx or the combination, XHX, resulted in a 41% and 51% respective reduction in viable cells in the population (p<0.0001 and p=0.0012, respectively; Figure 2.4B). This effect is not due to cell death and loss as a result of toxicity, since the 1mM Hx and XHX concentrations exhibit no evidence of toxic effects (Figure 2.4A). In contrast, higher concentrations of Hx at 3mM and 10mM show clear effects of toxicity (Figure 2.4A). The observed Hx- and XHX-dependent reduction in viable cell number, suggested that Hx and XHX, specifically, might induce suppression in the production of hematopoietic progenitor cells (HPCs), by promoting symmetric expansion of HSCs (which *de facto* prevents HPC production), or they might independently suppress HPC proliferation. Supplementation of CD34^{+} MPB cells with Hx and XHX resulted in a 1.5-fold and 1.7-fold increase, respectively, in the fraction of cells expressing CD133 (p<0.0001 & p=0.002, respectively; Figure 2.4C). This observed Hx- and XHX-dependent increase in the fraction of CD133^{+} cells suggested that either simple enrichment of CD133^{+} cells has taken place due to selective suppression of HPC

proliferation or that HSCs were expanded. As predicted, if SACK promoted symmetric expansion of HSCs, then the number of hematopoietic progenitor cells would be expected to decrease as the fraction of $CD133^+$ HSCs increases. No significant effects were observed in the fraction of cells expressing CD34 in SACK-treated cultures.

Although the SACK-effects observed with CD133 expression could be due to expansion in $CD133^+$ HSCs or better enrichment of SACK-dependent $CD133^+$ cells, there is another explanation. $CD34^+$ MPB cells cultured with Hx and XHX may increase the level of CD133 expression on each cell. However, this justification could be partly supported by a shift in the CD133 histogram with SACK-supplementation (Figure 2.3). However, no detectable shift is observed accounting for greater CD133 receptor expression as a response to SACK culture.

These effects of SACK-agents did not result in a SACK-dependent production of $CD133^+$ or $CD34^+$ cells (Figure 2.4D; Figure 2.5D). There could be several reasons for this outcome. On the one hand, culturing $CD34^+$ MPB cells for 5 days in a GF cocktail with Hx- and XHX-supplementation gives rise to extensive proliferation of HPCs. This effect reduced the sensitivity for detecting changes in $CD133^+$ and $CD34^+$ cell number related specifically to HSCs, because of the lack of exclusive detection. On the other hand, the optimal concentration of Hx and XHX may have not been tested. In order to investigate the latter, Hx was titrated at concentrations ranging from 0mM – 2mM. As determined from trypan blue exclusion, this range of concentrations exhibited no toxicity (Figure 2.5A). A dose-dependent reduction in the viable cells was observed with increasing Hx concentrations (Figure 2.5B). As discussed earlier, this observation suggested that the proliferation of HPCs might be suppressed with increasing Hx concentration, since this reduction was not due to toxic effects of Hx (Figure 2.5A-B). A dose-dependent increase in the frequency of $CD133^+$ cells was observed with increasing Hx concentration (Figure 2.5C). These observations together suggest that either Hx-supplementation selectively enriches for $CD133^+$ cells by directly reducing HPC production or, alternatively, that a population of $CD133^+$ HSCs may be promoted to symmetrically expand. Again, as in the initial studies (Figure 3.4), these effects with Hx did not translate into an increased number of $CD34^+$ or $CD133^+$ cells, as compared to control cultures (Figure 2.5D).

Conclusion

From these Phase I GF cocktail supplemented experiments, it was evident that Hx and XHX yielded significant reduction in viable cell number and increased the frequency of cells that expressed CD133^{+}. These effects were suggestive of SACK-dependent effects on a population of CD133^{+} HSCs. It is also evident that CD34 was not a useful marker for these analyses, since after 5 days of extensive proliferation, the majority of the cells still express CD34. Since HSC function is known to be dramatically reduced[3], CD34 was not used in subsequent studies. Although investigations into the optimal concentrations of Hx did not yield an absolute increase in CD133^{+} cells, they did confirm that the 1mM concentration is a good concentration to use in future experiments. The significant cell kinetic and CD133^{+} cell fraction effects observed with Hx- and XHX-dependent cultures was difficult to interpret, since the sensitivity for detecting any changes in CD133^{+} cells was not ideal, due to extensive proliferation of HPCs under GF cocktail supplemented conditions. Therefore, studies in Phase II experiments will focus on increasing the sensitivity for detecting SACK-dependent effects in cultured CD34^{+} MPB cells.
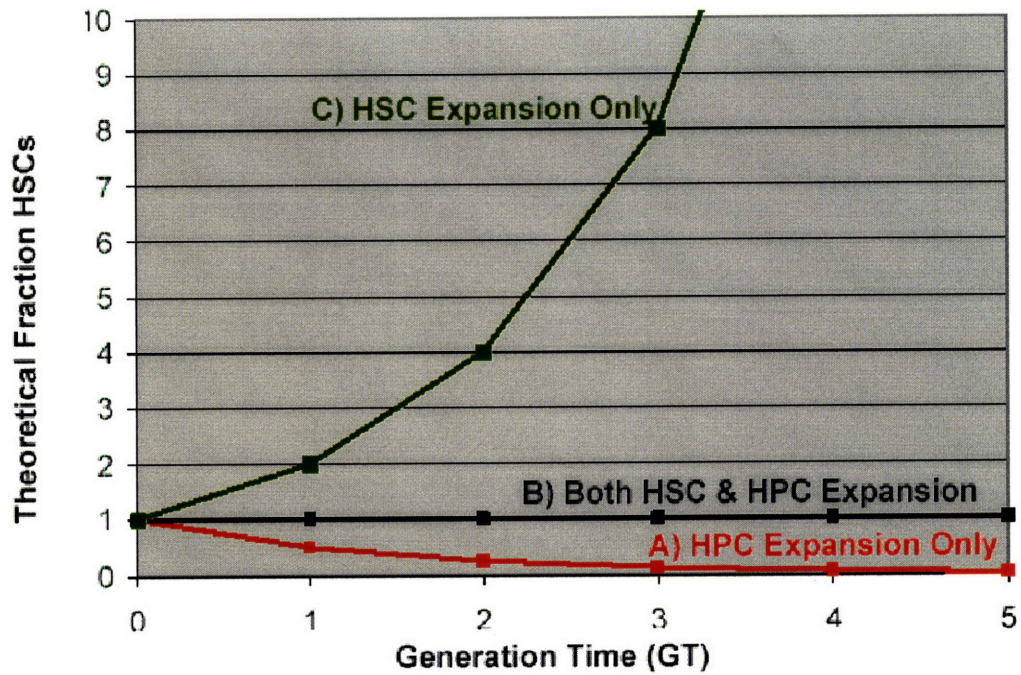
Figure 2.1 | Theoretical Effects of Cytokines on Different Cell Type Specificity on Hematopoietic Stem Cell (HSC) Population Fraction. Due to the heterogeneity in current HSC $CD34^+$ enriched populations, the following kinetic models propose various cell-specific effects on the theoretical fraction of HSCs. A) Exclusive induction of hematopoietic progenitor cell (HPC) expansion results in exponential dilution in the fraction of HSCs in the population. B) Induced proliferation of both HSCs and HPCs, at equal efficiency, maintains the relative frequency of HSCs, although HSC numbers increase. Although potentially advantageous for clinical applications, lack of *in vitro* specificity to track HSCs is problematic. C) Exclusive promotion of HSC expansion in an environment where HPC proliferation is suppressed results in exponential increase in the theoretical fraction and absolute number of HSCs.

Experimental Design – Phase I
Growth Factor (GF) Cocktail Experiments

GF Cocktail* (5 Days)

+ SACK Agents
Hx, Xn, Xs, or XHX

Harvest

Human CD34+ Mobilized Peripheral Blood (MPB)

In vitro Characterization
a) FACS → HSC-Associated Markers (CD34+ & CD133+)
b) Cell Kinetics → Cell Number, % Viability
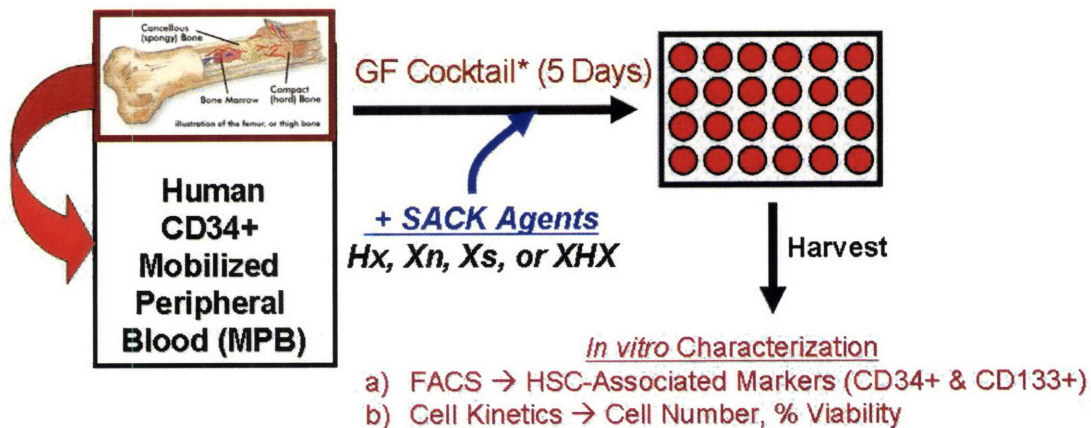
* GF Cocktail consists of SCF, TPO, Flt-3 ligand, IL-3, IL-6

Figure 2.2 | Experimental Design of Phase I, Growth Factor (GF) Cocktail Supplemented Studies. CD34$^+$ mobilized peripheral blood (MPB) cells were cultured for 5 days in serum-free HPGM (Hematopoietic Progenitor Growth Medium) supplemented with 50ng/ml Flt3 ligand, 50 ng/ml TPO, 25 ng/ml SCF, 20 ng/ml IL-3, and 20 ng/ml IL-6. CD34$^+$ MPB cells were cultured supplemented with hypoxanthine (Hx), xanthine (Xn), xanthosine (Xs) and an equal mixture of Xn, Hx, Xs (XHX). SACK-free, negative controls were not supplemented with purines. Cells were cultured for 5 days, harvested and quantified for CD34$^+$ & CD133$^+$ cell fraction and cell kinetics.
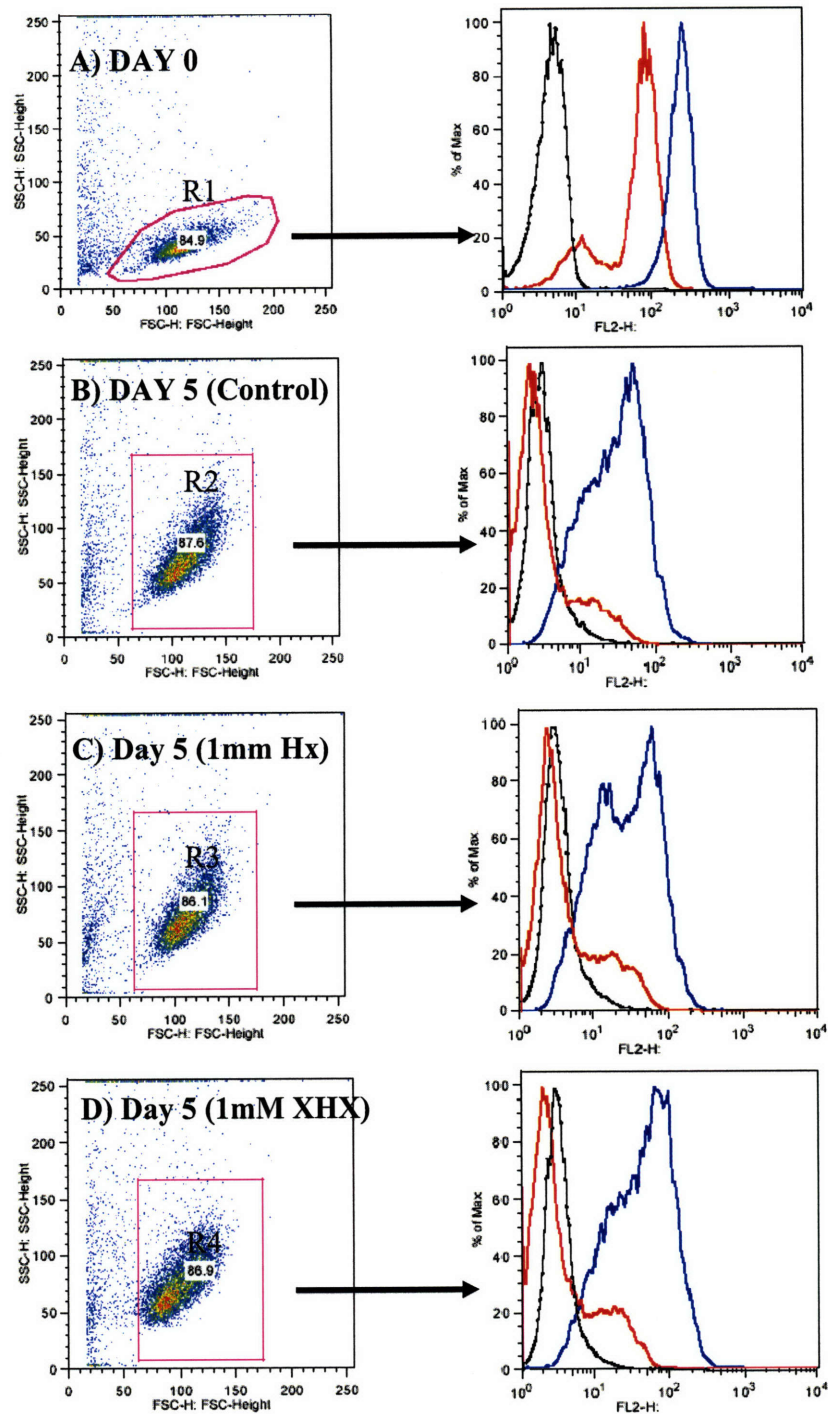
Figure 2.3 | Representative FACS Profiles of Uncultured (Day 0) and Cultured (Day 5) CD34$^+$ Mobilized Peripheral Blood (MPB) Cells in GF Cocktail. Fluorescent-activated cell sorting (FACS) profiles exhibiting expression patterns of IgG1-PE (black; isotype control), CD133-PE (red) and CD34-PE (blue) gated from the live, lymphocyte-sized fraction A) R1, for uncultured, day 0 cells, B) R2, day 5 cultured SACK-free controls, c) R3, day 5 Hx (1mM) cultured cells, and D) R4, day 5 XHX (1mM) culture cells. Scatter profiles represent side (SSC) vs. forward (FSC) scatter. Histograms represent the fluorescent profiles for various PE-conjugated antibodies.
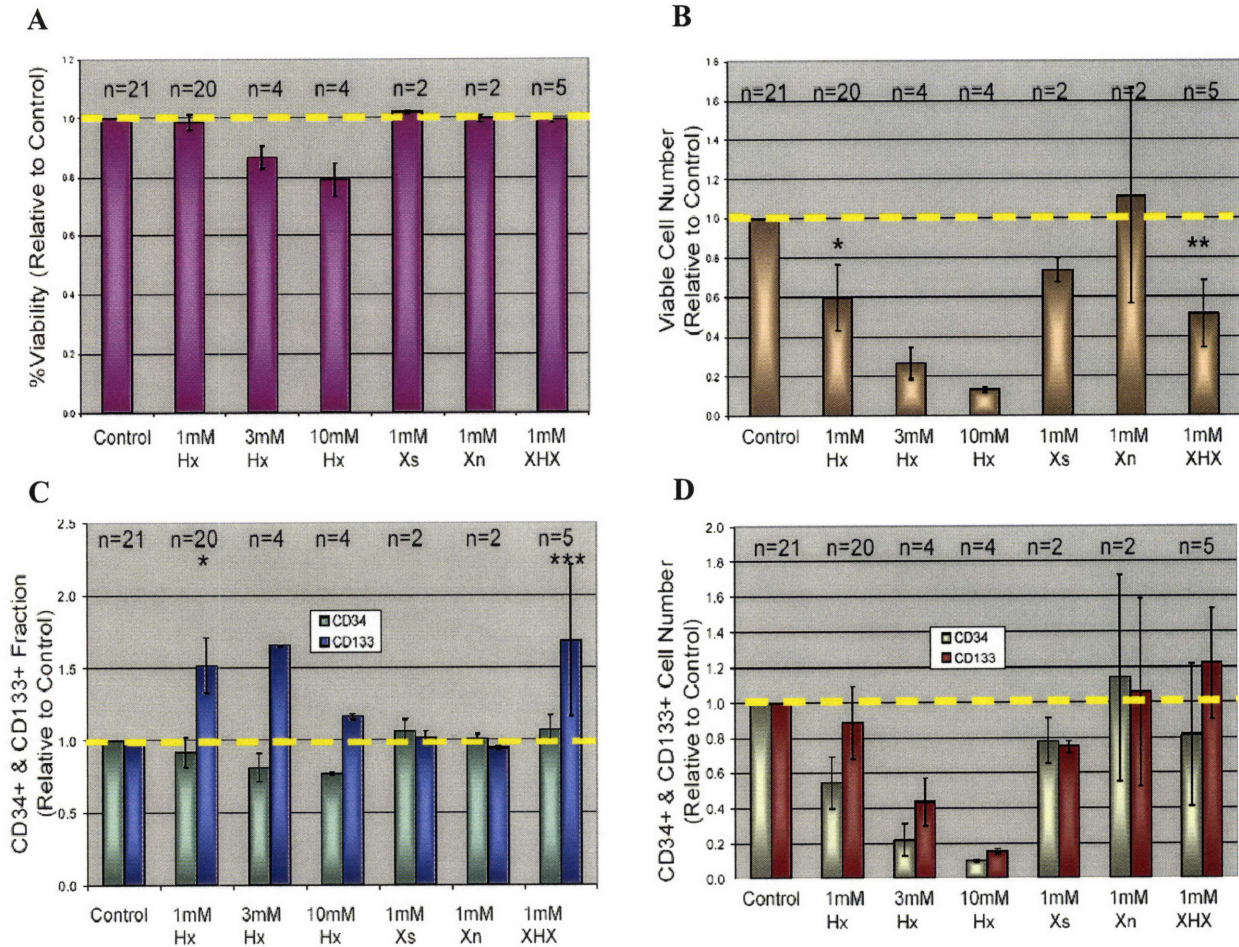
Figure 2.4 | SACK-Dependent Effects on CD34⁺ Mobilized Peripheral Blood (MPB) Cells Cultured for 5 Days with GF Cocktail Supplementation. Various SACK-agents were cultured at varying doses (including hypoxanthine [Hx], xanthosine [Xs], xanthine [Xn], and an equal mixture of Xs, Hx, and Xs [XHX]), in addition to SACK-free controls and investigated for SACK-dependent effects on the relative (to control) A) percent viability , B) total viable cell number, C) CD34⁺ and CD133⁺ cell fraction and D) absolute CD34⁺ and CD133⁺ cell number. Error bars = standard deviation for n individual assays. n = number individual assays, in general, performed in replicates of 2. Dashed (yellow) line represents the normalized control.

* $p<0.0001$, ** $p=0.0012$, *** $p=0.002$ for student's t-test for differences versus control.
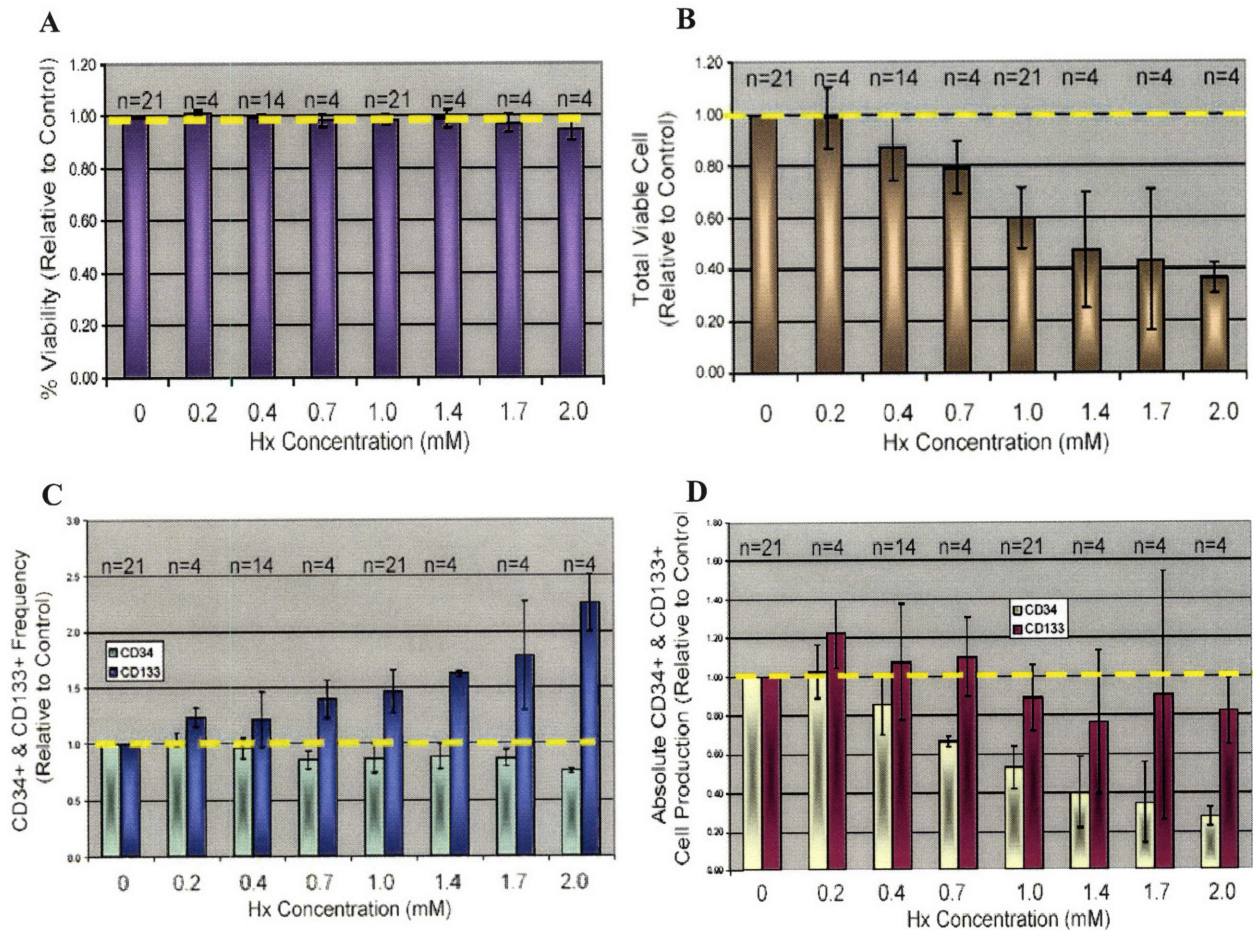
Figure 2.5 | Titration of Hx Concentration for Cell Kinetics Effects on CD34$^+$ Mobilized Peripheral Blood (MPB) Cells Cultured for 5 Days in GF Cocktail Supplementation. A titration of hypoxanthine (Hx) in the indicated range was investigated for Hx-dependent effects on the relative (to control) A) percent viability , B) viable cells, C) CD34$^+$ and CD133$^+$ cell fraction and D) absolute CD34$^+$ and CD133$^+$ cell number. Error bars = standard deviation for n individual assays. n = number individual assays, in general, performed in replicates of 2. Dashed (yellow) line represents the normalized control.

Bibliographical References

1.   Petzer, A., Zandstra, P., Piret, J. & Eaves, C. Differential cytokine effects on primitive (CD34$^+$CD38$^-$) human hematopoietic cells: novel responses to Flt3-ligand and thrombopoietin. *J. Exp. Med.* **183**, 2551-2558 (1996).

2.   Piacibello, W. et al. Negative influence of IL3 on the expansion of human cord blood in vivo long-term repopulating stem cells. *J Hematother Stem Cell Res.* **9**, 945-956 (2000).

3.   Madlambayan, G. J. et al. Dynamic changes in cellular and microenvironmental composition can be controlled to elicit in vitro human hematopoietic stem cell expansion. *Experimental Hematology* **33**, 1229-1239 (2005).

4.   Huang, S., Law, P, Francis, K, Palsson, BO, Ho, AD. Symmetry of initial cell divisions among primitive hematopoietic progenitors is independent of ontogenic age and regulatory molecules. *Blood* **94**, 2595-604 (1999).

5.   Punzel, M. et al. The symmetry of initial divisions of human hematopoietic progenitors is altered only by the cellular microenvironment. *Experimental Hematology* **31**, 339-347 (2003).

6.   Jaroscak, J. et al. Augmentation of umbilical cord blood (UCB) transplantation with ex vivo-expanded UCB cells: results of a phase 1 trial using the AastromReplicell System. *Blood* **101**, 5061-5067 (2003).

7.   Taghizadeh, R. R. & Sherley, J. L. Hematopoietic Stem Cell Therapy: Why Aren't We There Yet? *Cambrex Resource Notes*, **3**:2, 4-5 (2005).

8.   Jansen, J., Hanks, S., Thompson, J., Dugan, M. & Akard, L. Transplantation of hematopoietic stem cells from the peripheral blood. *J Cell Mol Med* **9**, 37-50 (2005).

9.   Sutherland, D., Keating, A. The CD34 antigen: structure, biology, and potential clinical applications. *J Hematother* **1**, 115-129 (1992).

10. Miraglia, S. et al. A Novel Five-Transmembrane Hematopoietic Stem Cell Antigen: Isolation, Characterization, and Molecular Cloning. *Blood* **90**, 5013-5021 (1997).

11. Yin, A. H. et al. AC133, a Novel Marker for Human Hematopoietic Stem and Progenitor Cells. *Blood* **90**, 5002-5012 (1997).

12. Kobari, L., Giarratana, MC, Pflumio, F, Izac, B, Coulombel, L, Douay, L. CD133$^+$ cell selection is an alternative to CD34$^+$ cell selection for ex vivo expansion of hematopoietic stem cells. *J Hematother Stem Cell Res.* **10**, 273-281 (2001).

13. Spangrude, G., Heimfeld, S, Weissman, IL. Purification and characterization of mouse hematopoietic stem cells. *Science* **241**, 58-62 (1988).

14. Sutherland, H., Eaves, CJ, Eaves, AC, Dragowska, W, Lansdorp, PM. Characterization and partial purification of human marrow cells capable of initiating long-term hematopoiesis in vitro. *Blood* **74**, 1563-1570 (1989).

15. Gallacher, L. et al. Isolation and characterization of human CD34⁻Lin⁻ and CD34⁺Lin⁻ hematopoietic stem cells using cell surface markers AC133 and CD7. *Blood* **95**, 2813-2820 (2000).

16. de Wynter, E. A. et al. CD34⁺AC133⁺ Cells Isolated from Cord Blood are Highly Enriched in Long-Term Culture-Initiating Cells, NOD/SCID-Repopulating Cells and Dendritic Cell Progenitors. *Stem Cells* **16**, 387-396 (1998).

17. Peichev, M. et al. Expression of VEGFR-2 and AC133 by circulating human CD34⁺ cells identifies a population of functional endothelial precursors. *Blood* **95**, 952-958 (2000).

18. Asahara, T. et al. Isolation of Putative Progenitor Endothelial Cells for Angiogenesis. *Science* **275**, 964-966 (1997).

19. Holyoake, T. L., Nicolini, F. E. & Eaves, C. J. Functional differences between transplantable human hematopoietic stem cells from fetal liver, cord blood, and adult marrow. *Experimental Hematology* **27**, 1418-1427 (1999).

20. Leor, J. et al. Human Umbilical Cord Blood-Derived CD133⁺ Cells Enhance Function and Repair of the Infarcted Myocardium. *Stem Cells* **24**, 772-780 (2006).

21. Sitnicka, E. et al. Human CD34⁺ hematopoietic stem cells capable of multilineage engrafting NOD/SCID mice express flt3: distinct flt3 and c-kit expression and response patterns on mouse and candidate human hematopoietic stem cells. *Blood* **102**, 881-886 (2003).

22. Storb, R. Allogeneic hematopoietic stem cell transplantation-Yesterday, today, and tomorrow. *Experimental Hematology* **31**, 1-10 (2003).

23. Bitan et al. Successful transplantation of haploidentically mismatched peripheral blood stem cells using CD133⁺-purified stem cells. *Experimental Hematology* **33**, 713-718 (2005).

24. Kuci, S. et al. Identification of a novel class of human adherent CD34- stem cells that give rise to SCID-repopulating cells. *Blood* **101**, 869-876 (2003).

Chapter 3

Ex vivo Culture and Characterization of SACK Effects on CD34^{+} Mobilized Peripheral Blood Cells in Growth Factor Starved Conditions (Phase II)

Rationale

Hematopoietic growth factors and cytokines (i.e., GF cocktail) promote extensive proliferation of committed hematopoietic progenitor cells (HPCs). As a result, although it was possible to detect SACK-dependent effects on cell number and CD133 frequency, the greater variance in the responses of HPCs made it difficult to evaluate the potential SACK-effects on HSCs. There are two major reasons for this. First, the markers CD133 and CD34 are not uniquely expressed on HSCs. From Phase I experiments (Chapter 2), there was evidence that suggests that CD133 was a relatively more specific HSC-associated marker than CD34. The observation that CD133 might be a more specific HSC-associated marker than CD34 has been also suggested in literature[1-6]. Second, as a result of the low specificity of *in vitro* markers for HSCs, low sensitivity for detecting HSCs was observed. In order to increase the *in vitro* sensitivity for detecting HSCs, the effect of growth factor starvation on HPC proliferation was evaluated. Previous studies in this laboratory indicated that some types of ASCs were relatively insensitive to removal of growth factors required by committed progenitor cells for proliferation. Specifically, rat hepatocyte and cholangiocyte adult stem cells derived by the SACK method were able to grow in a reduced growth factor environment[7]. The reason for their reduced dependency on growth factors was unclear, but it provided a strategy for selective repression of HPC proliferation. Additionally, it has been proposed that hematopoietic progenitor cells *in vivo* may negatively regulate HSC growth and expansion. Therefore, the presence of HPCs in a heterogeneous cell population such as CD34^{+} MPBs may prohibit HSC expansion *ex vivo* [8]. Consequently, culture of CD34^{+} MPBs in GF starved conditions was evaluated as a means to increase sensitivity for detecting SACK-dependent effects on CD133^{+} HSCs and simultaneously allowing for greater potential SACK-dependent HSC expansion as a result of reducing repressive effects of proliferating HPCs.

Materials & Methods

Experimental Method

CD34$^+$ MPBs were thawed and treated as previously described (Material & Methods, Chapter 2). CD34$^+$ cells were counted using a hemacytometer and the percentage of viable cells was determined using trypan blue dye exclusion. CD34$^+$ MPB cells were suspended in batch at a concentration of 10^5 CD34$^+$ MPBs per milliliter HPGM. The cells were then split into various conditions for controls and SACK-agents, Hx and XHX, both at a 1mM concentration. SACK agents were dissolved in 125mM sodium hydroxide at a stock concentration of 20mM. Control medium received the same volume of 125mM sodium hydroxide used for each respective SACK condition. CD34$^+$ MPB cells were then seeded at a density of 10^5 cells per ml per well of a 24 well plate. Two wells were pooled for each analysis and each condition was evaluated with at least two replicates. For flow cytometry analysis, at least 10,000 CD34$^+$ MPB cells were stained and analyzed for selected markers, as described previously (Material & Methods, Chapter 2). Cells were cultured at 37° C in a 5% CO_2 humidified incubator for 5 days unless noted otherwise. At the end of the culture period, cells were harvested by repeatedly pipeting contents of each well. For each well, viable cell number and percent viability was determined using hemacytometer counting with trypan blue exclusion dye. In addition, cells were stained and analyzed for CD34 and CD133, using flow cytometry. An isotype control antibody was used as a negative control for each marker antibody analyzed (Figure 3.1).

Propidium Iodide Exclusion Assay

Cultured cells were harvested and stained with 5µg/ml (final concentration) propidium iodide for 30 minutes at 37°C. Cells were immediately put on ice and analyzed for PI fluorescence using a FACSCalibur™ flow cytometer (Becton, Dickinson and Company, BD, Mountain View, CA). Data were analyzed using FlowJo software (Tree Star, Inc., San Carlos, CA).

Results

In order to verify that cultured cells can be technically distinguished based on cell viability, initial flow cytometry analyses were performed staining cells with propidium iodide (PI), a fluorescent stain for nucleic acids. Cell membrane integrity excludes PI from staining viable cells; therefore, viable cells exhibit no PI fluorescence. Figure 3.2 exhibits representative flow cytometry analyses of cultured cells stained with PI. Indeed, PI staining discriminated between live and dead cells. Cells cultured without growth factors (GF) for 5 days exhibit a distinct population in the flow scatter profile (total cells and R1; Figure 3.2A). When the total cell population (no gate) was analyzed for PI fluorescence, cells positive and negative for PI were observed (Figure 3.2B). However, when cells only in R1 were analyzed for PI fluorescence, it was evident that R1 gated cells in the flow scatter profile represented the viable cell population since they were negative for PI fluorescence (Figure 3.2C). In addition, a correlation for percent viability as determined from flow cytometry analyses and trypan blue exclusion exhibits strong association ($r^2 = 0.95$; Figure 3.2D). These results together suggest that viable and non-viable cells can be distinguished with precision.

CD34$^+$ MPB cells cultured without growth factors (GF) for 5 days exhibited an enrichment of CD133$^+$ cells (Figure 3.3). Uncultured CD34$^+$ MPB cells (Figure 3.3A), exhibited two distinct CD133$^+$ cell populations. After 5 days of culture, the highest expressing CD133$^+$ cells had either become CD133$^-$ or decreased their expression of CD133$^+$ (Figure 3.3B-D). When compared to GF cocktail supplemented cultures (Chapter 2, Figure 2.3), where the fraction of CD133$^+$ cells represented ~10%-20% of day 5 culture, with GF starved conditions, CD133$^+$ cells comprised ~40%-70% of the culture, depending on SACK-culture (Figure 3.3B-D).

CD34$^+$ MPB cells cultured without GFs exhibited an overall reduction in viable cell number after 5 days of culture (Figure 3.4A), as predicted. The number of viable cells found after 5 days of culture was significantly less than that of the starting population of 10^5 CD34$^+$ MPB cells. The viable cell number ranged from 35,000 to 60,000 cells, depending on the SACK culture (Figure 3.4A).

On the other hand, CD34$^+$ MPB cells cultured with GF cocktail supplementation conditions resulted in an overall 10- to 15-fold increase in viable cells after 5 days of

culture (compare Figure 3.4A to 3.4B at 5 days). Moreover, Hx- and XHX-dependent cultures exhibited a higher frequency of cells that expressed CD133. Approximately 40% of control cells expressed CD133, whereas approximately 65% of both Hx- and XHX-supplemented cells expressed CD133 (Figure 3.4C). When compared to the same SACK conditions supplemented with GF cocktail, the frequency of cells expressing CD133 declined from 85% to 10%-20% depending on the SACK-supplementation (Figure 3.4D). However, enrichment of CD133$^+$ cells due to selective loss of HPCs could be ruled out as an explanation for the increased CD133$^+$ expressing cells in GF starved conditions, since an overall net production of total cells was observed (Figure 3.4E).

A summary of the results obtained by culturing CD34$^+$ MPB cells in a growth factor starved condition revealed that Hx and XHX promoted 1.9-fold (p<0.0001) and 2.1-fold (p=0.0054) respective increase in percent viability, compared to the control SACK-free conditions (Figure 3.5A). This effect translated into a 1.6-fold (p<0.0001) and 1.7-fold (p=0.0058) increase in viable cells in Hx- and XHX-supplemented conditions, respectively, compared to SACK-free conditions (Figure 3.5B). Moreover, Hx- and XHX-cultured cells exhibited a 1.4-fold (p<0.0001) and 1.6-fold (p=0.0001) increase in the frequency of cells that express CD133, respectively, compared to control cultures (Figure 3.5C). Finally, for the first time, the culture of CD34$^+$ MPB cells in Hx- and XHX-supplemented cultures resulted in a 2.3- (p<0.0001) and 2.8-fold (p=0.0044) increase in the number of CD133$^+$ cells as compared to control SACK-free conditions (Figure 3.5D).

In an attempt to enhance the Hx- and XHX-dependent effects on CD133$^+$ cell production, CD34$^+$ MPB cells were cultured for longer time periods, specifically 8 and 14 days. Culturing CD34$^+$ MPB cells for 8 days in Hx- and XHX-supplemented medium resulted in 3.4-fold (p=0.006) and 6.4-fold (p=0.0269) increase in the number of Hx- and XHX-dependent CD133$^+$ cells, respectively, compared to control unsupplemented cultures (Figure 3.6A). Although cells cultured for 8 days exhibited greater fold CD133$^+$ cells, day 8 cultures didn't result in more CD133$^+$ cells than day 5 cultures (Figure 3.6B). A potential reason for less CD133$^+$ cells at day 8 compared to day 5 could be lack of viability in cultures. In fact, CD34$^+$ MPB cells cultured for more than 8 days resulted in low viability and low cell numbers (data not shown).

Discussion

In order to increase sensitivity for detecting SACK-dependent effects on the production CD133$^+$ cells, CD34$^+$ MPB cells were cultured in GF starved conditions for 5, 8, and 14 days. This approach may promote selective expansion of HSCs if they, like other reported ASCs, have a low GF requirement for SACK-induced proliferation[7]. In addition, the suppression of HPC growth caused by their GF-dependency may reduce HPC produced factors that repress HSC division. Cells cultured for 14 days in GF starved conditions exhibited prohibitive viability (data not shown). However, CD34$^+$ MPB cells cultured for 5 and 8 days exhibited specific SACK-dependent effects. After 5 days of culture, both Hx and XHX promoted increased cell viability relative to control conditions (Figure 3.5A), translating into a significant increase in viable cells produced with Hx- and XHX-supplementation (Figure 3.5B). These observations suggested that a subset of CD34$^+$ MPB cells that are SACK-responsive may be resistant to growth factor starvation. In an environment where the growth and survival of GF-dependent cells are prevented, Hx and XHX may promote the symmetric expansion of cells that are relatively insensitive to GF starvation. In addition, consistent with these observations is the possibility that Hx and XHX could be promoting survival of CD133$^+$ cells as well.

This result seems unlikely to be due to simple enrichment of SACK-dependent, GF-insensitive cells. This is not a plausible explanation since overall production of total cells (viable and non-viable cells) was observed (Figure 3.3E). Moreover, in GF starved conditions, in general, a greater fraction of viable cells are CD133$^+$ (compare Figure 3.3D to 3.3C). Specifically, 40%-65% of viable cells cultured in GF starved conditions expressed CD133 (Figure 3.3C), whereas only 10%-20% of viable cells cultured in GF cocktail supplemented conditions expressed CD133 (Figure 3.3D). In addition, cells cultured in Hx- and XHX- cultures exhibited a 1.4-fold (p<0.0001) and 1.6-fold (p=0.0001) respective increase in the fraction of viable cells that express CD133 (Figure 3.5D). This observation suggested that the population of viable cells that are resistant to growth factor starvation include CD133$^+$ cells and the frequency of these cells was increased in Hx- and XHX-supplemented conditions. The Hx- and XHX-dependent increase in the frequency of CD133$^+$ cells is consistent with the proposal that HSCs may be enriched under GF starved conditions and with Hx- and XHX- supplementation, this

CD133$^+$ population has increased (Figure 3.5C). The amplification translated into a 2.3-fold (p<0.0001) and 2.8-fold (p=0.0044) increase in the production of Hx- and XHX-responsive CD133$^+$ cells, respectively (Figure 3.5D). These results together suggest, for the first time, that Hx and XHX promoted *ex vivo* symmetric expansion of CD133$^+$ cells.

In order to increase the yield of SACK-dependent CD133$^+$ cells produced after 5 days, CD34$^+$ MPBs cells were cultured in GF starved conditions for 8 days. Indeed, a longer culture duration corresponded to a 3.4-fold (p=0.006) and 6.4-fold (p=0.0269) increase in the absolute number of Hx- and XHX-dependent CD133$^+$ cells, respectively, compared to control conditions (Figure 3.6A). The fold effects observed for the number of CD133$^+$ cells for 8 days is not statistically different from day 5 cultured cells (data not shown). In addition, a net decrease in the number of CD133$^+$ cells is detected when compared to day 5 cultures (Figure 3.6B). There could be several reasons for this observation. First, CD133$^+$ committed HPCs may remain in day 5 cultures yielding increased detection of CD133$^+$ cells. However, this is not plausible since survival of committed HPCs is repressed significantly between 48 and 120 hours (see Chapter 4, Figure 4.2). Therefore, it would be unlikely that HPCs could survive for more than 5 days. A second basis for this observation is loss of cell survival factors leading to cell loss. In fact, attempts to increase SACK-dependent CD133$^+$ cells by culturing for 14 days led to an excessive loss of viability. This suggests that although the SACK-dependent CD133$^+$ cells may be GF resistant, they may still depend on one or more of the cocktail GFs for their survival.

Conclusion

Culturing CD34$^+$ MPB cells for 5 and 8 days in GF starved conditions represses the proliferation of cells that are highly dependent on growth factors for their survival and proliferation. These cells are most likely committed hematopoietic progenitor cells since they are known to be highly mitogenic. A large fraction of the cells that remain after 5 and 8 days of culture in GF starved conditions express CD133$^+$ and expand in response to Hx- and XHX-supplementation. These observations indeed confirmed that suppressing proliferation of HPCs yields greater sensitivity for detecting SACK-dependent effects on CD133 cell expression. Additionally, expansion in Hx- and XHX-dependent CD133$^+$ cell may have been intensified due to negative inhibition of CD133$^+$ HSCs by HPCs. However, it is difficult to conclude this without more specific investigations. Yet, it is clearly evident that Hx- and XHX-dependent CD133$^+$ cells are missing critical survival factors for optimal growth and survival since the number of viable CD133$^+$ cells detected decreased after 8 days culture (compared to 5 days culture) and culture of these cells beyond 8 days was not observed.
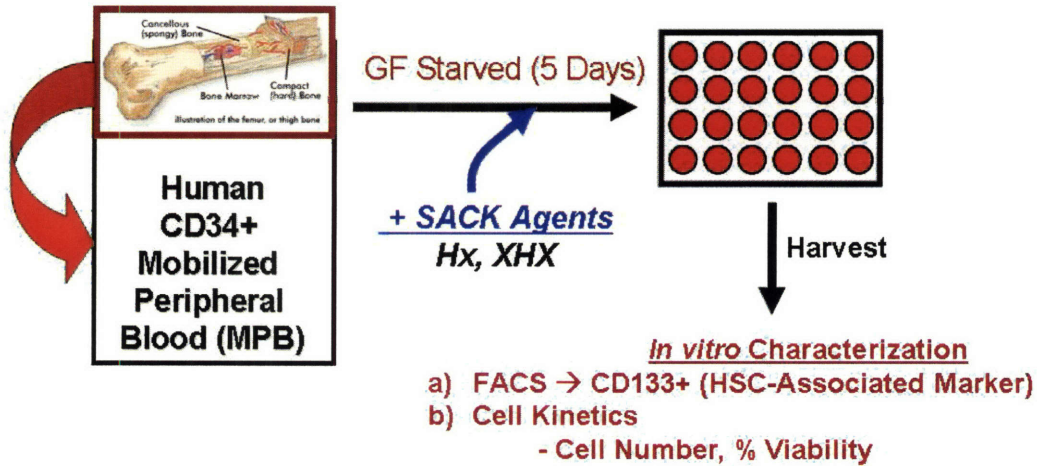
Figure 3.1 | Experimental Design of Phase II Growth Factor (GF) Starved Studies. CD34$^+$ mobilized peripheral blood (MPB) cells were cultured for 5 days in serum-free HPGM (Hematopoietic Progenitor Growth Medium). CD34$^+$ MPB cells were supplemented with hypoxanthine (Hx), xanthine (Xn), xanthosine (Xs) and an equal mixture of Xn, Hx, Xs (XHX). Cells were cultured for 5 days, or noted otherwise, harvested and quantified for CD133$^+$ cell fraction and cell kinetics.
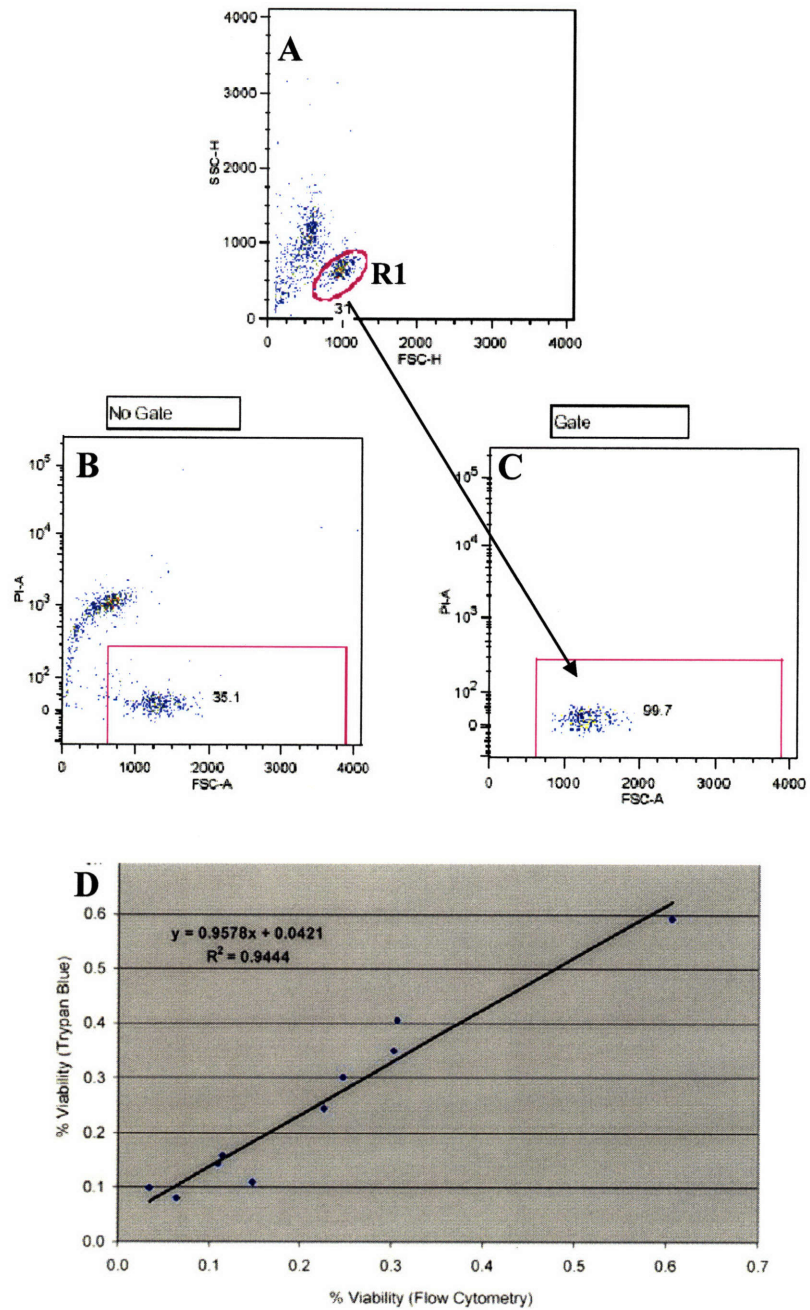
Figure 3.2 | Use of Propidium Iodide (PI) Exclusion to Confirm Live Cell Detection by Bivariate Scatter Profile. CD34^{+} MPB cells were cultured for 5 days. A) A side vs. forward scatter profile of Hx-cultured cells represents cells with varying scatter profiles. B) Total population profiles exhibit cells that are positive and negative for PI. C) R1 gated cells represent cell that are negative for PI. D) A regression correlation is exhibited for the percent viability of cultured CD34^{+} MPB cells (day 5) evaluated with trypan blue exclusion and flow cytometry.
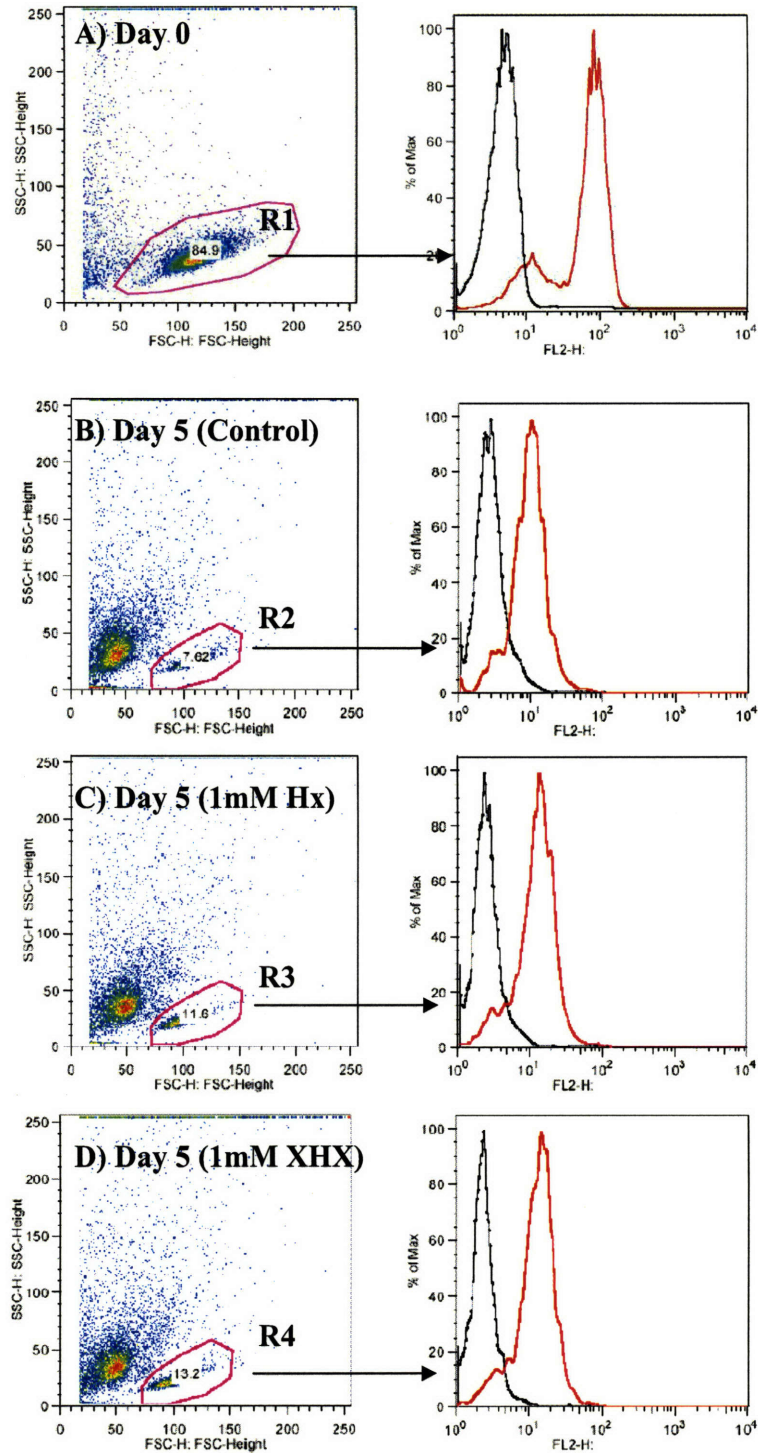
Figure 3.3 | Representative FACS Profiles of Uncultured (Day 0) and Cultured (Day 5) CD34$^+$ Mobilized Peripheral Blood (MPB) Cells in Growth Factor (GF) Starved Conditions. FACS profiles exhibiting expression patterns of IgG1-PE (black; isotype control) and CD133-PE (red) gated from the live, lymphocyte-sized fraction A) R1, for uncultured, day 0 cells, B) R2, day 5 cultured SACK-free controls, c) R3, day 5 Hx (1mM) cultured cells, and D) R4, day 5 XHX (1mM) culture cells. Scatter profiles represent side (SSC) vs. forward (FSC) scatter. Histograms represent the fluorescent profiles for various PE-conjugated antibodies.
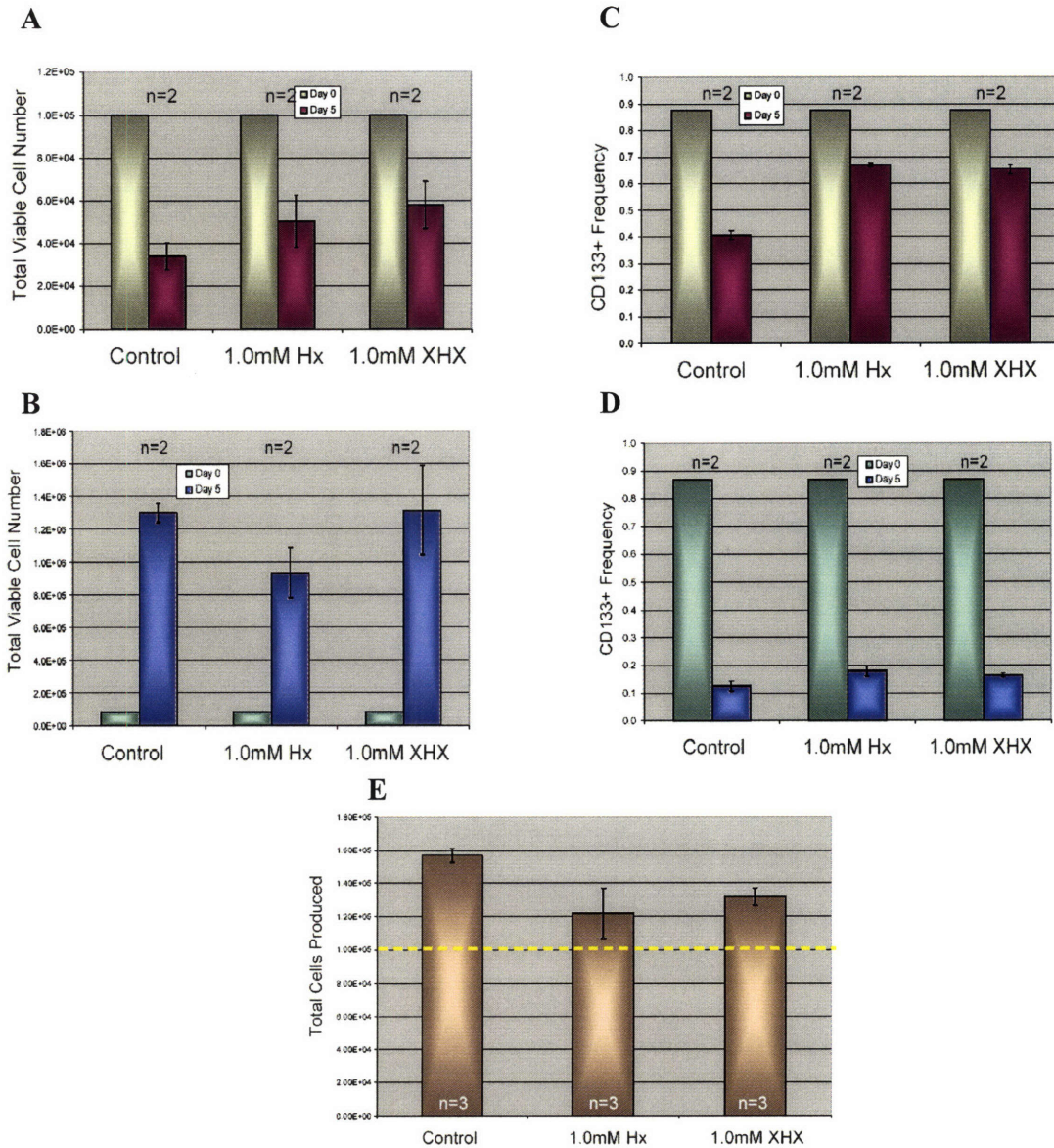
Figure 3.4 | Cell Kinetic & CD133 Effects of GF Starvation on CD34+ Mobilized Peripheral Blood (MPB) Cells, as compared to GF Cocktail Supplemented Studies. Viable cell number for Hx, XHX and SACK-free controls were determined after 5 days culture in A) GF starved and B) GF cocktail supplemented conditions. The respective fraction CD133 expression for Hx, XHX, and controls were determined after 5 days culture in C) GF starved and D) GF cocktail supplemented conditions. E) Total cell production was determined for GF starved cultured in control, Hx and XHX conditions. Error bars = standard deviation for n individual assays. n = number individual assays, in general, performed in replicates of 2. Dashed (yellow) line represents the normalized control.
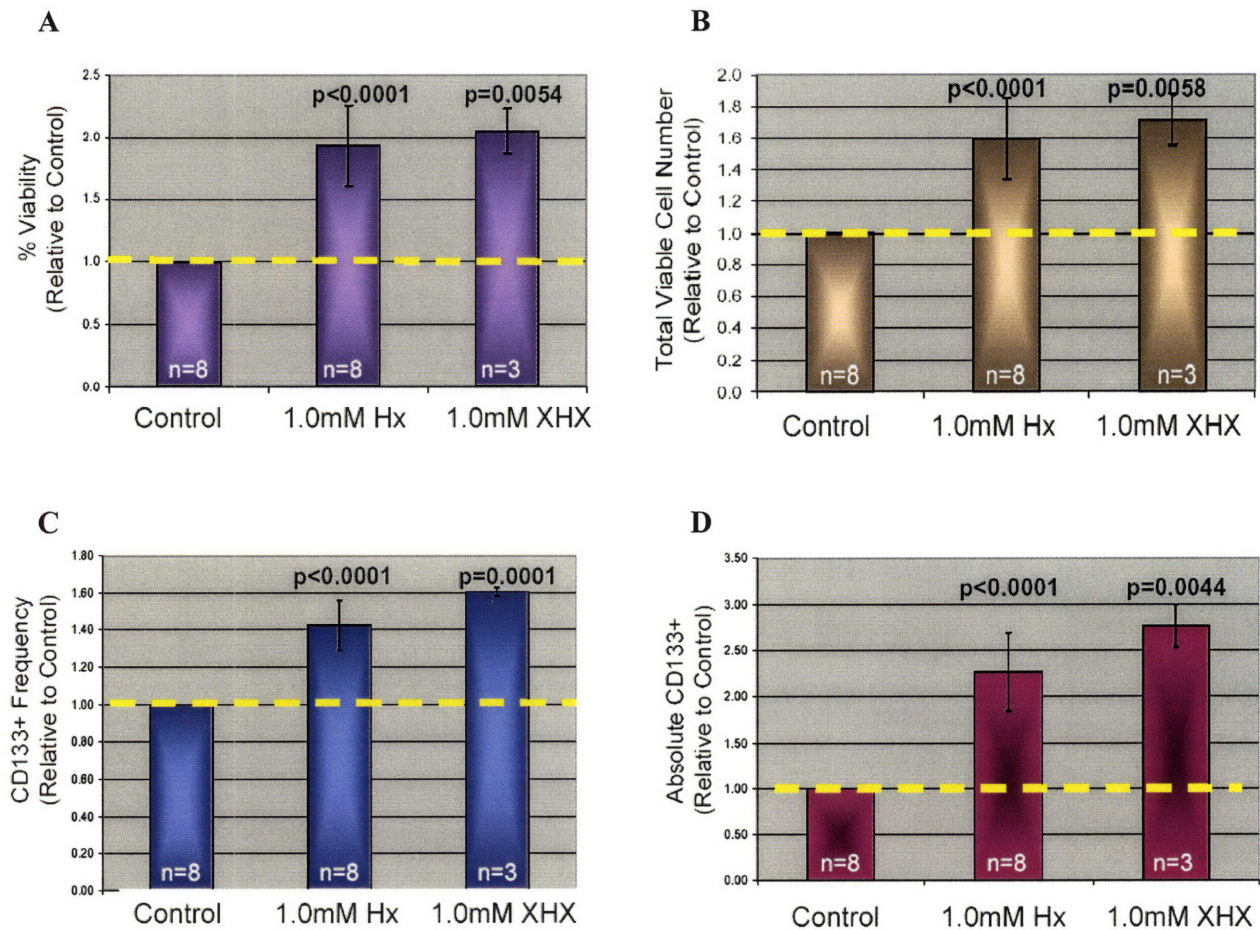
Figure 3.5 | Hx- and XHX-Dependent Effects on CD34$^+$ Mobilized Peripheral Blood (MPB) Cells Cultured for 5 Days in GF Starved Conditions. CD34$^+$ MPB cells were cultured with Hx- and XHX-supplementation with controls and investigated for SACK-dependent effects relative to control. A) Percent viability B) viable cell number C) CD133$^+$ cell fraction D) Absolute CD133$^+$ cell number. Derivations of p-values are determined from Student t-test for one group. Error bars = standard deviation for n individual assays. n = number individual assays, in general, performed in replicates of 2. Dashed (yellow) line represents the normalized control.

A

B
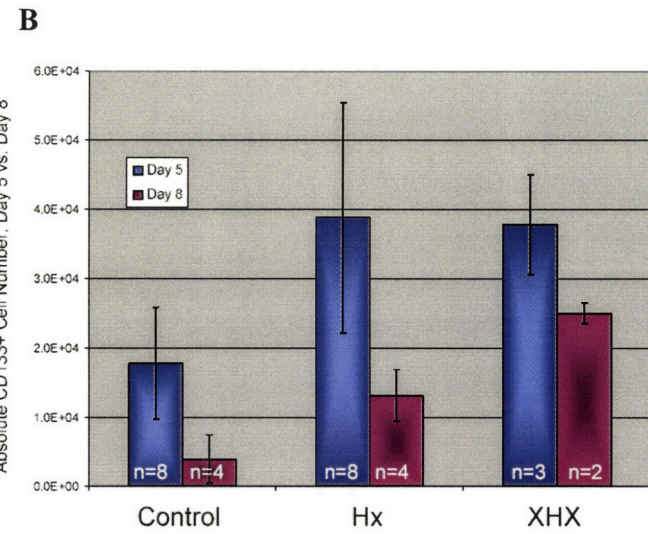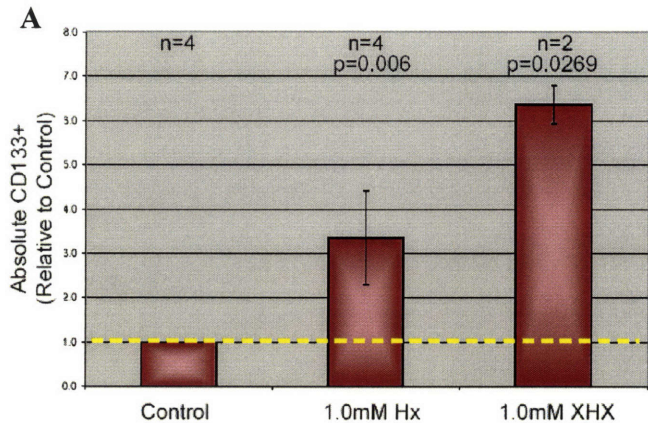
Figure 3.6 | Hx- and XHX-Dependent Effects on CD34$^+$ Mobilized Peripheral Blood (MPB) Cells Cultured for 8 Days in GF Starved Conditions. A) CD34$^+$ MPB cells were cultured without (control) or with Hx- or XHX-supplementation for 8 days and investigated for SACK-dependent effects relative to control for absolute CD133$^+$ cell number. B) Absolute CD133$^+$ cells from Day 5- and 8-cultures without (control) or with Hx- or XHX-supplementation in GF starved conditions. Derivations of p-value are determined from (One-Group) Student t-test. Error bars = standard deviation for n individual assays. n = number individual assays, in general, performed in replicates of 2. Dashed (yellow) line represents the normalized control.

Bibliographical References

1. Bhatia, M. AC133 expression in human stem cells (Review). *Leukemia* **15**, 1685-1688 (2001).

2. Bitan et al. Successful transplantation of haploidentically mismatched peripheral blood stem cells using $CD133^+$-purified stem cells. *Experimental Hematology* **33**, 713-718 (2005).

3. Leor, J. et al. Human Umbilical Cord Blood-Derived $CD133^+$ Cells Enhance Function and Repair of the Infarcted Myocardium. *Stem Cells* **24**, 772-780 (2006).

4. Gallacher, L. et al. Isolation and characterization of human $CD34^-Lin^-$ and $CD34^+Lin^-$ hematopoietic stem cells using cell surface markers AC133 and CD7. *Blood* **95**, 2813-2820 (2000).

5. Wagner, W. et al. Molecular evidence for stem cell function of the slow-dividing fraction among human hematopoietic progenitor cells by genome-wide analysis. *Blood* **104**, 675-686 (2004).

6. Kuci, S. et al. Identification of a novel class of human adherent $CD34^-$ stem cells that give rise to SCID-repopulating cells. *Blood* **101**, 869-876 (2003).

7. Crane, G., Taghizadeh, R. R. & Sherley, J. L. Adult Rat Hepatic Stem Cells Exhibit Asymmetric Adifferentiation In Vitro. *Submitted* (2006).

8. Madlambayan, G. J. et al. Dynamic changes in cellular and microenvironmental composition can be controlled to elicit in vitro human hematopoietic stem cell expansion. *Experimental Hematology* **33**, 1229-1239 (2005).

Chapter 4

Ex Vivo Culture and Characterization of SACK Effects on CD34$^+$ Mobilized Peripheral Blood Cells After Growth Factor Starvation & HSC Survival Factor Addition (Phase III)

Rationale

Specific survival factors were investigated in order to promote survival of SACK-dependent CD133$^+$ cells, without promoting growth and survival of committed hematopoietic progenitor cells (HPCs). It was determined from Phase II studies (Chapter 3) that GF starved conditions yielded net Hx- or XHX-dependent CD133$^+$ cell production relative to SACK-free control conditions after 5 and 8 days of culture. However, culture beyond 8 days resulted in prohibitive cell death. In order to overcome this limitation, attempts were made to balance inhibition of HPC growth by GF starvation with promotion of survival of SACK-dependent CD133$^+$ cells with specific survival factors (SFs).

Materials & Methods

Experimental Method

Figure 4.1 diagrams the experimental approach for survival recovery analyses. CD34$^+$ MPBs were thawed and treated as previously described (Material & Methods, Chapter 2). CD34$^+$ cells were cultured for varying time periods without GFs (GF starvation) and then specific survival and growth factors were added to the culture for the remaining culture time. For flow cytometry analysis, at least 10,000 CD34$^+$ MPB cells were stained and analyzed for various markers, as described previously (Chapter 2, Materials & Methods).

Wnt & Notch Delta-like ligand 4 (DLL4)

Recombinant mouse Wnt-3a (R&D Systems, Minneapolis, MN) was dissolved in a 1% solution of bovine serum albumin in phosphate buffered saline (1% BSA/PBS) and added directly to cell cultures to a concentration of 25ng/ml. Recombinant human Notch DLL4 was provided by Dr. Max Wicha (University of Michigan School of Medicine, Ann

Harbor, MI) dissolved in a 1% solution of human serum albumin in PBS (1% HSA/PBS). DLL4 was added directly to cell cultures at a concentration of 1μM. Each recombinant protein was aliquoted and stored at -80°C for not more than 6 months.

Cell Cycle Analysis

Cell cycle analysis was performed on both uncultured and cultured CD34^{+} MPB cells, in order to quantify the fraction of cells dividing in cultures. Cultured cells were sorted for viable cells based on scatter using a FACSAria™ flow cytometer (Becton, Dickinson and Company, Mountain View, CA). After cell sorting, viability was determined using a trypan blue and hemacytometer (See Chapter 2 Materials & Methods). Viable cells were re-suspended in approximately 500μl of ice-cold PBS and mixed. Then cold (-20° C) ethanol was added, drop by drop, while vortexing to prevent clumping and were fixed overnight at 4°C. The next day, fixed cells were centrifuged to remove the ethanol. After removal of ethanol, the cell pellets was washed with FACS Buffer and re-centrifuged. After centrifugation and re-suspension in 200μl of FACS Buffer, propidium iodide (PI) and RNase A was added to a final concentration of 50μg/ml. The cells were incubated at 37°C for 30 minutes. Samples were protected from light and stored at 4°C until flow cytometry analysis.

<u>Results</u>

In order to investigate the length of time to culture CD34^{+} MPB cells without GFs before survival factor addition, CD34^{+} MPB cells were cultured without GFs for different periods of time. On days 0, 1, 3, and 5, cell samples from SACK-supplemented and control cultures were collected to determine percent viability and viable cell number (Figure 4.2). After one day of culture, the percent viability dropped from 95% to 40%-70% (Figure 4.2A), but corresponded to modest effects on viable cell number, with the exception of HX-supplemented cultures (Figure 4.2B). However, by day 3, the percent of viable cells dropped to 10%-30%, corresponding to a 50%-80% reduction in viable cells. It is noteworthy that Hx- and XHX-supplemented cultures exhibited better survival in most cases, being greatest after one day of GF starvation (Figure 4.2B). In order to maximize the loss of SACK-independent cells while preserving SACK-dependent cells, a

time point between 24-72 hours was chosen. Specifically, 44 hours was designated for future analyses to allow sufficient time for repression of HPC number before subsequent enhancement of SACK-dependent cell survival with the addition of specific survival factors (Figure 4.2).

In order to determine which, if any, of the main components of the GF cocktail promoted SACK-dependent CD133$^+$ cell survival, CD34$^+$ MPB cells were cultured for 44 hours without GFs, followed by addition of TPO, SCF, or Flt3 ligand alone and as the complete GF cocktail (Figure 4.3). These all enhanced Hx-dependent viability and viable cell number (Figure 4.3A, B). However, only TPO and Flt3 ligand did so without also promoting growth in SACK-free control conditions (Figure 4.3B, compare to control data). TPO and Flt3 ligand alone promoted a significant Hx-dependent increase in the frequency of CD133$^+$ cells (Figure 4.3C). The GF cocktail supplemented cells exhibited the least fold (1.3-fold) increase in the frequency of Hx-dependent CD133$^+$ cells (Figure 4.3C), at a similar magnitude as that of GF starved controls (1.3-fold; Figure 4.3C). TPO and Flt3 ligand gave rise to the greatest fold increase in Hx-dependent CD133$^+$ cell frequency (1.9; p=0.01 and 2.5; p=0.02, respectively), as compared to the control GF starved conditions (1.3; Figure 4.3C). These effects translated into an overall enhancement in the production of Hx-dependent CD133$^+$ cells. However, only TPO and Flt3 ligand enhanced Hx-dependent CD133$^+$ cell production without promoting CD133$^+$ cell production in SACK-free controls supplemented with each respective survival factor (Figure 4.3D). TPO and Flt3 ligand promoted 3.8-fold (p=0.29) and 5.5-fold (p=0.04) increase in Hx-dependent CD133$^+$ cells (Figure 4.3D), respectively. However, only Flt3 ligand promoted Hx-dependent CD133$^+$ cells production at a statistically significant level (p=0.04; Figure 4.3D).

Despite the level of statistical significance obtained for Hx-dependent CD133$^+$ cell production, after 44 hours of GF starvation with subsequent Flt3 ligand addition for the remaining 5 days culture time in initial studies (Figure 4.3), variability in these experiments was problematic. Specific factors were investigated to determine the source of the observed variability. One factor considered was Flt3 ligand might be rapidly utilized and depleted from culture medium by cells. However, studies replenishing Flt3 ligand at 24 hour intervals after initial 44 hour GF starvation exhibited no effect on Hx-

dependent CD133$^+$ cell production (data not shown). The opposite effect might have also been true. The Flt3 ligand concentration used might have been at too high a concentration. This was proposed since at saturating levels, Flt3 ligand might act as a mitogen, rather than a survival factor. However, decreasing the Flt3 ligand concentration from 50ng/ml to 12.5ng/ml did not improve Hx-dependent CD133$^+$ cell production (data not shown). Technical factors such as the stability of cryopreserved human hematopoietic stem cell enriched populations and changes in temperature during shipping that might alter the post-thaw Hx-dependence of CD34$^+$ MPB cells were evaluated. CD34$^+$ MPB cells from the same donor, but shipped at various times were compared and found to have no significant effect on Hx-dependent CD133$^+$ cell production. Another possible factor was that the optimal SACK-agent concentration might change under conditions of survival factor recovery. Therefore, a titration was performed for Hx from 0mM – 2mM. Varying the concentration of Hx did not yield improved Hx-dependent CD133$^+$ cell production with Flt3 ligand addition at 44 hours. Because the Flt3 ligand carrier solution contained human serum albumin (HSA), it was evaluated for independent SACK effects. Human serum albumin might have had bound purine nucleotides. An investigation found that HSA alone did not promote increased numbers of CD133$^+$ cells and it was not the source of the observed variability (data not shown). The serum-free conditioned based medium, HPGM, was also investigated as the source of variable SACK-dependent CD133$^+$ cell production. Another conditioned medium, Stemline II (Sigma, St. Louis, MO), was used instead of HPGM. Likewise, Stemline II medium did not enhance detection of SACK-dependent CD133$^+$ cells (data not shown).

When Flt3 ligand was added to cultures at 24 hour intervals, varying the time of GF starvation and Flt3 ligand survival effects, a source of variability was noted (Figure 4.4A). In these experiments, only XHX-supplemented conditions were evaluated. In each of two independent experiments, XHX induced an increase in CD133$^+$ cells for all intervals of Flt3 ligand addition, including no Flt3 ligand addition for the entire 5 day period (Figure 4.4). Consistent with earlier GF starvation studies, longer periods of GF starvation resulted in progressive reduction in the number of CD133$^+$ cells in both control and XHX-supplemented cultures. In one experiment, the optimal XHX effect occurred when Flt3 ligand was added after 72 hours of GF starvation (Figure 4.4B, D). In an

independent second experiment, it occurred at 48 hours (Figure 4.4C, E). These two experiments exemplified the experiment-to-experiment variability previously observed and indicated that one important source was the length of GF starvation before addition of SFs.

In order to reduce this variability, other survival factors were investigated. In particular, Notch Delta-like ligand (DLL4) was investigated as a putative survival factor to enhance SACK-dependent CD133$^+$ cell survival with fewer effects on HPCs. When Notch DLL4 was added to CD34$^+$ MPB cells at day 0 of GF starvation (Figure 4.5A), CD34$^+$ MPB cells cultured for 5 days exhibited comparable percent viability and viable cell number to GF starved conditions (Figure 4.5B, C). Moreover, the frequency of cells that express CD133$^+$ exhibited a significant XHX-dependent effect (Figure 4.5D), which translated into a significant XHX-dependent absolute number of CD133$^+$ cells (Figure 4.5E). Although Flt3 ligand maintained greater viability and survival when added to CD34$^+$ cell at day 0 compared to Notch DLL4 (data not shown), there was a greater XHX-dependent effect on the fraction and absolute number of CD133$^+$ cells (Figure 4.5 C, D; DLL4 compared to Flt3 ligand at 0 hours of GF starvation).

Discussion

In order to increase survival of SACK-induced CD133$^+$ cells and at the same time suppress the growth of HPCs, CD34$^+$ MPB cells were cultured without GFs for 44 hours, with subsequent addition of specific factors known to promote survival and proliferation of CD34$^+$ cells (Figure 4.1). After 72 hours of GF starvation, there was a significant loss in viable cells suggesting that a majority of HPCs that were heavily dependent on GFs for their survival and proliferation were inhibited (Figure 4.2). A 44 hour GF starvation period was chosen in order to minimize irreversible effects on SACK-expanded CD133$^+$ cells, proposed to include HSCs. With subsequent addition of TPO, SCF, and Flt3 ligand or the GF cocktail, only Flt3 ligand and TPO specifically promoted survival of Hx-dependent CD133$^+$ cells (Figure 4.3B). Moreover, the majority of the viable Hx-dependent cells cultured in TPO and Flt3 ligand were CD133$^+$ (Figure 4.3C). On the other hand, cells cultured with GF cocktail supplementation showed a 60%-80% reduction in CD133$^+$ cells, likely due to dilution of CD133$^+$ cells by the production of

CD133⁻ hematopoietic cells. However, although TPO, SCF, Flt3 ligand alone and the GF cocktail gave rise to enhanced Hx-dependent CD133$^+$ cells, only TPO and Flt3 ligand did so without promoting SACK-free CD133$^+$ cell production (Figure 4.3D). Flt3 ligand gave rise to the higher degree of Hx-dependent CD133$^+$ cell production at a statistically significant level (p=0.04). These findings suggest that Flt3 ligand acts as a survival factor for Hx-dependent CD133$^+$ cells.

Flt 3 ligand is a type III tyrosine kinase receptor expressed mainly by primitive hematopoietic cells[1-3]. Flt3 ligand has little direct effect on committed progenitor cell proliferation, but in a combination with other cytokine and growth factors it synergizes to enhance proliferation of CD34$^+$ cell populations[4,5]. These observations are consistent with the hypothesis that Flt3 ligand acts as a HSC survival factor. On the other hand, GF cocktail promotes proliferation and differentiation of CD34$^+$ hematopoietic cells. These data raise the possibility that SACK-free control cultured cells with GF cocktail supplementation may promote asymmetric self-renewal of HSCs, thereby producing HPCs that are dilute CD133$^+$ cells and HSCs.

Although GF starvation for 44 hours, and subsequent Flt3 ligand addition, resulted in significant SACK-dependent CD133$^+$ cell production (Figure 4.3), this procedure proved to yield highly variable results. A number of factors were investigated, including Flt3 ligand depletion by CD34$^+$ MPB cells and, conversely, excessive Flt3 ligand; donor cell variability; non-optimal Hx concentration; potential SACK effects by human serum albumin; and non-optimal base medium. None of these factors were found to significantly impact the variability in SACK-dependent CD133$^+$ cells. The time of GF starvation and Flt3 ligand addition was identified as an important source of variability in SACK-dependent CD133$^+$ cell production (Figure 4.4). In two independent experiments where GF starvation and Flt3 ligand addition time were varied (Figure 4.4A), two different times of optimal SACK-dependent CD133$^+$ cell production were observed (Figure 4.4 B vs. C, D vs. E). Therefore, it appears that GF-starved CD34$^+$ MPB cells differ in SACK response, depending on when a SF is restored. If not enough time is allotted for HPC repression, then while the growth of the majority of HPCs may be contained, the addition of Flt3 ligand may promote the growth of the remaining viable HPCs. Flt3 ligand is not a specific survival factor for HSCs. Flt3 ligand knockout mice

show defects in primitive hematopoietic cells, as well as natural killer and dendritic cells[6,7]. As a result, if there are any viable HPCs, then they will be promoted to proliferate by Flt3 ligand, leading to a variable SACK response, if as postulated, these agents primarily affect the cell kinetics pattern of rare HSCs.

Since there is an overall reduction in viable cells with this culture method, the argument can be made that SACK-dependent culture simply maintains the survival (Figure 4.6A), but does not promote the proliferation of a sub-population of CD34$^+$ MPB cells that are SACK-induced. There are two lines of evidence that suggest that Hx or XHX promote proliferation of cultured CD34$^+$ MPB cells. First, cells cultured without GFs and rescued with Flt3 ligand exhibit an overall production of total cells (viable and non-viable; Figure 4.6B). This suggests that cell proliferation has taken place with this culture method. Second, cell cycle analysis on cultured viable cells shows an increase in cycling S-phase fraction. Culturing cells with this method increases the fraction of cycling cells when compared to uncultured cells (S=0.99%; Figure 4.6C). Specifically, cells cultured in Hx or XHX exhibit 4.7% and 5.6% of cells in S-phase of the cell cycle (Figure 4.6E, F). This corresponds to a 1.9-fold and 2.3-fold increase in cycling cells in Hx- and XHX-cultures, respectively, compared to cells cultured without Hx or XHX (Figure 4.6D). Taken together, these results suggest that CD34$^+$ MPB cells cultured without GFs and rescued with Flt3 ligand promotes proliferation of cells. In addition, SACK-induced culture increases the cycling fraction of cultured cells.

A more HSC-specific survival factor was needed that would, ideally, have two specific properties: it would not promote proliferation of contaminating HPCs while simultaneously promoting survival of HSCs. Wnt and Notch Delta-like ligand 4 were both investigated as putative HSC survival factors (see Chapter 1). Wnt did not exhibit any significant survival effects on SACK-dependent CD133$^+$ cells. When Notch DLL4 was added to cells from the start of GF starvation, it resulted in a 1.9-fold SACK-dependent increase in CD133$^+$ cell production after 5 days of culture (Figure 4.5F). This result was comparable to the highest SACK-dependent effects observed with addition of Flt3 ligand between 48-72 hours of GF starvation (Figure 4.5F). However, DLL4 supplementation, unlike Flt3 ligand, obviates the need for restoring SFs after a GF starvation period, because it has minimal effects on the production of SACK-free

CD133$^+$ cells. DLL4 yields reduced viable cells than Flt3 ligand (added at day 0; Figure 4.5B, C), indicating that DLL4 resulted in greater enrichment for SACK-dependent CD133$^+$ cells than Flt3 ligand. Therefore, DLL4 may be a more specific CD133$^+$ cell survival factor than Flt3 ligand. Although the viable cell numbers are remarkably low in DLL4 supplemented cultures, more of the viable cells are SACK-dependent, suggestive that DLL4 may be more specific to maintaining survival of HSCs, as previously suggested[8-11]. Flt3 ligand may act as a general hematopoietic cell survival factor, maintaining survival of HSCs, in addition to promoting survival of HPCs and other cells. In fact, Flt3 ligand has also been shown to maintain survival and promote proliferation of dendritic cells[6,7].

Conclusion

These *in vitro* studies identify a novel, previously undescribed type of human CD133$^+$ hematopoietic cell defined by its response to purine nucleoside precursors. A summary of their properties include that they:

1) are found in mobilized peripheral blood
2) initially express CD34$^+$, since they are CD34 selected
3) express CD133$^+$
4) have reduced requirements for growth factors, but are not indispensable
5) have increased survival and growth by Flt3 ligand and Delta-like ligand 4 (DLL4)
6) have increased survival and proliferation by SACK-agents.

The SACK-dependent CD133$^+$ cells derived with this method are proposed to represent asymmetrically self-renewing HSCs shifted to symmetric self-renewal with increased numbers and reduced production of committed HPC progeny.

Experimental Design – Phase III
Survival Factor Experiments
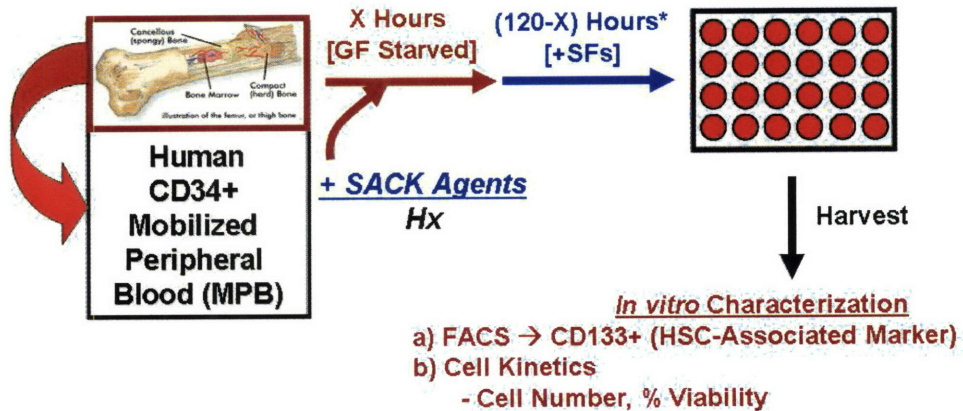
* HSC Survival Factors (SF) → TPO Only , SCF Only, Flt-3 Ligand Only, or GF Cocktail

Figure 4.1 | Experimental Design of Phase III Survival Factor Approach to SACK Expansion of Human HSCs. CD34^{+} mobilized peripheral blood (MPB) cells were cultured for varied time (X hours) in serum-free HPGM (Hematopoietic Progenitor Growth Medium) without GFs. Thereafter, specific factors were added to promote survival of SACK-dependent CD133^{+} cells. Cells were cultured for a total of 5 days, harvested and characterized for CD133^{+} expression and cell kinetics.

A

Total Viable Cells

B

% Viability
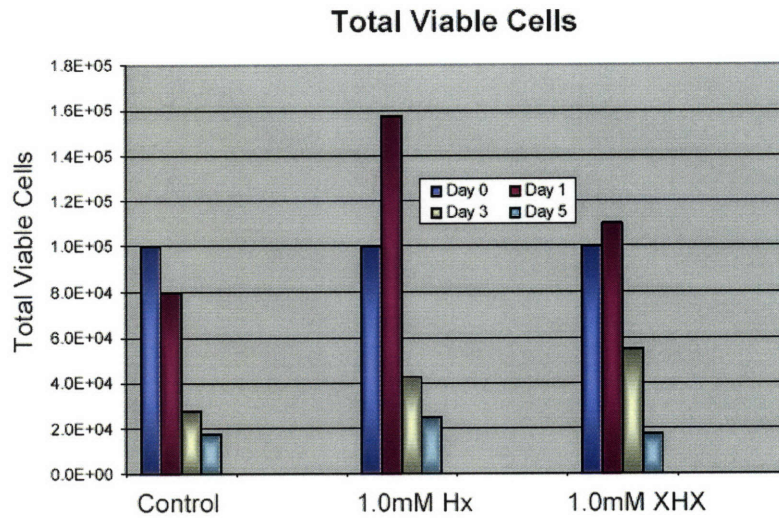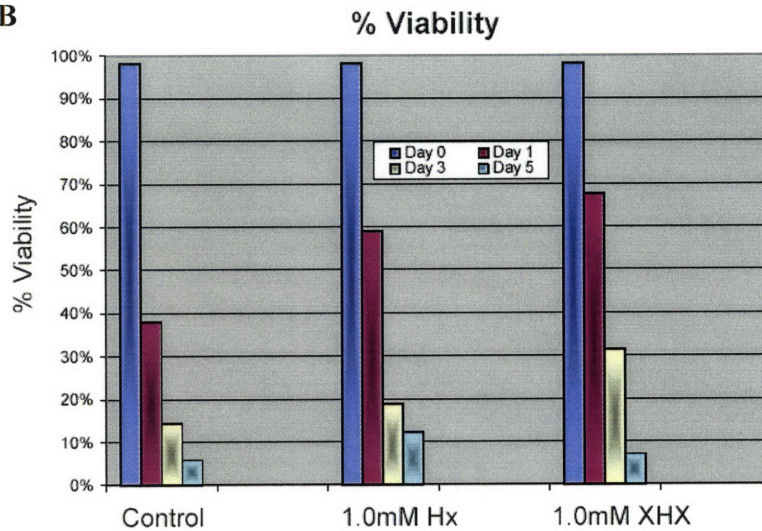
Figure 4.2 | Time Course for Suppression of SACK-Independent Hematopoietic Progenitor Cell (HPC) Survival and Proliferation. CD34^{+} mobilized peripheral blood (MPB) cells were cultured for 0 to 5 days in serum-free HPGM (Hematopoietic Progenitor Growth Medium) supplemented with or without Hx or XHX. On day 0 (blue bar), 1 (red bar), 3 (yellow bar), and 5 (cyan bar), cell samples were analyzed. A) Percent viability and B) viable cell numbers were determined at each respective time point for controls.
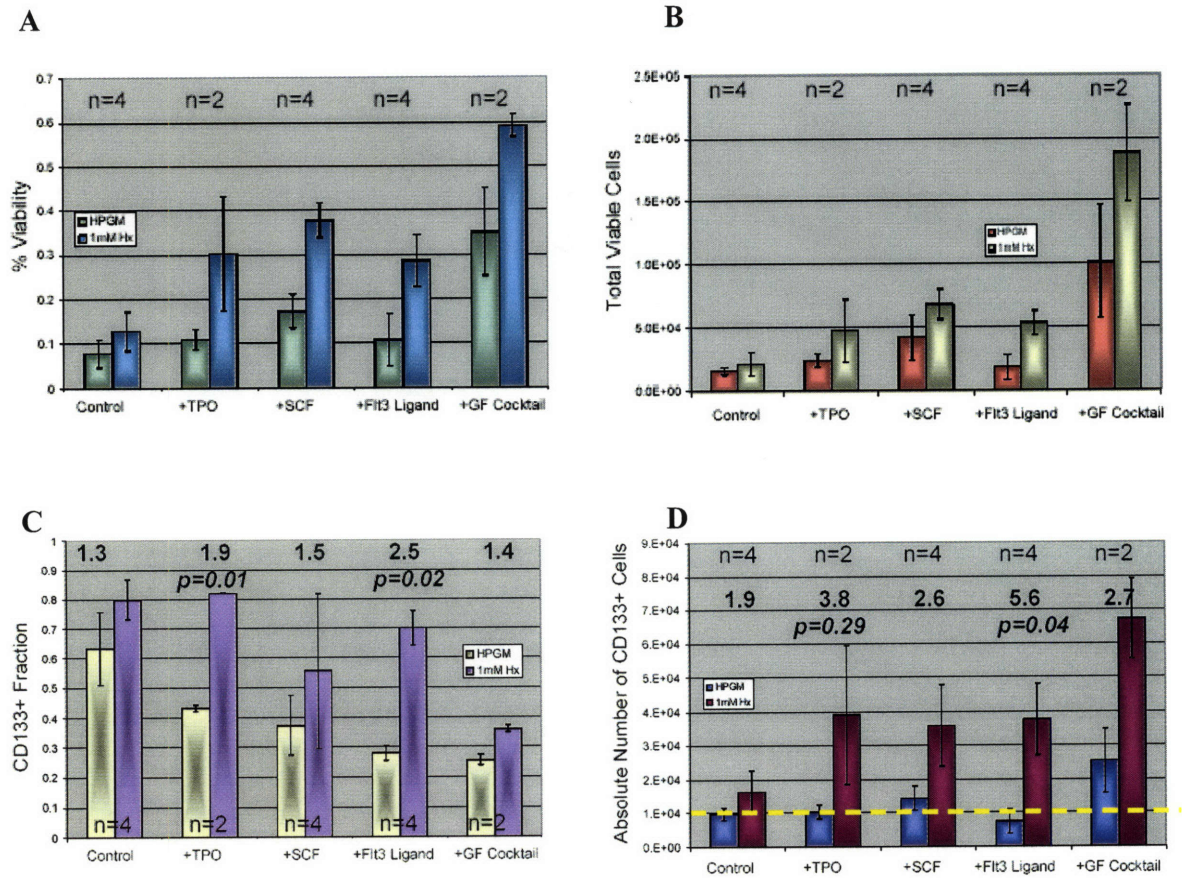
Figure 4.3 | Evaluation of Specific Survival Factors for Enhanced Hx-Dependent CD133$^+$ Cell Production. CD34$^+$ mobilized peripheral blood (MPB) cells were cultured for 44 hours without GFs followed by addition of TPO (thrombopoietin), stem cell factor (SCF), Flt3 ligand, and the GF cocktail, for the remainder of the 5 days. Cells were cultured with or without Hx. At day 5, cells were harvested and analyzed for A) percent viability, B) viable cells, C) CD133$^+$ fraction, and D) absolute number of CD133$^+$ cells. Derivations of p-values are determined from student paired t-tests. Error bars = standard deviation for n individual assays. n = number individual assays, in general, performed in replicates of 2. Dashed (yellow) line represents the normalized control.

A

Survival Factor Addition, Time (hr) 0 24 44 72 96 120

Growth Factor Free
Flt3L

B

C

D

E
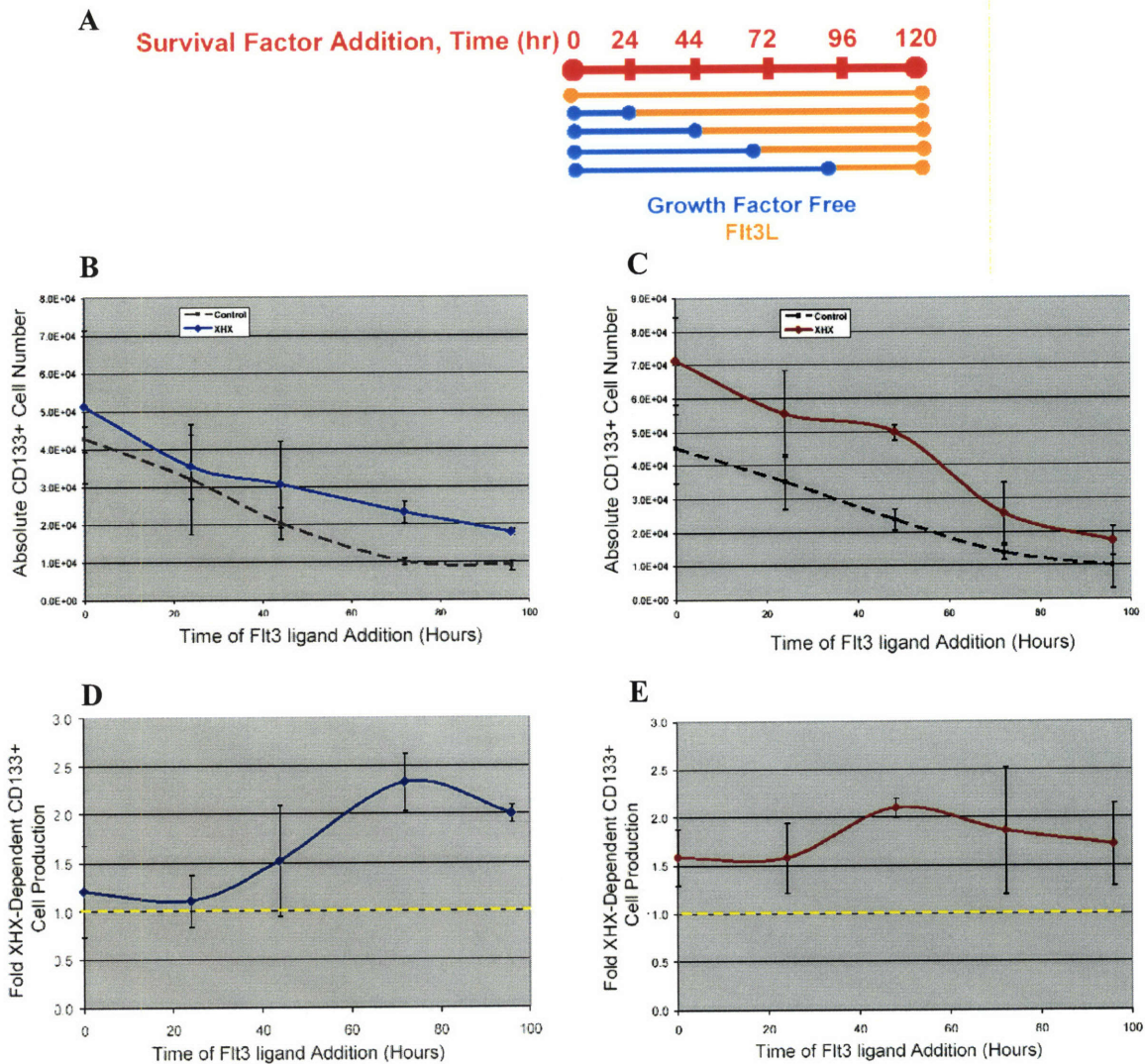
Figure 4.4 | Evaluation of the Effect of Time of GF Starvation and Flt3 Ligand Addition on XHX-Dependent CD133$^+$ Cell Production. CD34$^+$ MPB cells were cultured, supplemented with or without XHX. At every 24 hour interval, Flt3 ligand was added to GF starved cultures for a total of 5 days culture. A) Diagram of Flt3 ligand addition scheme. In two independent experiments, after 5 days of culture, cells were harvested and analyzed for B & C) absolute CD133$^+$ cell production in two independent experiments. D & E) Respective fold increase in CD133$^+$ cell number in response to XHX-supplementation. Error bars = standard deviation for duplicate assays. Each respective data point represents duplicate (n=2) assays. Dashed (yellow) line represents the normalized control.
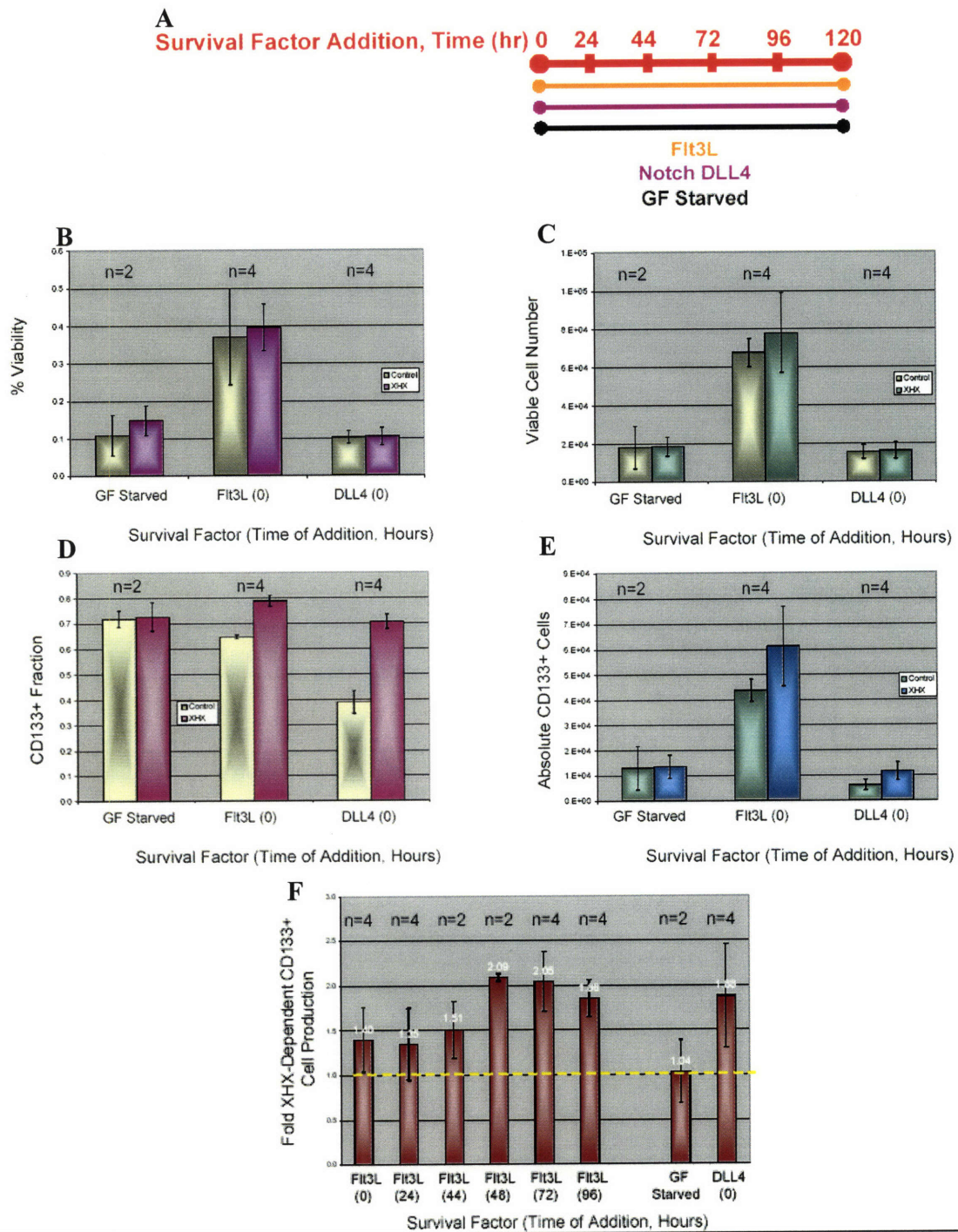
Figure 4.5 | Investigations into XHX-Dependent Effects of Notch Delta-Like Ligand (DLL4) as a More Specific Survival Factor (SF) of XHX-Dependent CD133$^+$ Cell Production. CD34$^+$ MPB cells were cultured with or without XHX. A) Diagram of cell culture scheme. B) Percent viability, C) viable cell number, D) CD133$^+$ fraction, and E) absolute production of CD133$^+$ cells are shown for GF starved Flt3 ligand- or DLL4-supplemented cultures for 5 days. F) A summary of the fold XHX-dependent CD133$^+$ cell production was determined after 5 days of culture under varying additions of Flt3 ligand and DLL4. Time of SF addition is shown in parentheses. Error bars = standard deviation for n individual assays. n = number of individual assays, in general, preformed in replicates of 2. Dashed (yellow) line represents the normalized control.
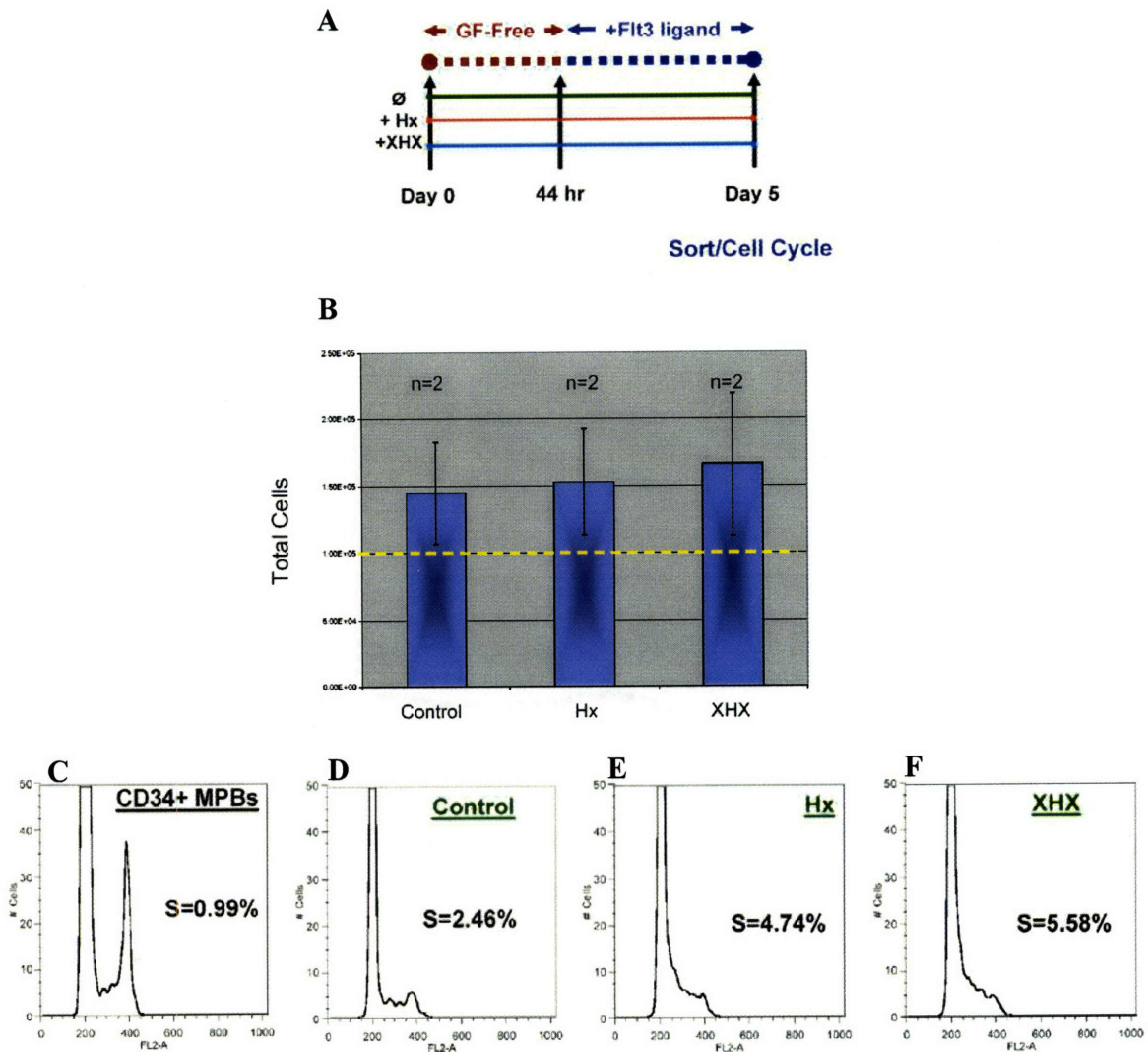
Figure 4.6 | Proliferation and Cell Cycle Analysis of CD34⁺ MPB Cells Cultured without GFs and Addition of Flt3 Ligand. A) Diagram of cell culture scheme. B) Total cells (viable & non-viable) cells are determined for SACK-free (control), Hx, and XHX. Cell cycle analysis was determined for C) uncultured CD34⁺ MPBs, D) cultured control, E) Hx-cultured, and F) XHX-cultured cells. Error bars = standard deviation for a duplicate assay. Each respective bar represents duplicate (n=2) assays.

Bibliographical References

1. Sitnicka, E. et al. Human CD34$^+$ hematopoietic stem cells capable of multilineage engrafting NOD/SCID mice express flt3: distinct flt3 and c-kit expression and response patterns on mouse and candidate human hematopoietic stem cells *Blood* **102**, 881-886 (2003).

2. Rosnet, O. et al. Human FLT3/FLK2 gene: cDNA cloning and expression in hematopoietic cells. *Blood* **82**, 1110-1119 (1993).

3. Matthews, W., Jordan, C. T., Wiegand, G. W., Pardoll, D. & Lemischka, I. R. A receptor tyrosine kinase specific to hematopoietic stem and progenitor cell-enriched populations. *Cell* **65**, 1143-1152 (1991).

4. Zhang, S. et al. Essential Role of Signal Transducer and Activator of Transcription (Stat)5a but Not Stat5b for Flt3-dependent Signaling. *J. Exp. Med.* **192**, 719-728 (2000).

5. Broxmeyer, H. et al. Flt3 ligand stimulates/costimulates the growth of myeloid stem/progenitor cells. *Exp Hematol* **23**, 1121-1129 (1995).

6. McKenna, H. J. et al. Mice lacking flt3 ligand have deficient hematopoiesis affecting hematopoietic progenitor cells, dendritic cells, and natural killer cells. *Blood* **95**, 3489-3497 (2000).

7. Maraskovsky, E. et al. Dramatic increase in the numbers of functionally mature dendritic cells in Flt3 ligand-treated mice: multiple dendritic cell subpopulations identified. *J. Exp. Med.* **184**, 1953-1962 (1996).

8. Karanu, F. N. et al. The Notch Ligand Jagged-1 Represents a Novel Growth Factor of Human Hematopoietic Stem Cells. *J. Exp. Med.* **192**, 1365-1372 (2000).

9. Karanu, F. N. et al. Human homologues of Delta-1 and Delta-4 function as mitogenic regulators of primitive human hematopoietic cells. *Blood* **97**, 1960-1967 (2001).

10. Kumano, K. et al. Notch1 but Not Notch2 Is Essential for Generating Hematopoietic Stem Cells from Endothelial Cells. *Immunity* **18**, 699-711 (2003).

11. Lauret, E. et al. Membrane-bound Delta-4 Notch ligand reduces the proliferative activity of primitive human hematopoietic CD34$^+$CD38low cells while maintaining their LTC-IC potential. *Leukemia* **18**, 788-797 (2004).

Chapter 5

In vivo Characterization of SACK Effects on CD34$^+$ Mobilized Peripheral Blood Cells in Non-Obese Diabetic/Severe Combined Immunodeficient Mice
(Phase V)

<u>Rationale</u>

Several *in vivo* xenogeneic transplant models have been developed utilizing immunodeficient mice and fetal sheep as hosts for study of human hematopoietic stem cells (HSCs)[1-3]. A major limitation in these models is the low level of human cell chimerism that is obtained in the animals. Nevertheless, these models have been used to compare *in vivo* repopulation potential of human hematopoietic cell populations manipulated *ex vivo*.

The transplantation assay available in mice has been instrumental in defining and characterizing the most primitive elements of the mouse hematopoietic system[4]. A similar *in vivo* approach has become available for human hematopoiesis. Numerous groups have transplanted primitive human hematopoietic cells into different mouse mutants in an attempt to develop a reproducible transplantation assay[2,4]. In particular, intravenous injection of human hematopoietic precursors into sublethally irradiated severe combined immunodeficient (SCID) and non-obese diabetic/SCID (NOD/SCID) mice provides engraftment of primitive human hematopoietic cells that proliferate and differentiate to multiple lineages in bone marrow (BM) and spleen[5-7]. The transplanted human cells home to the marrow microenvironment and engraft the ablated murine BM, where they proliferate and differentiate to produce LTC-IC (long-term culture-initiating cells), CFC (colony forming cells), and immature and mature myeloid, erythroid and lymphoid cells. The engrafting human cells have been defined as SCID-repopulating cells (SRC)[8,9].

The NOD/SCID human HSC repopulation assay is widely utilized and has proven extremely useful in verifying that transplanted cells maintain their functional ability to self-renew and produce differentiated human hematopoietic cells. The NOD/SCID transgenic model is a suitable model, since these animals have multiple defects in innate and adaptive immunity that minimizes host immune responses against transplanted cells. However, although proven to be effective models for determining *in vivo* properties of

transplanted cells, these models are not ideal. For instance, NOD/SCID mice have low sensitivity. So, a high number of cells needs to be transplanted in order to observe engraftment[10,11]. One potential reason for this limitation is that although the mice are impaired in dendritic (antigen presenting cell) function, T cells and immunoglobulin, the animals have a low level of natural killer cell activity[10]. Another drawback is that in order to have adequate statistical power, many animals must be transplanted.

In order to evaluate the *in vivo* properties of SACK-dependent CD133$^+$ cells, both uncultured and cultured human CD34$^+$ mobilized peripheral blood (MPB) cells were transplanted into non-obese diabetic/severe combined immunodeficient mice (NOD/SCID). Transplantation of cells into NOD/SCID mice allowed for the evaluation of the engraftment potential of cells and their capacity to give rise to multilineage committed cells of both the myeloid and lymphoid lineages. In addition, this assay allowed for the concomitant evaluation for the significance of the SACK-dependent production of CD133$^+$ cells.

Materials & Methods

SACK Cultures

CD34$^+$ MPB cells were cultured for 44 hours without growth factors, followed by Flt3 ligand addition for 5 days of total culture time. (At the time of NOD/SCID investigations, findings with Notch DLL4 had not been determined. NOD/SCID studies are underway to evaluate *in vivo* engraftment potential of cells in DLL4-supplemented cultures). Twenty-four hours prior to transplantation, mice were sublethally irradiated. At the time of culture initiation, uncultured cells were transplanted into NOD/SCID mice as positive controls. In order to follow effects in terms of total engraftment activity, transplantations were designed based on culture well equivalents (CWE) instead of fixing cell number. The CWE approach avoids misinterpreting changes in HSC fraction as changes in HSC number. After 5 days of culture, cells were harvested from control (i.e. SACK-free, Ø), Hx- and XHX-supplemented cultures and transplanted at varying doses (i.e. CWE). After at least 8 weeks, mice were euthanized by CO_2-asphyxiation, and bone marrow, peripheral blood and spleen were all harvested for each mouse. Cells were

stained with fluorescent antibodies against specific cell surface antigens and analyzed by flow cytometry (Figure 5.1).

Cell Transplantation in NOD/SCID mouse model

NOD/LtSz scid/scid (NOD/SCID) mice were supplied by Jackson Laboratories (Bar Harbor, ME) and maintained in the Massachusetts Institute of Technology (MIT) Division of Comparative Medicine (DCM) animal facilities under institutional regulations. All animals were handled under sterile conditions and maintained in microisolator cages. One week prior to transplantation, mice were put on an antibiotic regiment (Septra in sterilized drinking water) for the remainder of the study. Pre-transplantation, mice were given a total body irradiation at 6 to 8 weeks of age with 300 cGy from a ^{137}Cs source. Twenty-four hours post irradiation, mice were given a single retro-orbital injection of: (1) uncultured human CD34$^+$ cells; (2) cells harvested from SACK supplemented or control cultures; or (3) sterile PBS to assess background host HSC regeneration levels. Transplanted cells were injected in 300μl of sterile PBS. For each described injection, 5-10 mice were used. Mice were euthanized by CO$_2$-asphyxiation at least 8 weeks post-transplantation to assess the number and types of human cells detected in murine bone marrow (BM) harvested from femurs and tibias, in addition to peripheral blood and spleen.

Flow Cytometry Detection of Human Cells in Murine Bone Marrow, Peripheral Blood, and Spleen

Bone marrow cells were flushed from the femurs and tibias of each mouse using a 1.0ml syringe and 26-gauge needle. Cells were flushed using Fischer Medium (Quality Biological, Gaithersburg, MD), 5% fetal bovine serum (FBS; JRH Biosciences, Lenexa, KS) and 1% penicillin/streptomycin (P/S, Invitrogen, Carlsbad, CA). Cells from peripheral blood and spleen were obtained, respectively, through cardiac puncture and mechanical dissociation. To prepare cells for flow cytometry analysis, contaminating red blood cells were lysed using 8.3% ammonium chloride, with the remaining cells washed in FACS Buffer. The cells were then re-suspended at 5x10^5 cells and washed with FACS buffer to block non-specific binding sites. After centrifugation, cells were stained with

5μg monoclonal antibodies specific for human CD45, CD33, CD38, CD19, CD34 (all from BD Biosciences, Franklin Lakes, NJ), and CD133 (Miltenyi Biotech, Auburn, CA) directly labeled with fluorescein isothiocyanate (FITC), R-phycoerythrin (PE), or allophycoerythrin (APC) for 30 minutes at 4°C. Cells for each sample were also stained in parallel with isotype control antibodies (Caltag, Burlingame, CA) and unstained samples for FACS compensation. At least 50,000 cells were analyzed from flow cytometry analyses using a FACSCalibur™ flow cytometer (Becton, Dickinson and Company, Mountain View, CA). Successful engraftment by human hematopoietic cultures was defined as the presence of at least 0.1% of human CD45$^+$ and 0.01% CD33 and CD38 positive cells.

Results

Uncultured CD34$^+$ MPB cells transplanted into NOD/SCID mice resulted in human cell engraftment in the bone marrow, as demonstrated by anti-human CD45 detection by flow cytometry (Figure 5.2). Bone marrow lymphoid and myeloid cells are exhibited as expressing low and high scatter profiles, respectively (R1; Figure 5.2A). Gated R1 cells express a population of cells that are distinctly CD45$^+$ (R2; Figure 5.2B). Gated cells from R1 and R2, exhibit a specific population of cells that express CD33 (Figure 5.2C) and CD38 (Figure 5.2D). Cells that express CD45, CD33, and CD38 in mice engrafted at a 5 CWE dose are not detected in mock transplanted mice (Figure 5.2E-H).

Three independent experiments were performed evaluating CD34$^+$ MPB cells cultured for 44 hours without GFs, with subsequent Flt3 ligand addition for the remaining 5 days. In the first experiment, 2 out of 2 mice transplanted with uncultured CD34$^+$ MPB cells engrafted at 5 CWEs (1.5% and 1.5%; data not shown). No engraftment was observed for mock transplanted (0/4) or uncultured cells transplanted at 0.5 CWEs (0/1). Mice transplanted with cultured control (Ø; 0/4), Hx- (0/1) or XHX-supplemented (0/3) cells exhibited no engraftment at 2 CWEs (data not shown).

In a second study, 1 out of 6 mice (mouse L4) transplanted with 2 CWEs of XHX-supplemented cells exhibited significant expression of CD45 (0.19%; Figure 5.3A), whereas 3 out of 4 mice (H1-H3) transplanted with uncultured CD34$^+$ MPB cells at 5

CWEs exhibited significant CD45 engraftment (0.14%, 0.20%, 0.22%; Figure 5.3A). Additionally, mouse L4 exhibited distinct myeloid (CD33) and lymphoid (CD38) engraftment, as did the control mice H1-H3 (Figure 5.3B). However, mouse L4 exhibited a 2.3-fold (p=0.05) greater frequency of human lymphoid cells than uncultured CD34$^+$ MPB cells at 5 CWEs (0.04% ± 0.02%), even though a 2.7-fold reduction in myeloid (CD33) expression is detected in mouse L4, compared to mice H1-H3 (Figure 5.3B). Uncultured CD34$^+$ MPB cells transplanted into NOD/SCID mice at 0.5 CWEs did not exhibit engraftment in 2 out of 2 mice, as was also the case with cultured SACK-free (Ø; 0/4) and Hx cultured cells (0/5; Figure 5.3A, B of any animals). No significant engraftment was observed in the spleen and peripheral blood of any animals (data not shown).

In a third independent study, 1 out of 4 XHX-transplanted mice (AG1) at 2 CWEs resulted in significant CD45$^+$ engraftment (10.6%). In addition, 4 out of 5 Hx-transplanted mice (F1, F2, F4, F5) resulted in significant CD45$^+$ engraftment (0.11%, 3.9%, 0.11%, and 0.31%, respectively; Figure 5.3C). On the other hand, only 1 out of 4 SACK-free (Ø) transplanted mice (AE4) resulted in significant CD45$^+$ engraftment (3.1%; Figure 5.3C). Control mice transplanted at 5, 2, and 0.5 CWEs of CD34$^+$ MPB cells resulted in 2 out of 2 mice (AB1=28.0% & AB2=10.7%), 4 out of 4 mice (AD1-AD4, 18.1%, 4.5%, 6.9%, and 20.7%, respectively), and 1 out of 2 (AC2=0.55%) mice that engrafted with significant CD45$^+$ human cell expression, respectively (Figure 5.3C). All mice that exhibited significant CD45$^+$ human cell engraftment demonstrated significant expression of both CD33 and CD38 positive cells (Figure 5.3D). Most notably was mouse AG1, transplanted with XHX-cultured CD34$^+$ MPB cells, which exhibited 2.6-fold (p=0.01) greater CD33$^+$/CD38$^+$ cell engraftment at 2 CWEs, as compared with uncultured CD34$^+$ MPB cells transplanted at 5 CWEs (1.5% ± 0.04; Figure 5.3D).

In the second experiment, significant human CD45$^+$ cell expression was observed in the spleen and peripheral blood of transplanted mice (Figure 5.4A, B, respectively). XHX-transplanted mice displayed 0.64%, 0.33% and 4.1% human CD45$^+$ cell engraftment (AG1, AG2, and AG3, respectively) in the spleen (Figure 5.4A) of 2 CWE transplanted NOD/SCID mice. Of these mice, only AG2 exhibited significant human CD45$^+$ cell engraftment (0.76%) in the peripheral blood (Figure 5.4B). Furthermore,

NOD/SCID mice transplanted with Hx-supplemented cells (2 CWE) demonstrated 0.17%, 0.91%, 0.23%, and 0.55% human $CD45^+$ cell engraftment (AF, AF2, AF4, and AF5, respectively; Figure 5.4A) in the spleen. Of these mice, only mouse AF2 and AF5 displayed significant $CD45^+$ engraftment (0.89% and 0.31%, respectively; Figure 5.4B) in the peripheral blood. Mice transplanted with culture controls (i.e. SACK-free, Ø) at 2 CWEs showed evidence of engraftment in mouse AE3 and AE4 (0.52% and 0.81%, respectively, Figure 5.4A) in the spleen. In the peripheral blood, mouse AE1, AE2, and AE4 exhibited significant engraftment (1.8%, 0.81%, and 0.19%, respectively; Figure 5.4B). All eight mice transplanted at varying doses of uncultured $CD34^+$ MPB cells exhibited evidence of engraftment in the spleen (Figure 5.4A). In the spleen, mice transplanted at 5 CWEs exhibited 3.2% and 2.0% engraftment, whereas mice transplanted at 0.5 CWEs displayed 0.1% and 0.2% engraftment (Figure 5.4A). Additionally, mice transplanted at 2 CWEs engrafted with 1.2%, 0.87%, 0.30%, and 0.98% engraftment in the spleen (Figure 5.4A). In the peripheral blood, 7 out of 8 uncultured, control animals engrafted. At 5 CWEs, mice AB1 and AB2 exhibited 1.4% and 2.5%, respectively (Figure 5.4B), whereas for mice transplanted at 0.5 CWEs, only AC2 demonstrated significant engraftment (1.3%; Figure 5.4B). Mice transplanted with uncultured $CD34^+$ MPB cells at 2 CWEs displayed 1.8%, 0.13%, 0.38%, and 3.2% engraftment in the peripheral blood (Figure 5.4B).

NOD/SCID transplantation studies were also performed using cultured cells in GF starved conditions for 8 days supplemented with Hx or XHX, along with SACK-free controls (Ø). In two independent studies, no mice exhibited $CD45^+$ engraftment, except positive control mice (Figure 5.5). Mice transplanted with uncultured $CD34^+$ MPB cells at 5 CWEs demonstrated 22.0%, 36.6%, 40.1%, and 14.3% engraftment (Figure 5.5). Table 5.1 summarizes *in vivo* transplantation of NOD/SCID mice with cultured and uncultured $CD34^+$ MPB cells at varying doses from examined conditions.

Discussion

In vivo injection of $CD34^+$ MPB cells allows for the evaluation of the engraftment and multilineage differentiation capacity of transplanted hematopoietic stem cells. Specifically, direct comparisons based on the dose of cells transplanted and number of

engrafted (i.e. greater than 0.1% CD45^{+} expression) animals allows for the rough approximation of the relative number of HSCs in compared cell populations, or more specifically, SCID-repopulating cells (SRC)[12,13]. These determinations are based on the assumption that one HSC (or SRC) can yield long-term multilineage engraftment in an animal. This model necessitates the application of Poisson statistics. When uncultured CD34^{+} MPB cells are transplanted into NOD/SCID mice at varying doses (i.e. culture well equivalents, CWE), distinct engraftment is observed (Figure 5.2). At 5 CWEs of CD34^{+} MPB cells, 11 out of 12 total (~92%) transplanted mice exhibit CD45^{+} engraftment in bone marrow. In addition, all 11 engrafted mice display multilineage engraftment (Figure 5.3B, D; Table 5.1). Decreasing the transplantation dose 10-fold, from 5 CWEs to 0.5 CWEs, results in significant reduction in engraftment (1 out of 7, ~14%; Table 5.1). 100% of mice transplanted with CD34^{+} MPB cells at 2 CWEs result in engraftment (4 out of 4; Figure 5.3C & Table 5.1). This corresponds to an SRC frequency of approximately 1 SRC in 1.3 CWEs (i.e. 1 SRC in 76,900 CD34+ MPB cells) in uncultured CD34^{+} MPB cells (Figure 5.6). All animals that engrafted, as demonstrated by significant CD45^{+} expression, resulted in multilineage engraftment (Figure 5.3B, C; Table 5.1). Engrafted cells exhibit distinct expression for CD33 and CD38. CD33 is an early myeloid progenitor cell marker that is also expressed on monocytes and granulocytes[14,15], whereas, CD38 is an early B and T cell marker[16]. When both CD33 and CD38 are expressed on one cell, it suggests that the cell is a myeloid and lymphoid unspecified cell, otherwise referred to as a multipotent progenitor cell (MPC). MPCs are produced solely from self-renewal of HSCs since MPCs are not capable of self-renewal[17,18]. Therefore, detection of MPCs in transplanted mice is consistent with the presence of HSCs in CD34^{+} enriched MPB cell populations (Figure 5.3D).

CD34^{+} MPB cells cultured without GFs for 44 hours, with subsequent Flt3 ligand addition, also give rise to significant engraftment, albeit at an overall reduced efficiency. Mice transplanted at 2 CWEs with SACK-free (Ø) cultured CD34^{+} MPB cells result in only 1 out of 13 (8%) mice showing evidence of engraftment in the bone marrow (Figure 5.3; Table 5.1). The sole mouse that exhibited human CD45 engraftment (AE4=3.1%) displayed 0.95% CD33^{+}/CD38^{+} multilineage engraftment (Figure 5.3D). In the spleen, 2 out of 13 (15%) mice exhibit human engraftment, while in the peripheral blood, 3 out of

13 (23%) animals demonstrate engraftment (Figure 5.4, Table 5.1). Due to the varied observed engraftment in peripheral blood and spleen from experiment-to-experiment, bone marrow was used as the standard for engraftment determinations.

Transplantation of SACK-supplemented cultured cells exhibits increased engraftment compared to SACK-free cultured cells. XHX-cultured cells engraft in 2 out of 13 mice (15%). Therefore, XHX-cultured cells results in 1.9-fold greater efficiency than SACK-free cultured cells. This result suggests that culturing of $CD34^+$ MPB cells in XHX-supplemented culture results in an increase in SRCs. Specifically, one XHX-transplanted mouse (L4; at 2 CWEs) engrafted (0.19%) at comparable levels to uncultured controls at 5 CWEs (0.14%, 0.2%, and 0.22%; Figure 5.3A; Table 5.1). In addition, mouse L4 exhibited 2.3-fold improved lymphoid engraftment compared to uncultured $CD34^+$ MPB cells at 5 CWEs, although myeloid expression is reduced in mouse L4, not unlike mouse H2 (Figure 5.3B). XHX-transplanted mice also demonstrate engraftment in the spleen (3 out of 13 mice) and peripheral blood (1 out of 13; Figure 5.4; Table 5.1).

Transplantation of Hx-supplemented cultured cells results in the best engraftment efficiency of any of the cultured conditions. Specifically, 4 out of 11 (36%) total mice transplanted with cells from Hx-cultures engraft with significant $CD45^+$ human expression (p=0.14 by Fisher's Exact Test compared to mice transplanted with SACK-free cultured cells; Figure 5.3, Table 5.1), corresponding to a 4.5-fold increase in engraftment efficiency, compared to SACK-free cultured cells. This result suggests that an expansion in SRCs has been achieved with Hx-supplemented culture. Again, all mice that express CD45 in their bone marrow, also express CD33 and CD38 (0.06% – 0.84%; Figure 5.3D). Furthermore, 36% of mice transplanted with Hx-supplemented cells exhibit engraftment in the spleen (4/11) and 18% in the peripheral blood (2/11; Figure 5.4; Table 5.1).

Although the overall efficiency of engraftment was significantly reduced by culturing $CD34^+$ MPB cells, there were significant effects of Hx- and XHX-cultured cells. Specifically, XHX-transplanted cells demonstrated a 2.3-fold and 2.6-fold increase in the lymphoid and multilineage engraftment, as compared with 5 CWE uncultured controls (Figure 5.3B, D). This suggests that XHX-cultured cells may promote greater

self-renewal of HSCs, therefore giving rise to greater numbers of MPCs. The presence of MPCs strongly suggests the existence of self-renewing HSCs, since MPCs are not predicted to survive in the mice for 8 weeks, given that MPCs do not self-renew. Alternatively, XHX may promote symmetric expansion of HSCs *ex vivo*, therefore giving rise to greater numbers of MPCs *in vivo*. Additionally, Hx- and XHX-transplanted mice demonstrated increased efficiency in SRC engraftment, compared to SACK-free cultured cells (Figure 5.3, Table 5.1). Overall, 6 out of 24 (25%) SACK-transplanted animals give rise to human CD45 and multilineage (CD33/CD38) engraftment in the bone marrow, as compared to the 1 out of 13 (8%) animals transplanted with SACK-free cultured $CD34^+$ MPB cells (Figure 5.3, Table 5.1). This suggests that although the culture scheme may be reducing the overall number of SRCs, SACK-dependent culture contains a greater number of these cells, either by promoting HSC survival or expansion. Because total cell number does increase in culture (Chapter 4; Figure 4.6B) with SACK agents, a component of the increase can be attributed to expansion of cells with SRC activity (i.e. HSCs).

Flt3 ligand may be acting as a survival factor for SRCs, as previously suggested. This is evident since mice transplanted with GF starved cells for 8 days give rise to no engraftment, independent of SACK-supplementation (n=16; Figure 5.5). Along with Flt3 ligand supplemented transplantations, this observation suggests that long-term GF starvation significantly reduces the efficiency of SRC engraftment in NOD/SCID mice. Although a reduced efficiency in engraftment is observed with mice transplanted with cells supplemented with Flt3 ligand, engraftment is still possible, suggestive that GF starvation for 44 hours and Flt3 ligand does, indeed, maintain the survival of a fraction of cells that possess the potential to engraft into NOD/SCID mice and give rise to myelolymphoid lineage cells.

Although a 1.9-fold and 4.5-fold engraftment efficiency was observed with mice transplanted with XHX- and Hx-supplemented cells, respectively (relative to SACK-free cultured cells), when compared to mice transplanted with uncultured cells, it is clear that *ex vivo* culture of $CD34^+$ MPBs without GFs, followed by Flt3 ligand reduces the number of SRCs that engraft mice. However, transplantation of Hx-cultured cells into NOD/SCID mice at 2 CWEs yields equivalent SRC activity as 0.75 CWE of uncultured

CD34$^+$ MPB cells (Figure 5.6). Since the proliferation of committed HPCs is repressed by GF starvation culture for 44 hours, cultured cells are predicted to be at least 1.5-fold enriched for HSCs (or SRCs). This is determined by taking the ratio of the number of uncultured cells transplanted at 0.75 CWE (75,000) to the number of Hx-cultured cells transplanted at 2 CWE (50,000). Although repression of HPCs was a necessary procedure to detect net expansion of SACK-dependent CD133$^+$ cells *ex vivo*, it is not the ideal culture procedure for determining SRC activity in *in vivo* NOD/SCID investigations. There are several reasons for this statement. First, GF starvation significantly reduces the number of committed HPCs in culture and, therefore, reduces the total number of cells that are transplanted into NOD/SCID mice. This is may be an important consideration since the marrow seeding efficiency of intravenously transplanted human cells that successfully home to the bone marrow microenvironment is less than 10%[19,20]. Therefore, a significant reduction in viable cells will naturally reduce the engraftment efficiency of transplanted cells. Second, although HPCs may be problematic for detecting SACK-dependent effects on cultured CD34$^+$ MPB cells *in vitro*, the presence of HPCs for *in vivo* engraftment may be important. Not only might it increase the probability that a SRC will successfully reach the marrow microenvironment, but it might also have potential positive effects in promoting engraftment in NOD/SCID mice. For instance, HPCs may decrease the short-term morbidity and mortality of NOD/SCID mice, since the HPCs will give rise to immediate differentiated myeloid and lymphoid cells, reducing irradiation-induced anemia, although it is not clear whether human cells have functional capacity in the mouse. HPCs or other cell types (i.e. stromal cells) may also be important for conditioning the bone marrow microenvironment for successful HSC homing and residence in the niche[6,19]. This effect may also relate to the fact that other investigators have been successful in engrafting NOD/SCID mice transplanted with GF cocktail induced cells[21-23]. Therefore, ongoing studies aim to investigate engraftment efficiency in mice transplanted with GF cocktail cultured CD34$^+$ MPB cells, supplemented with Hx and XHX. Additionally, although Flt3 ligand demonstrated survival effects in cultured CD34$^+$ MPB cells, Delta-like ligand 4 (DLL4) may promote greater engraftment efficiency by specifically promoting SRC survival. So a combination of DLL4, GF

cocktail, and Hx or XHX may be the necessary components to maintain HSC survival, support HPC proliferation, and promote symmetric expansion of HSCs, respectively.

Conclusion

CD34$^+$ MPB cells cultured for 44 hours without GFs, followed by Flt3 ligand addition results in overall reduction in engraftment efficiency, when transplanted into NOD/SCID mice, compared to uncultured cells. However, culture with Flt3 ligand maintains the survival of SRCs (HSCs), when compared to cells that were cultured and transplanted into NOD/SCID mice without GFs. Culture of CD34$^+$ MPB cells in Hx- and XHX-supplemented conditions results in 4.5-fold and 1.9-fold increase in engraftment efficiency, respectively. This SACK-dependent effect on cultured CD34$^+$ MPB cells, while repressing proliferation of HPCs, suggests that Hx- and XHX-supplemented cultures have increased SRC activity. In order to increase the overall efficiency of cultured cells, future *in vivo* transplantation investigations of SACK-induced expansion of HSCs need to be evaluated in conditions that promote proliferation of HPCs (i.e. GF cocktail) resulting in increased conditioning for HSC homing and residence in the bone marrow microenvironment.

Cell Culture Scheme
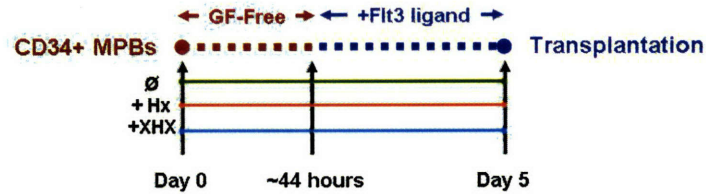
Mice Transplantation Scheme

Day -7 → Antibiotic regiment initiated
Day -1 → NOD/SCID mice sublethally irradiated with 300 cGy γ-radiation
Day 0 → NOD/SCID mice transplanted with cells retro-orbitally
~ Day 60 → NOD/SCID mice sacrificed (BM, Blood, and Spleen harvested)

Figure 5.1 | Experimental Design for *In Vivo* Transplantation of Cultured CD34$^+$ MPB Cells. CD34$^+$ MPB cells were cultured without GFs for 44 hours, with subsequent Flt3 ligand addition for a total of 5 days culture time. Cells were harvested and transplanted into non-obese diabetic/severe combined immunodeficient (NOD/SCID) mice.
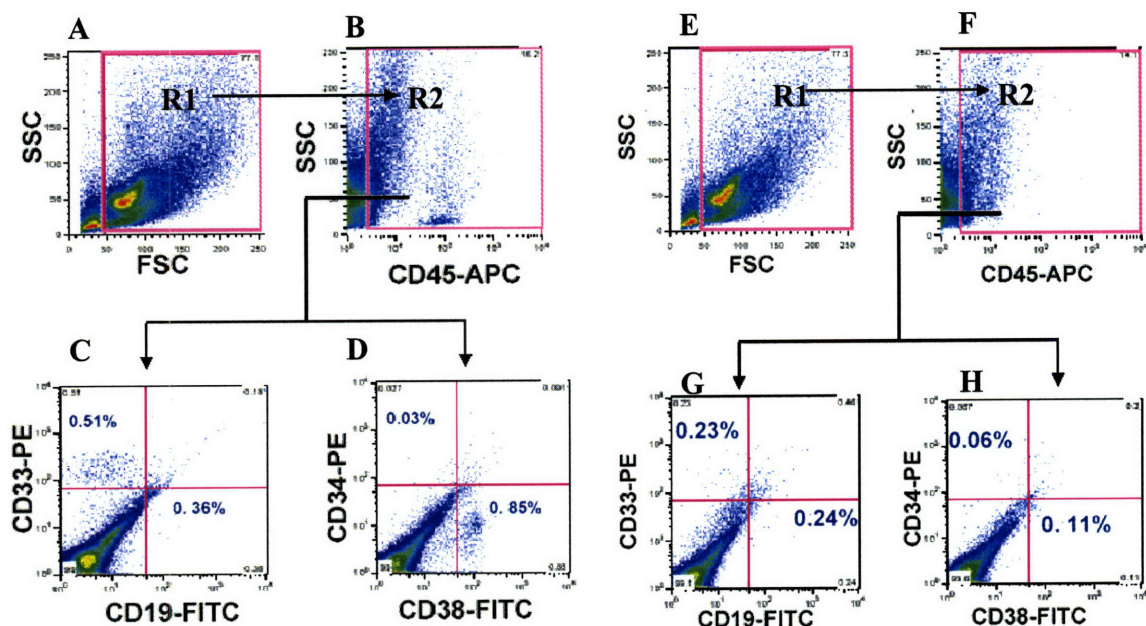
Figure 5.2 | Representative Flow Cytometry Bivariate Plots for Bone Marrow Cells from NOD/SCID Mice Transplanted with Uncultured CD34$^+$ MPB Cells. Bone marrow cells from NOD/SCID mice were evaluated for expression of the indicated cell surface antigens. A-D) Cells from mouse transplanted with 5 cell well equivalents (5×10^5) of uncultured CD34$^+$ MPB cells. E-H) Cells from a mock transplanted control mouse. Live cells in the R1 gate were evaluated for CD45$^+$ cells in R2. In independent 3-color analyses, CD45$^+$ cells in R2 were evaluated for either CD33/CD19 expression (C & G) or CD34/CD38 expression (D & H).

A

B
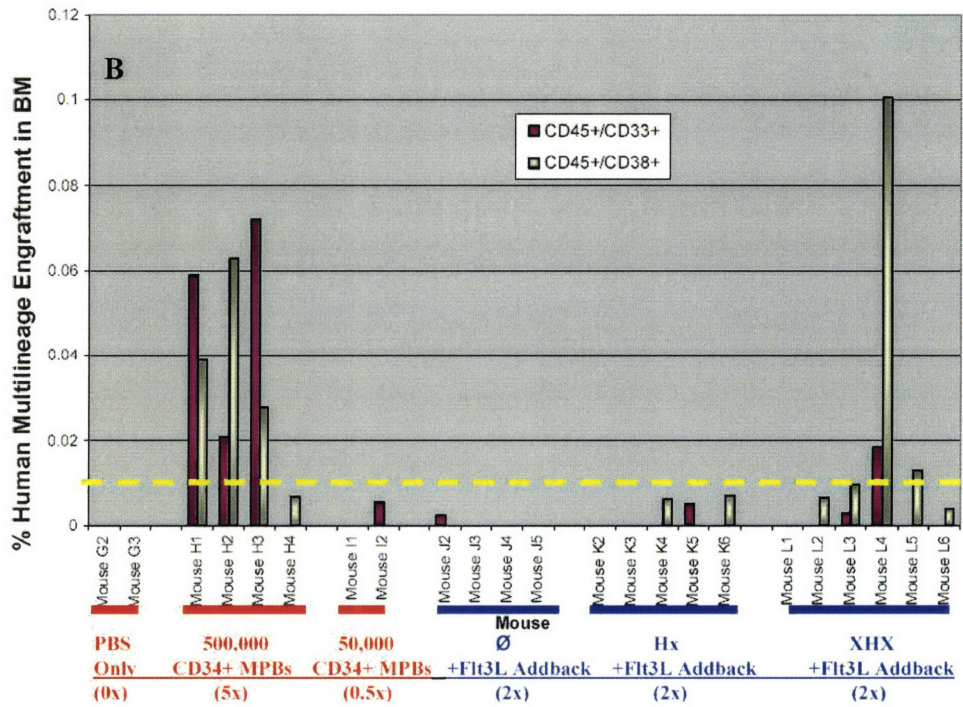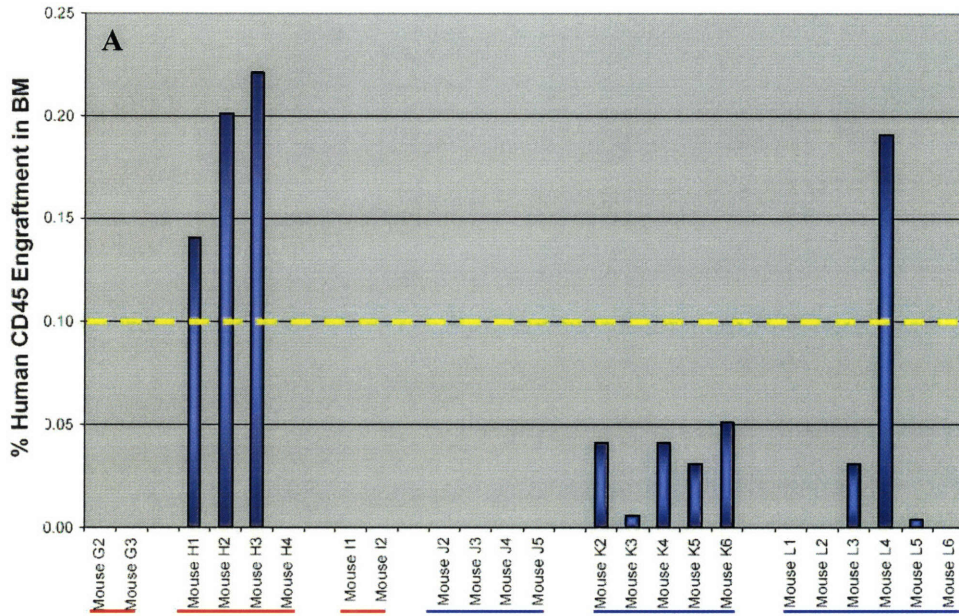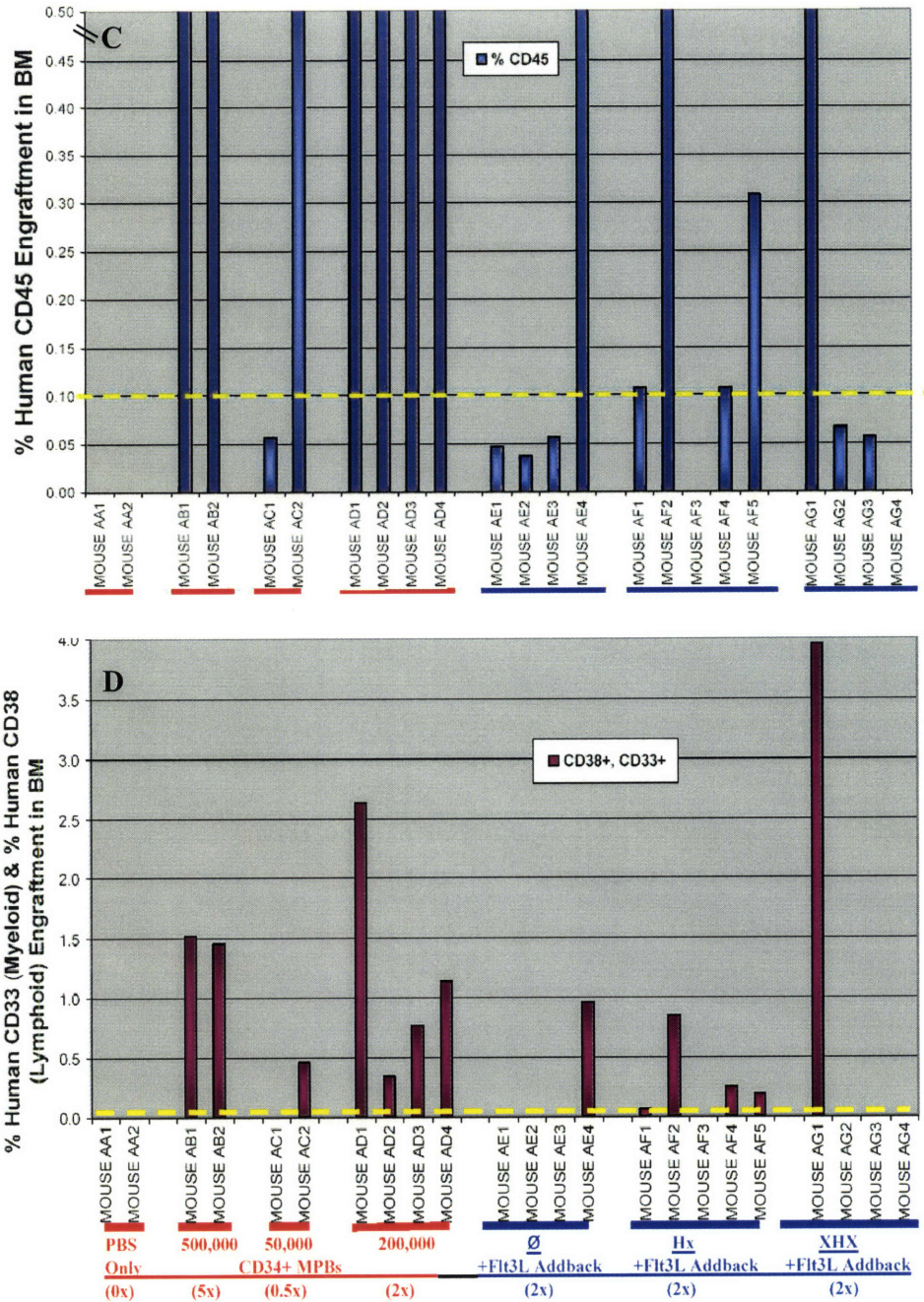
Figure 5.3 | *In Vivo* Engraftment in the Bone Marrow of NOD/SCID Mice Transplanted with Cultured (Day 5 GF Starved and Flt3 Ligand Addition) and Uncultured CD34⁺ MPB Cells. Two independent experiments are shown for each mouse for A & C) CD45⁺ expression and B & D) each respective multilineage engraftment for CD33 (myeloid) and CD38 (lymphoid) expression. Mice were transplanted with uncultured control cells (0, 5, 0.5, and 2 CWEs), in addition to SACK-free (Ø), Hx and XHX cultured cells at 2 CWEs. Transplanted mice were considered engrafted by human CD34⁺ MPB cells if expression was above 0.1% for CD45⁺ and 0.01% for CD33⁺/CD38⁺ expression (dotted yellow lines).
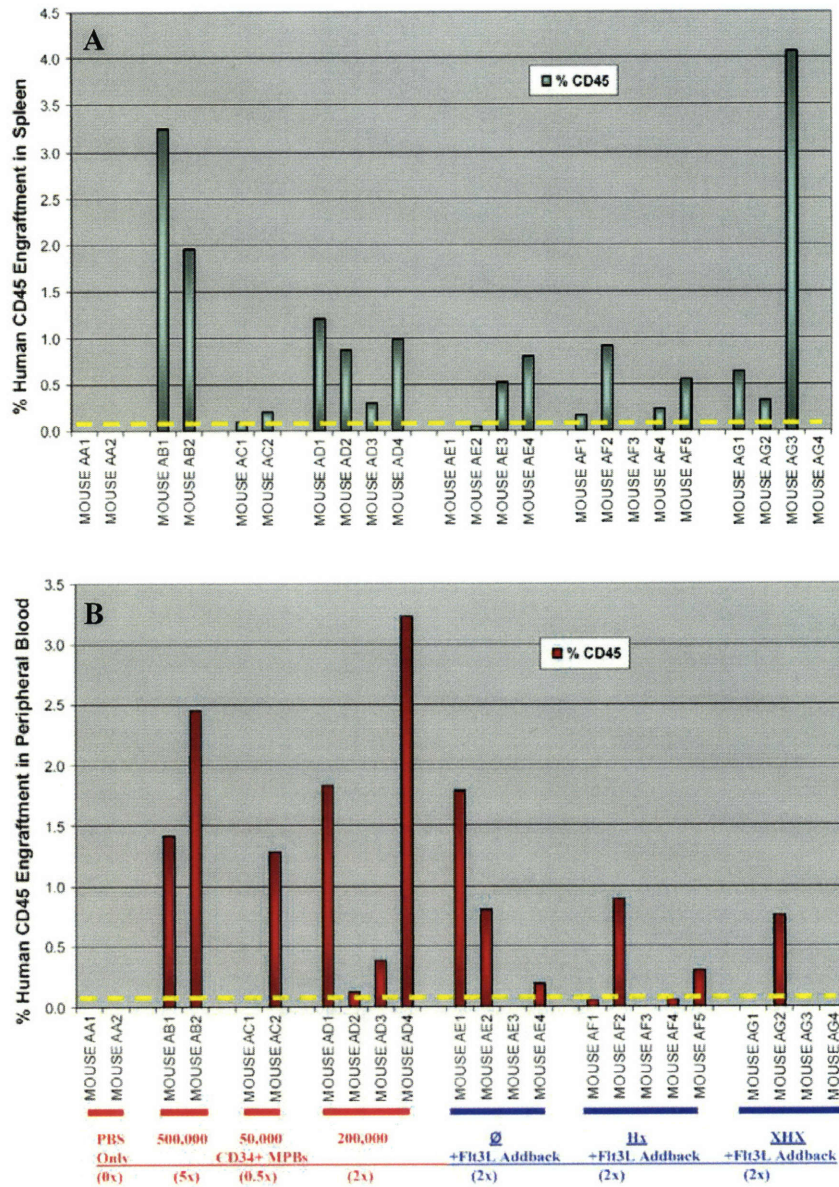
Figure 5.4 | *In Vivo* Engraftment in the Spleen and Peripheral Blood of NOD/SCID Mice Transplanted with Cultured (Day 5 GF Starved and Flt3 Ligand Addition) and Uncultured CD34$^+$ MPB Cells. CD45 engraftment results in the A) spleen and B) peripheral blood of transplanted NOD/SCID mice. Mice were transplanted with uncultured control cells (0, 5, 0.5, and 2 CWEs cell dose), in addition to SACK-free (Ø), Hx- and XHX-supplemented cells at 2 CWEs. Transplanted mice were considered engrafted by human CD34$^+$ MPB cells if CD45 expression was above 0.1% (dotted yellow lines).
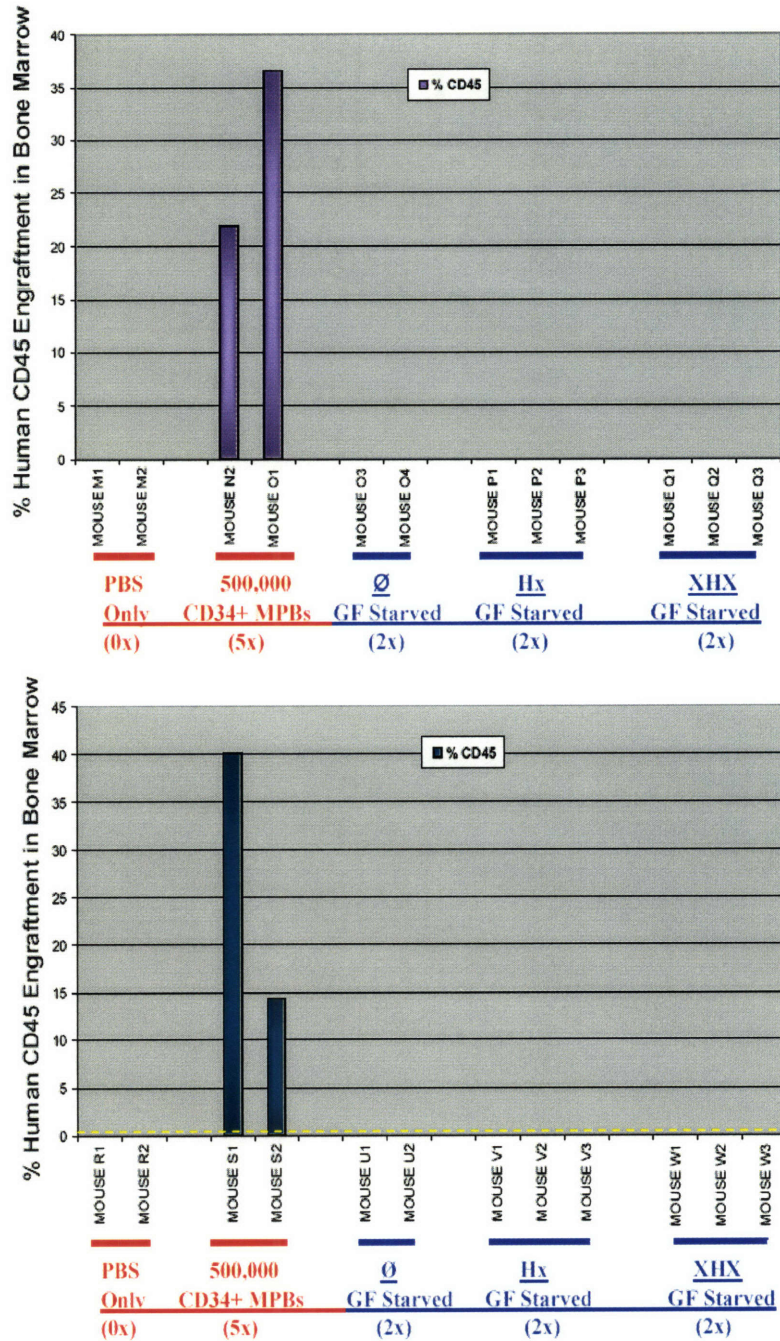
Figure 5.5 | *In Vivo* Engraftment in the Bone Marrow of NOD/SCID Mice Transplanted with Cultured (Day 8 GF Starved) and Uncultured CD34$^+$ MPB Cells. Two independent investigations for CD45 engraftment by cultured day 8 GF starved cells in SACK-free (Ø), Hx- and XHX-supplemented media (2 CWE) in the bone marrow of transplanted mice. In addition, mice were transplanted with uncultured control cells (0 and 5 CWEs). Transplanted mice were considered engrafted by human CD34$^+$ MPB cells if CD45 expression was above 0.1% (dotted yellow lines).

CWE	UNCULTURED Bone Marrow	Ø	CULTURED Hx	XHX
0	0/11 (0%)	-----	-----	-----
0.5	1/7 (14%)	-----	-----	-----
2	4/4 (100%)	1/13 (8%)	4/11 (36%)	2/13 (15%)
5	11/12 (92%)	-----	-----	-----

CWE	UNCULTURED Spleen	Ø	CULTURED Hx	XHX
0	0/11 (0%)	-----	-----	-----
0.5	2/7 (29%)	-----	-----	-----
2	4/4 (100%)	2/13 (15%)	4/11 (36%)	3/13 (23%)
5	2/12 (17%)	-----	-----	-----

CWE	UNCULTURED Peripheral Blood	Ø	CULTURED Hx	XHX
0	0/11 (0%)	-----	-----	-----
0.5	1/7 (14%)	-----	-----	-----
2	4/4 (100%)	3/13 (23%)	2/11 (18%)	1/13 (8%)
5	2/12 (17%)	-----	-----	-----

Table 5.1 | Summary of *In Vivo* Engraftment of Transplanted NOD/SCID Mice in the Bone Marrow (BM), Spleen and Peripheral Blood. A summary for all experiments are shown for CD45$^+$ expression. The percent engraftment of uncultured control CD34$^+$ MPB cells at 0, 0.5, 2, and 5 CWEs is shown, as well as cultured CD34$^+$ MPB cells in SACK-free (Ø), Hx and XHX supplemented cells at 2 CWEs for bone marrow, spleen and peripheral blood. SACK-effects on cultured cells were investigated for GF starved, followed by Flt3 ligand addition conditions. Transplanted mice were considered engrafted by human CD34$^+$ MPB cells if CD45 expression was above 0.1%.

The chart shows:
- Y-axis: % of CD45+ Engrafted Mice (ranging from -20% to 120%)
- X-axis: Culture Well Equivalents (CWE) (ranging from 0 to 6)
- Equation annotation: y=(48.71%)x, R²=0.987, p=0.07
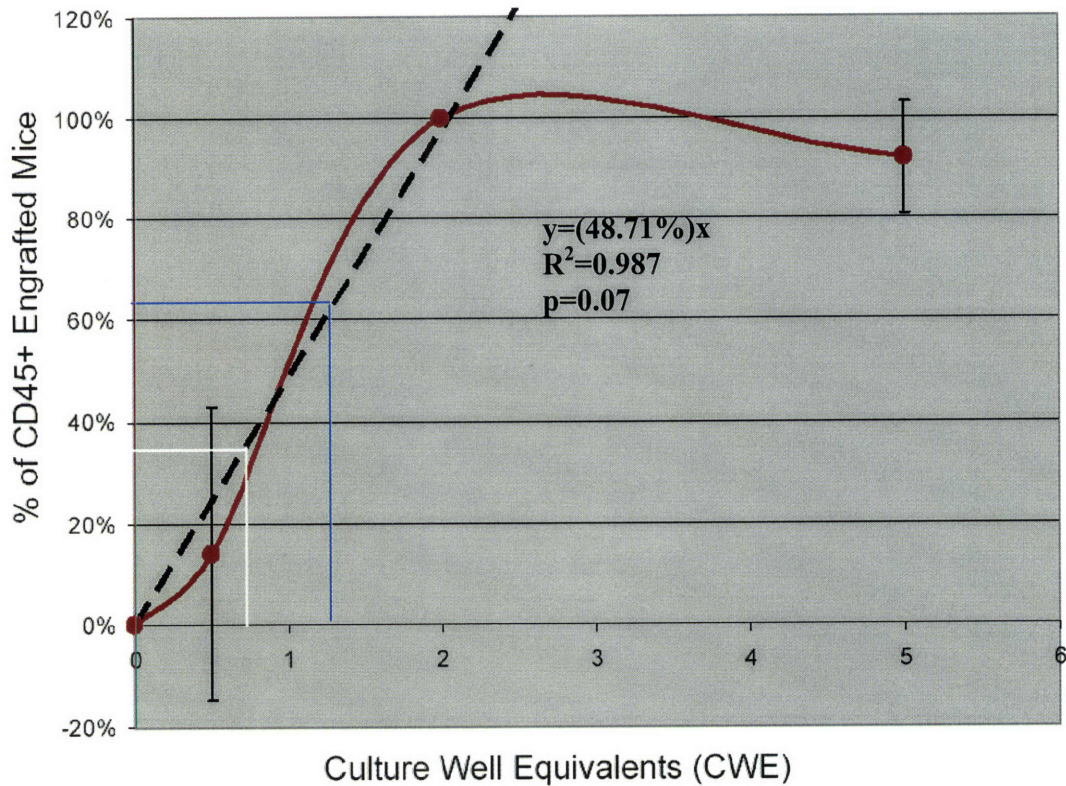
Figure 5.6 | *In Vivo* **Engraftment in the Bone Marrow of NOD/SCID Mice Transplanted with Uncultured CD34⁺ MPB Cells.** Percent of mice engraftment (i.e. engraftment efficiency) is illustrated as a function of culture well equivalents (CWE). Bone marrow cells that express CD45/CD33/CD38 were considered as engrafted. Dotted line exhibits a linear relationship between engraftment efficiency and CWE. White (solid) line represent the CWE of uncultured CD34⁺ MPB cells corresponding to 36% engraftment efficiency, as observed in mice transplanted with Hx-supplemented cells. Blue (solid) line corresponds to 63% engraftment for Poisson statistics. Error bars = standard deviation for n=5 independent animal studies.

115

Bibliographical References

1.   Larochelle, A., Vormoor, J, Lapidot, T, Sher, G, Furukawa, T, Li, Q, Shultz, LD, Olivieri, NF, Stamatoyannopoulos, G, Dick, JE. Engraftment of immune-deficient mice with primitive hematopoietic cells from beta-thalassemia and sickle cell anemia patients: implications for evaluating human gene therapy protocols. *Hum Mol Genet.* **4**, 163-172 (1995).

2.   Kyoizumi, S., Baum, CM, Kaneshima, H, McCune, JM, Yee, EJ, Namikawa R. Implantation and maintenance of functional human bone marrow in SCID-hu mice. *Blood* **79**, 1704-1711 (1992).

3.   Zanjani, E., Ascensao, JL, Harrison, MR, Tavassoli, M. Ex vivo incubation with growth factors enhances the engraftment of fetal hematopoietic cells transplanted in sheep fetuses. *Blood* **79**, 3045-3049 (1992).

4.   Kamel-Reid, S., Dick, JE. Engraftment of immune-deficient mice with human hematopoietic stem cells. *Science* **242**, 1706-1709 (1988).

5.   Cashman, J. D. et al. Kinetic Evidence of the Regeneration of Multilineage Hematopoiesis From Primitive Cells in Normal Human Bone Marrow Transplanted Into Immunodeficient Mice. *Blood* **89**, 4307-4316 (1997).

6.   Nolta, J., Hanley, M. & Kohn, D. Sustained human hematopoiesis in immunodeficient mice by cotransplantation of marrow stroma expressing human interleukin-3: analysis of gene transduction of long-lived progenitors. *Blood* **83**, 3041-3051 (1994).

7.   Pflumio, F. et al. Phenotype and function of human hematopoietic cells engrafting immune- deficient CB17-severe combined immunodeficiency mice and nonobese diabetic-severe combined immunodeficiency mice after transplantation of human cord blood mononuclear cells. *Blood* **88**, 3731-3740 (1996).

8.   Wang, J. C. Y., Doedens, M. & Dick, J. E. Primitive Human Hematopoietic Cells Are Enriched in Cord Blood Compared With Adult Bone Marrow or Mobilized Peripheral Blood as Measured by the Quantitative In Vivo SCID-Repopulating Cell Assay. *Blood* **89**, 3919-3924 (1997).

9.   Fuchs, E., Segre, JA. Stem cells: a new lease on life. *Cell* **100**, 143-155 (2000).

10. Shultz, L. et al. Multiple defects in innate and adaptive immunologic function in NOD/LtSz-scid mice. *J Immunol* **154**, 180-191 (1995).

11. Till, J., McCulloch, E. A direct measurement of the radiation sensitivity of normal mouse bone marrow cells. *Radiat Res* **14**, 1419-1430 (1961).

12. van der Loo, J. C. M. et al. Nonobese Diabetic/Severe Combined Immunodeficiency (NOD/SCID) Mouse as a Model System to Study the Engraftment and Mobilization of Human Peripheral Blood Stem Cells. *Blood* **92**, 2556-2570 (1998).

13. Bhatia, M., Wang, J. C. Y., Kapp, U., Bonnet, D. & Dick, J. E. Purification of primitive human hematopoietic cells capable of repopulating immune-deficient mice. *PNAS* **94**, 5320-5325 (1997).

14. Bernstein, I. D. et al. Treatment of acute myeloid leukemia cells in vitro with a monoclonal antibody recognizing a myeloid differentiation antigen allows normal progenitor cells to be expressed. *Journal of Clinical Investigation* (1987).

15. Terstappen, L., Hollander, Z., Meiners, H. & Loken, M. Quantitative comparison of myeloid antigens on five lineages of mature peripheral blood cells. *J Leukoc Biol* **48**, 138-148 (1990).

16. Deaglio, S. et al. Human CD38 ligand. A 120-KDA protein predominantly expressed on endothelial cells. *J Immunol* **156**, 727-734 (1996).

17. Fleming, W. et al. Functional heterogeneity is associated with the cell cycle status of murine hematopoietic stem cells. *J. Cell Biol.* **122**, 897-902 (1993).

18. Manz, M., Miyamoto, T., Akashi, K. & Weissman, I. Prospective isolation of human clonogenic common myeloid progenitors. *PNAS* **99**, 11872-11877 (2002).

19. Cashman, J. D. & Eaves, C. J. High marrow seeding efficiency of human lymphomyeloid repopulating cells in irradiated NOD/SCID mice. *Blood* **96**, 3979-3981 (2000).

20. Yahata, T. et al. A highly sensitive strategy for SCID-repopulating cell assay by direct injection of primitive human hematopoietic cells into NOD/SCID mice bone marrow. *Blood* **101**, 2905-2913 (2003).

21. Piacibello, W. et al. Engraftment in Nonobese Diabetic Severe Combined Immunodeficient Mice of Human CD34^{+} Cord Blood Cells After Ex Vivo Expansion: Evidence for the Amplification and Self-Renewal of Repopulating Stem Cells. *Blood* **93**, 3736-3749 (1999).

22. Sitnicka, E. et al. Human CD34^{+} hematopoietic stem cells capable of multilineage engrafting NOD/SCID mice express flt3: distinct flt3 and c-kit expression and response patterns on mouse and candidate human hematopoietic stem cells. *Blood* **102**, 881-886 (2003).

23. Madlambayan, G. J. et al. Dynamic changes in cellular and microenvironmental composition can be controlled to elicit in vitro human hematopoietic stem cell expansion. *Experimental Hematology* **33**, 1229-1239 (2005).

Chapter 6
Fluorescence Tracking of Adult Stem Cells (ASCs)

CFP & YFP, but not GFP, Provide Stable Fluorescent Marking of Adult Rat Hepatic Stem Cells

Rouzbeh R. Taghizadeh and James L. Sherley

**Biological Engineering Division,
Biotechnology Process Engineering Center, Center for Cancer Research,
Center for Environmental Health Sciences,
Massachusetts Institute of Technology, Cambridge, MA, 02139**

Key Words: *adult stem cell, green fluorescent protein, GFP toxicity, cyan fluorescent protein, yellow fluorescent protein, differentiation.*

Correspondence: James L. Sherley, M.D., Ph.D., 77 Massachusetts Avenue, 16-743b, Cambridge, MA, 02139, Massachusetts Institute of Technology; Telephone: 617-258-8853; Fax: 617-258-8648; e-mail: jsherley@mit.edu

Abstract

The stable expression of reporter genes in adult stem cells (ASC) has important applications in stem cell biology. The ability to integrate a non-cytotoxic, fluorescent reporter gene into the genome of ASCs with the capability to track the marked ASCs and their progeny is particularly desirable for *in vivo* repopulation studies. The use of fluorescent proteins has greatly aided the investigations of protein and cell function on short time-scales (hours). In contrast, the obtainment of stably expressing cell strains with low variability in expression for use in studies of longer time-scales (months) is often problematic. This difficulty is due, in part, to the cytotoxicity of the most commonly used fluorescent protein, green fluorescent protein (GFP), most importantly in adult stem cells. To avoid GFP-specific toxicity effects and, therefore, obtain stable, long-term expressing fluorescent adult stem cells, we evaluated cyan fluorescent protein (CFP) and yellow fluorescent protein (YFP), in addition to GFP, as cell markers. For these studies, we used adult rat hepatic stem cells expanded in our laboratory. Although we were unable to establish stable GFP-expressing strains, we did obtain stable fluorescent clones (up to 140 doublings) expressing either CFP or YFP. When fluorescently marked ASCs were induced to produce differentiated progeny cells, stable fluorescence expression was observed. This property is essential for future studies to track fluorescently marked ASCs and their differentiated progeny for *in vivo* repopulation studies.

Introduction

Fluorescent proteins have become widely used as viable markers for positively identifying and tracking expressing cells in many *in vitro* and *in vivo* studies. The most widely used, green fluorescent protein (GFP), cloned from *Aequorea victoria*, does not require substrates or cofactors and can be used in a variety of species[1,2]. Among its various uses as a marker, GFP has been used for transient studies of cell apoptosis[3], cytoskeletal dynamics[4], and inhibitory gene expression[5]. Since no cofactors are needed for the native GFP protein to develop fluorescence, it has been possible to use it as a marker in many different organisms. For instance, transgenic *Drosophila melanogaster*[6], zebrafish[7,8], mice[9-12] and rats[13,14] have been successfully produced using wild-type GFP. Although successful in obtaining stable GFP-expressing transgenic animals, attempts to develop *in vitro* cell lines stably expressing GFP have been largely unsuccessful[2,3,15-18].

Currently in adult stem cell (ASC) research, there is a critical need for methods to verify ASCs *in vitro* and track their progeny in *in vivo* repopulation studies. Since markers that uniquely identify ASCs are unknown, the accepted method to confirm the 'stemness' of a cell population is by transplantation of cells into animals after injury to targeted tissues. If ASCs are present at significant levels in the transplanted cell population, the animal survives with repair of the damaged tissue. However, in these experiments, there is uncertainty as to whether the tissue has been repaired by the transplanted cells, by activated resident host ASCs, or by host cells recruited from another tissue source altogether. To overcome these uncertainties, methods to identify the transplanted cells and their descendents have been favored. Ideally, these methods need to identify donor cell progeny independent of subsequent differentiation status.

Though attractive as an *in vivo* tracking tool in ASC repopulation assays, GFP has several drawbacks. One shortcoming of GFP is that it can induce cell death. Intense excitation of the protein *in vitro* for extended periods can generate free radicals that are quite toxic to cells[15]. The inability to obtain constitutively expressing GFP cell strains may also be related to DNA methylation effects. In the presence of an irreversible inhibitor of methyl transferase, C3A human hepatoblastoma cells transfected with GFP showed a significantly greater retention of GFP expression and exhibited higher levels of GFP production[19]. As a result, GFP has been more successfully used extensively as a

viable marker for mostly short time-scale experiments (hours), whereas attempts to establish long-term (months) GFP-expressing cell strains have been mostly unsuccessful[2,3,15-18]. The reported efficiency of establishing stable, constitutively expressing cell lines is extremely low[18].

GFP-expressing transgenic mice are readily available[9-12] and are a possible source for GFP-labeled cells. These mice are uniformly green with the exceptions of hair and red blood cells. However, there are still barriers to their use as a source of fluorescently marked ASCs. One major drawback is that, for many tissues, methods do not exist for efficient isolation of ASCs. Additionally, GFP-transgenic mice do not offer a solution for tracking ASCs derived from other species for which transgenic technology has not been developed.

Due to similar difficulties in developing adult stem cells with constitutive GFP expression, we evaluated two variants of GFP, cyan fluorescent protein (CFP) and yellow fluorescent protein (YFP) that have different excitation-emission profiles and, therefore, may have less toxicity associated with their free radical by-products. An early screen of *A. victoria* mutants produced CFP which has an emission spectrum below that of GFP due to a $Tyr^{66} \rightarrow Trp^{66}$ substitution[20,21]. Similarly, YFP has been rationally designed on the basis of the GFP crystal structure to red-shift the absorbance and emission spectra with respect to GFP. Based on these differences, we evaluated whether CFP and YFP might allow for stable, long-term fluorescence in adult hepatic stem cells derived in our laboratory. We were able to establish stable, long-term expressing ASC strains. When these fluorescently marked ASCs were induced to produce differentiated progeny cells, stable expression of fluorescence was maintained. Our findings indicate that CFP and YFP are more suitable markers for ASC studies *in vitro* and predict that they will be better markers for *in vivo* studies, as well.

Materials & Methods

Cells

Previously derived[22] adult rat hepatic stem cell strain, Lig-8, was maintained in Dulbecco's Modified Eagle Medium (DMEM; Life Technologies, Carlsbad, CA, USA) supplemented with 10% dialyzed fetal bovine serum (DFBS, JRH Biosciences, Lenexa,

KS), 1% Penicillin/Streptomycin (Life Technologies, Carlsbad, CA, USA), and 400μM xanthosine (Xs; Sigma-Aldrich, St. Louis, Missouri, USA) in a 37°C humidified incubator with a 5% CO_2 atmosphere.

Plasmids

Amplified plasmids for transfection were isolated by Qiagen (Valencia, CA, USA) column fractionation as specified by the supplier and further purified by cesium chloride equilibrium density gradient centrifugation. Transfections were performed using 5 μg of pEGFP-N3 vector plasmid (Clontech Laboratories, Palo Alto, CA, USA) under the control of a cytomegalovirus (CMV) promoter. In addition, the pEGFP-N3 vector contains a neomycin resistance gene insert under the control of the simian virus-40 (SV40) promoter conferring resistance to the antibiotic Genetecin™ (Life Technologies, Carlsbad, CA, USA). The CFP and YFP derivatives of pEGFP-N3 were prepared by digestion and complete removal of the EGFP insert using BamH1 and Not1 endonucleases (New England Biolabs, Beverly, MA, USA). The respective CFP or YFP insert was ligated into the vector after gel purification.

Transfection

Lig-8 cells were seeded at 1/10th confluency in a 75-cm² flask (Corning, Corning, NY, USA) one day prior to transfection. Lig-8 cells were then independently transfected with the CFP, YFP or GFP expression plasmids using Cytofectene (BioRad Laboratories, Hercules, CA, USA), per manufacturer's suggested instructions. Approximately 1.5 x 10⁶ cells (1/5th confluency in 75-cm² flask) were transfected for 16-20 hours and then given two phosphate buffer saline (PBS) washes, followed by supplementation with regular growth medium. The transfected cells were cultured for an additional 42-48 hours. After this time period, the transfected cells were replated at 1/6th density in parallel in 10–cm² plates (Corning, Corning, NY, USA). After overnight culture, the culture medium was replaced with medium supplemented to 0.5 mg/ml Genetecin™ to select for stably transfected cell clones.

Clonal Cell Viability

Propidium iodide (PI; Sigma, St. Louis, MO, USA) was added directly to media and cells at 5 μg/ml to determine viability of clonal cells at 14 days of culture. A Nikon super high pressure mercury lamp was used to image PI cells using a Nikon epifluorescent microscope.

Derivation of Fluorescent Protein-Expressing Clones

After 14 days in culture, transfected cells from each 10-cm^2 plate were trypsinized and each transferred into a 75-cm^2 flask with selection medium maintained thereafter. After two days, the transfected cells were re-seeded at 1000 cells each into five individual 10-cm^2 dishes. Resistant colony formation was assessed after 10-14 days of culture in selection medium, with medium changes every 3 days. After this time, colonies were counted and scored as non-expressing (B1; 0% of cells in the colony were expressing fluorescent protein), semi-expressing (B2; estimated 25-75% of cells in the colony were expressing fluorescent protein) or fully-expressing (B3; $\cong$ 100% of the cells in the colony were expressing fluorescent protein). Several isolated colonies were selected within cloning cylinders (Bellco Glass, Vineland, NJ, USA), harvested by trypsinization, transferred to 25-cm^2 flasks (Corning, Corning, NY, USA), and allowed to expand for 10-14 days, until the flask was >90% confluent. At that point, cells from the 25-cm^2 flasks were trypsinized and transferred into a 75-cm^2 flasks. Within 3-4 days, the flasks were 90% confluent. After trypsinization, ~80% of the cells in cultures of expanded clones were frozen in liquid nitrogen[22] for early passage stocks. The remaining cells were maintained in culture and passaged for at least 24 weeks (estimated 140 population doublings). Three of the CFP-expressing clonal strains, B1-X, B2-X and B3-X, were subsequently evaluated for this study.

Flow Cytometry and Fluorescence Microscopy

A FACStar Plus™ flow cytometer (Becton, Dickinson and Company, Franklin Lakes, NJ, USA) was used to quantify the fraction of fluorescent cells in populations. The FACStar Plus was equipped with two coherent Innova 90 lasers for visible and ultraviolet argon lines. Data acquisition and analyses were performed with Cell Quest

software (Becton, Dickinson and Company, Franklin Lakes, NJ, USA) and Summit analyses software (Cytomation, Inc, Fort Collins, CO), respectively. The non-transfected parent Lig-8 ASC strain was used as a negative control for all analyses to account for background cell auto-fluorescence. Cell populations were analyzed using both flow cytometry and epifluorescence microscopy using a Nikon TE300 microscope system with DAPI/GFP/CFP/YFP filters. A Hamamatsu digital camera and OpenLab imaging system were used for digital imaging.

Differentiation Induction

Cells were treated for 9 days with 20 ng/ml epidermal growth factor (EGF) and 0.5 ng/ml transforming growth factor β (TGF-β) (Life Technologies, Carlsbad, CA, USA), in the same culture medium, except that the DFBS was reduced to 1%. The details of the differentiation induction protocol will be reported elsewhere[23].

<u>**Results**</u>

Using CFP, YFP or GFP as independent fluorescent protein markers, we transfected respective expression plasmids into a previously described rat hepatic ASC strain, Lig-8[22]. Asymmetric self-renewal associated with asymmetric cell kinetics is the defining feature of ASCs[22,24]. Lig-8 cells were derived based on their asymmetric cell kinetics[24]. Lig-8 cells asymmetrically self renew, cycle with asymmetric cell kinetics, and produce differentiated progeny with mature hepatocyte properties[22,25]. The differentiated progeny cells express transcription factors and protein antigens that are specific for hepatocyte development and maturation, respectively. Hepatocyte-specific phenotypes include binucleation, albumin secretion, and expression of inducible cytochrome P450s[22,25]. Consistent with their ASC character, Lig-8 cells divide and produce one daughter that responds to TGF-β (transforming growth factor- β) induced differentiation, whereas the other, stem cell daughter is insensitive[23]. The same asymmetric self-renewal property was observed when hepatocytic maturation of differentiating progeny was induced in three-dimensional hydrogels[25]. Based on well-defined ASC properties, Lig-8 cells were ideal for evaluation of effects of GFP, CFP, and YFP in ASCs.

We found that transfections with the GFP gene construct yielded transfected colonies 50-fold less efficiently than transfections with the analogous CFP- or YFP-gene constructs (Table 6.1). In addition, the GFP-transfected cultures gave rise to no long-term cell strains, whereas both CFP- and YFP- transfected clones had 100% clonability (Table 6.1). Furthermore, it was determined that cells that were transiently-expressing GFP appeared to be undergoing cell death, as GFP-expressing cells were simultaneously positive for propidium iodide (PI) (Figure 6.1). PI is impermeable to intact membranes but readily penetrates the membranes of non-viable cells and binds to DNA or RNA, causing orange fluorescence. The cells eventually rounded up and detached from the culture dish, while still expressing GFP and PI (Figure 6.1). Expanded CFP and YFP clones expressed the respective fluorescent proteins stably for at least 24 weeks in culture (~ 140 doublings; e.g., CFP in Figure 6.2). Clones that were successfully derived exhibited a range of CFP- or YFP- expressing cell fractions. As a result, these clones were characterized as non-expressing (B1; 0% of cells in the colony express fluorescent protein, *data not shown*), semi-expressing (B2; at least 25-75% of cells in the colony expressed fluorescent protein, but not all [Figure 6.3 a-f]); or fully-expressing (B3; approximately 100% of the cells in the colony expressed fluorescent protein [Figure 6.3 g-l]). Although cell strains were derived from both CFP and YFP expressing colonies, only CFP cell strains were further evaluated.

Although, as colonies, the CFP-expressing cell strains exhibited the fluorescent properties described, with further propagation in culture, the fluorescence for one of the transfected clones decreased (B2-X in Figure 6.2). Moreover, cells derived from an initially non-expressing B1 colony began to express CFP (Figure 6.2; B1-X) at levels comparable to continuously, fully-expressing B3 clones (Figure 6.2; B3-X) during clonal propagation. Qualitatively, the B2-X and B3-X CFP-expressing clones maintained their initially observed fluorescent properties. Although there was some variation in expression seen in the early stages of clonal analysis, expression stabilized with propagation and low variability was observed for at least 24 weeks (estimated 140 population doublings). B2-X exhibited the greatest fluctuation in fluorescence expression (Figure 6.2), but did not change in its basic character.

Stable fluorescent protein expression did not alter the essential properties of the parent adult hepatic stem cell strain, Lig-8 (*data not shown*). We have found that, because of their asymmetric self-renewal property, the parent Lig-8 hepatic ASCs are resistant to complete differentiation by TGF-β, EGF and serum deprivation[23]. Under conditions of TGF-β, the cells produce differentiated progeny cells by asymmetric cell divisions that allow them to retain their undifferentiated ASC state[23]. To evaluate CFP expression in differentiated progeny cells, the three CFP expressing fluorescent ASC strains (B1-X, B2-X and B3-X) were examined after culture under EGF/TGF-β-induced differentiation conditions. All strains exhibited similar morphological and cell kinetic properties observed for the non-transfected parental Lig-8 strain (*data not shown*). As observed in Figure 6.4, the B3-X cell clone under normal conditions yielded a uniform culture (a-c), whereas under differentiation conditions, the culture yielded a heterogeneous collection of varying morphological cell types. Specifically, there were production of cells that had relatively larger morphology (Figure 6.4, d-f; arrows), with respect to the culture under normal conditions.

The level of CFP expression after induction of differentiated progeny did not vary significantly relative to the normal (undifferentiated) conditions for the B1-X clones which became positive during its expansion (Figure 6.2). However, although exhibiting stable fluorescence expression under differentiating conditions, B1-X and B3-X cells displayed a statistically significant increase [60% (p<0.0091) and 91% (p<0.0018), respectively) in median fluorescence under differentiating conditions (60% and 91%, respectively). However, the B2-X and B3-X clones showed small (15% and 9%, respectively) but statistically significant (p<0.027 and p<0.019, respectively) reductions in fluorescent cell fractions (Figure 6.5). Thus, although the three cell strains were derived from three independent clones and displayed differing fluorescent cell fractions (Figure 6.3), their fluorescence fraction did not vary by more than 15% when differentiated progeny cells were produced (Table 6.2). The estimated fraction of differentiated progeny in these experiments is ≥ 80%[23], indicating that a majority of differentiated cells retain a high level of fluorescence.

Discussion

    This report is a first study to look at GFP-, CFP-, and YFP-transgenes in side-by-side experiments in the same ASC strain. We evaluated the use of these transgenes for the derivation of stable, long-term fluorescence-expressing adult hepatic stem cell clones. We were able to attain transient GFP-expressing clones, but due to either the toxicity and/or methylation associated with GFP, were unable to propagate these clones as stable, long-term GFP-expressing hepatic ASC strains (Table 6.1). Given the failure to even establish clones from colonies with extinguished GFP fluorescence, cytotoxicity seems to be the primary problem.

    GFP gene transfections gave rise to transient expressing cells for up to 72-96 hours post-transfection (Figure 6.1 a-b, d-e, g-h). As the culture continued, intact, adherent cells positive for GFP-expression began to round up, detach and lose viability, indicated by propidium iodide (PI) (Figure 6.1 c, f, i). Eventually, every adherent, GFP-expressing cell rounded up, became suspended, and was positive for PI (Figure 6.1, j-l). Although these experiments were done with three varying GFP plasmid constructs, the most success was obtained at 72-96 hours post-transfection. Needless to say, all attempts yielded no stable, GFP-expressing cell lines. These observations, cumulatively, suggest that the GFP protein is toxic to the cells, as a strong, inverse correlation is observed between GFP expression and cell viability.

    Other studies[15,16] have obtained similar results using various GFP plasmids. One group in particular[15] examined several variants of GFP plasmids resulting in many of the GFP-expressing cells contracting, rounding-up and dying, which was confirmed by decreasing luciferase activity and increasing CPP32-activity, a cysteine protease that plays a direct role in the proteolytic digestion of cellular proteins responsible for progression to apoptosis.

    Our work with GFP confirms that the GFP protein product has toxic side-effects in at least one type of ASC, whereas the CFP and YFP protein, translated from the same plasmid vector construct is well tolerated by these cells. This conclusion can also explain the transfection efficiency and clonability data derived in our analyses. Table 6.1 summarizes the relative transfection efficiency and clonal expansion outcomes for the various fluorescent proteins studied in our work. Since transfection efficiency is an

indicator of success for the transfer and integration of genes into cells, it is possible that due to GFP-related toxicity, both CFP- and YFP-genes transfect the adult hepatic stem cells approximately 47- and 45-fold better, respectively, than the analogous GFP gene. Cloning efficiency (clonability) data further confirms the difficulties observed with stable, long-term transduction with GFP; since 100% of CFP- and YFP- clones gave rise to cell strains, whereas none of the GFP-derived colonies gave rise to stable clones (Table 6.1). This is further evidence that due to GFP-dependent toxicity, GFP cannot be utilized as a stable fluorescent reporter in these adult hepatic stem cells.

In contrast, the acquisition of both CFP- and YFP-expressing hepatic ASC derivatives (Figure 6.3) was straightforward. Due to initial variability in fluorescence expression fraction, several clones were selected that represented the population's range of expression frequency. The designated ranges of expression were non-expressing (B1), semi-expressing (B2) or fully-expressing (B3; Figure 6.2 & Figure 6.3). The differing frequencies of expression might be due to early random extinction events in the growth of single cell clones or due to the action of specific CFP and YFP inhibitors. When CFP-expressing clones were further propagated to develop strains, one non-expressing B1 clone began to express CFP at high-levels (Clone B1-X; Figure 6.2; Table 6.2). This may have occurred due to the loss of initial CFP inhibition in the clonal cell or because of a very low rate of stable gene expression. Additionally, due to the short time period in which this phenotypical change occurred (i.e., within 6 population doublings), the explanation of rare fluorescent contaminants can be ruled out. It is unlikely that a few fluorescent cells would have adequate time to proliferate sufficiently to give rise to a predominantly fluorescent culture in such a short period of time. Although it is reasonable that this fluctuation in fluorescence expression could have occurred in initially non-GFP-expressing clones, it is unlikely since this was not observed in numerous trials and clones. Additionally, if cells began to express GFP, it is unlikely that the cells would have survived, as suggested from our transiently-derived GFP clones.

The remaining CFP-expressing cell clones, B2-X and B3-X, maintained their initial fluorescence properties throughout their examined 24 week time period in culture (Figure 6.2). All three cell clones retained a high level of fluorescent expression at 24 weeks of culture (approximately 140 population doublings), even though clone B1-X

initially showed decreasing expression (Figure 6.2). Not surprisingly, the semi-expressing B2-X cell strain exhibited greater variation in its CFP-expression, since this culture contains the greatest mixture of fluorescent- and non-fluorescent expressing cells (Figure 6.3).

Our success in deriving stable, fluorescence-expressing cell strains with CFP or YFP, and failure with GFP may be due to differences in the emission spectra between the proteins. It is possible that free-radicals are not formed in the case of CFP and YFP; but if they are generated, they may exist in lower amounts compared to GFP for the same amount of excitation energy. Another possible explanation is that the radicals formed in the case of CFP and YFP are imbedded in the protein, preventing reactivity with other vital cellular nucleophiles (e.g. DNA, proteins). Additionally, CFP- and YFP-radicals may be more efficiently quenched and, therefore, deactivated by other molecules in the cell. Even so, it seems paradoxical that it is possible to derive stable transgenic GFP-expressing animals[9-12] but not stable expressing cultured cells. However, cells in culture may have insufficient compounds that quench free radicals. *In vivo*, organ systems like the liver may supply a sufficient quantity of such compounds (e.g. quinones, glutathione) to counter effects of GFP-dependent free radical formation. However, there is evidence that over-expression of GFP in transgenic mice can cause dilated cardiomyopathy[26] and may compromise developmental competence of embryos[27].

When the CFP-expressing cell strains (B1-X, B2-X and B3-X) were placed under differentiation conditions after 120 doublings, either no or only modest reductions in fluorescence cell fractions were observed relative to normal culture conditions (Figure 6.5; Table 6.2). However, although exhibiting stable fluorescence expression under differentiating conditions, B1-X and B3-X cells displayed a statistically significant increase [60% ($p<0.0091$) and 91% ($p<0.0018$), respectively) in median fluorescence under differentiating conditions (60% and 91%, respectively). This increase in fluorescence may be directly related to an increase in the median cell size of the population, since it has been observed that as Lig-8 cells differentiate, they produce large hepatocytes[23] (Figure 6.4, d-f; arrows). Nonetheless, this stability in fluorescence is important, since it suggests that CFP is expressed independent of the differentiation state of progeny cells. Stable fluorescence expression in our *in vitro* differentiation studies is a

valid predictor of stable expression in *in vivo* differentiation, since TGF-β is a ubiquitous differentiation growth factor, especially in the liver[28]. The high stability in fluorescence expression under both normal and differentiating conditions can ideally be used in transplantation studies to evaluate the *in vivo* repopulation properties of these cells.

The importance of this report is underscored by recent reports concluding statistically significant amplification of hematopoietic stem cells by forced expression of specific genes. For instance, the gene transfer of the *HOXB4* gene into human hematopoietic stem cells (HSCs) was reported to result in an overall approximately 2-fold increase in total and CD34$^+$ cells, normalized to a transfer of a control EGFP gene construct[29]. This 2-fold increase and eventual significant overall increase in *in vivo* repopulation efficiency caused by *HOXB4* regulation could be interpreted as the result of increased cell death in EGFP-controls due to fluorescent toxicity and not due to the expansion of HSCs using *HOXB4* regulation, as suggested. Similarly, in another report using recombinant HIV transactivating (TAT)-HOXB4 protein[30], TAT-GFP was used as a control for the *in vivo* expansion and pluripotency of HSCs. It was concluded that TAT-GFP was ineffective in supporting HSC expansion, whereas TAT-HOXB4 resulted in a net expansion of 20-fold over control values. Again, this data may be interpreted as resulting from the toxicity-dependent effects of the GFP gene, used as the control for gene transfer.

Availability of stable, long-term marked ASCs has important applications in advancing the ASC biology field. Currently, there are no tissue-specific ASC markers that would allow for easy characterization and validation. One example is the expansion of HSCs in culture, currently a major obstacle in the field. Although markers have been found that promote enrichment of ASCs from specific tissues[31,32], these are not sufficient for determining the 'stemness' in any general sense. Currently, the main method that is used to establish the 'stemness' of an ASC population is transplantation of cells into animals and determination of whether the cells can regenerate damaged tissues. However, our group is currently working to develop *in vitro* functional identifiers[22-24].

In some tissue models, determining repopulation efficiency is simpler than in others. For bone marrow repopulation studies, the output metric is reconstitution of viable recipient animals after donor cell transplant. Few ASC studies have this ideal feature of

functional reconstitution. Most of these studies depend on *in vivo* cell histology to indicate effective tissue repopulation. Studies of this sort have led to debates regarding issues of ASC plasticity[33]. If a faithful cell marker is not tracked in transplanted ASCs, then uncertainty arises; since it is not clear whether the transplanted cells or host cells are responsible for results. In some tissue models, such as the liver, where the tissue has the capacity for active proliferation, tracking of transplanted cells is even more crucial. The described method will allow for the development of stable, long-term fluorescence-expressing ASCs in culture will greatly assist in resolving current controversial issues, including ASC plasticity in animal repopulation assays.

Notwithstanding the current controversy regarding ASC plasticity and cell fusion[33-35], our findings with GFP call for re-evaluation of conclusions based on the transduction of GFP-transgenes into manipulated ASC populations. Additionally, our findings establish important quality control concepts for developing and implementing methods and tools for future ASC therapeutics that employ gene transfer. Our experience highlights the importance of careful *in vitro* characterization of genetically marked cell populations before transplant.

Fluorescent Marker	Avg. Colony Number/ 10-cm^2 dish	Relative Transfection Efficiency	Number of Clones Picked	Number of Cell Strains Derived	Cloning Efficiency
GFP	1.3 (n=10)	0.02	8	0	0%
CFP	64 (n=3)	1.00	6	6	100%
YFP	61 (n=3)	0.95	6	6	100%

Table 6.1 | Relative transfection efficiency of fluorescent gene markers and cloning efficiency of selected transfected cell colonies. Transfection efficiency is defined as the average number of colonies/ number of cells transfected/μg DNA. Cloning efficiency (clonability) is defined as the number of cell lines derived/number of clones picked.

Condition	% CFP Fluorescence (mean ± SD; n=2)
B1-X	
Undifferentiated	94 ± 0.02
Differentiated	94 ± 0.88
B2-X	
Undifferentiated	33 ± 1.6
Differentiated	28 ± 0.87
B3-X	
Undifferentiated	87 ± 0.32
Differentiated	79 ± 2.3

Table 6.2 | Quantitative comparison of the CFP-fluorescent cell fractions of cultures under undifferentiated and differentiated conditions. Flow cytometry quantification of the R2 region of flow histograms (as shown in Figure 6.5) for three fluorescent cell clones (same as Figure 6.2). Data are the average % fluorescent cells at 24 weeks in cultures ± standard deviation (SD). Cells were analyzed under normal culture conditions (undifferentiated) and under conditions that increase differentiated progeny (differentiation), as described in the text.
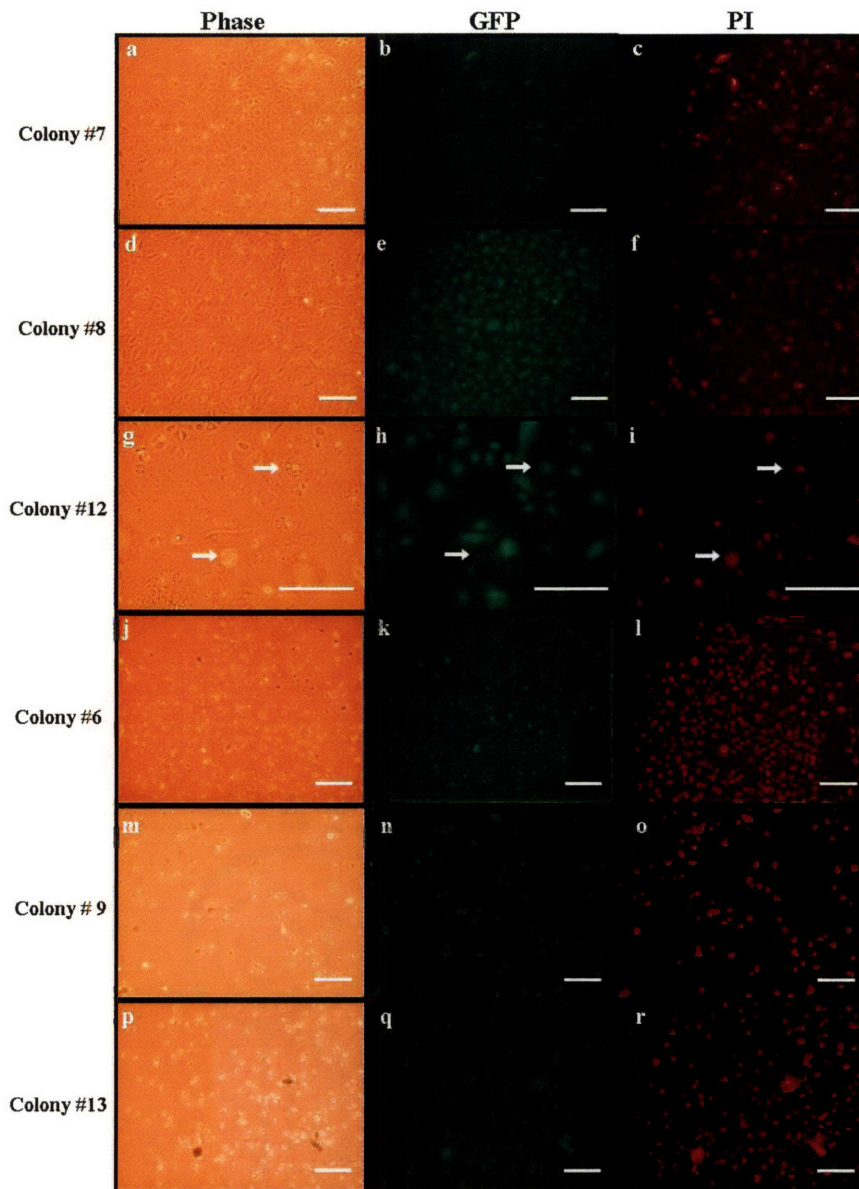
Figure 6.1 | Transient, short-term expression of GFP fluorescence expression of the hepatic adult stem cell strain, Lig-8 due to GFP cytotoxicity. Adult hepatic stem cell strain, Lig-8, was transfected with the pEGFP-N3 expression vector. Shown are images of 6 independent colonies transiently expressing Lig-8 GFP cell colonies 72-96 hours post-transfection Shown are the phase (a, d, g, j, m, p), GFP-fluorescent (b, e, h, k, n, q) and propidium iodide (PI) fluorescent (c, f, i, l, o, r) images of 6 GFP-expressing colonies. Arrows indicate cells double-positive for GFP and PI. Scale bar is equivalent to 100 μm.
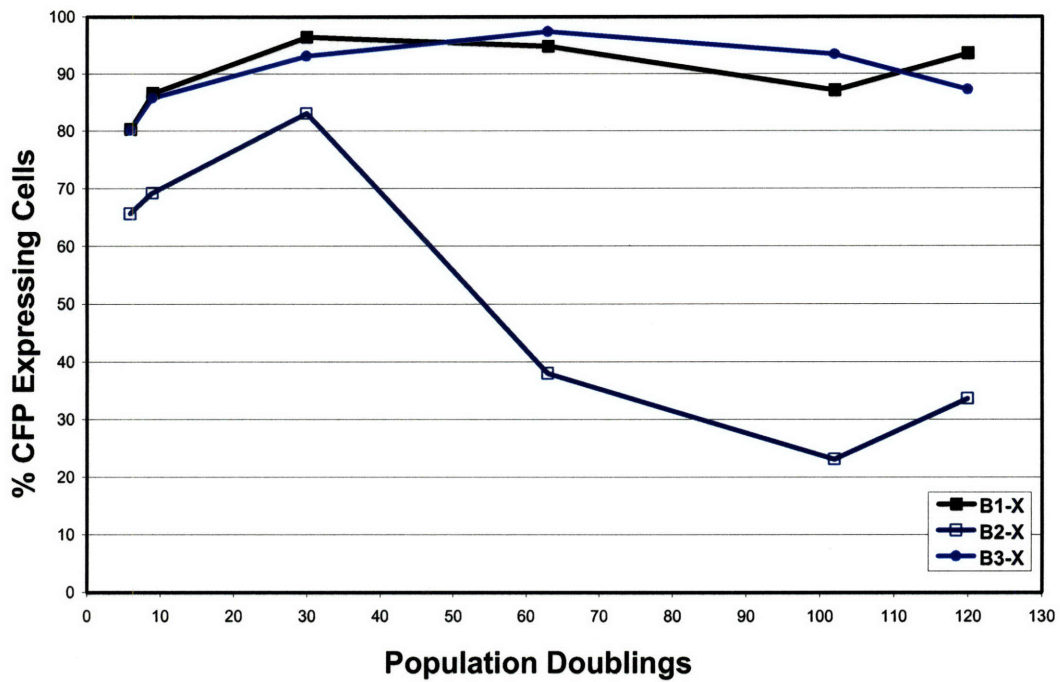
Figure 6.2 | Stable, long-term expression of CFP fluorescence in stably transfected adult stem cell clones. Three cell clones expanded from CFP transfected colonies, B1-X, B2-X and B3-X (as described in text), were propagated and serially analyzed for CFP expression. At the indicated number of population doublings, the percentage of fluorescence-expressing cells was determined by flow cytometry for each specified clone. The cells have been passaged for a maximum of 140 population doublings.

Phase	Fluorescence	Merge
a	b	c

CFP B2

| d | e | f |

YFP B2

| g | h | i |

CFP B3

| j | k | l |

YFP B3
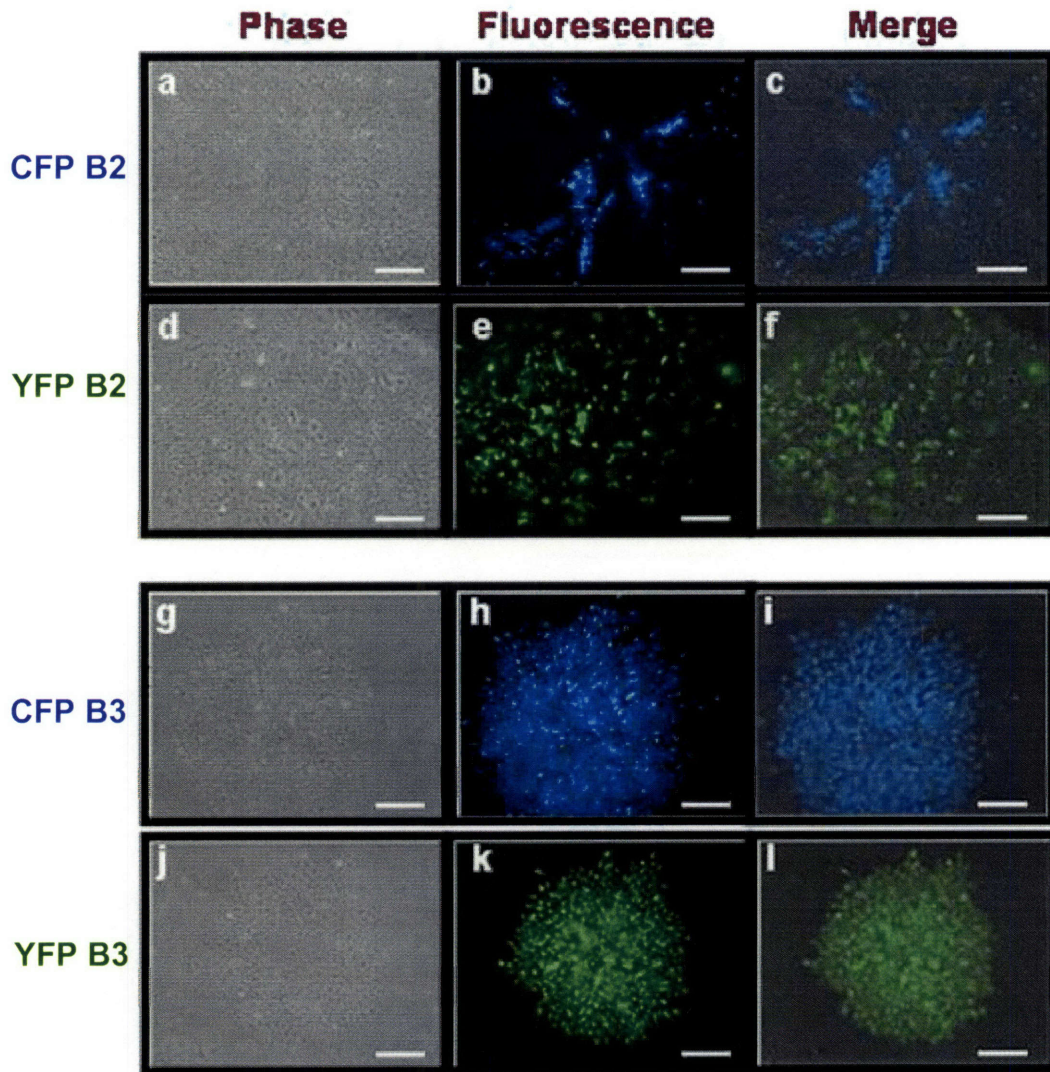
Figure 6.3 | Fluorescent protein (CFP or YFP)-expressing colonies from adult hepatic stem cells. Adult hepatic stem cell strain, Lig-8, was transfected with either a CFP or YFP expression vector. Shown are colonies with approximately 20-75% of the cells expressing (B2) and colonies with essentially 100% of the cells expressing (B3). Shown are the phase (a, d, g, j), fluorescent (b, e, h, k) and merged (c, f, i, l) images of CFP- and YFP- expressing colonies. Scale bar is equivalent to 100 μm.

136
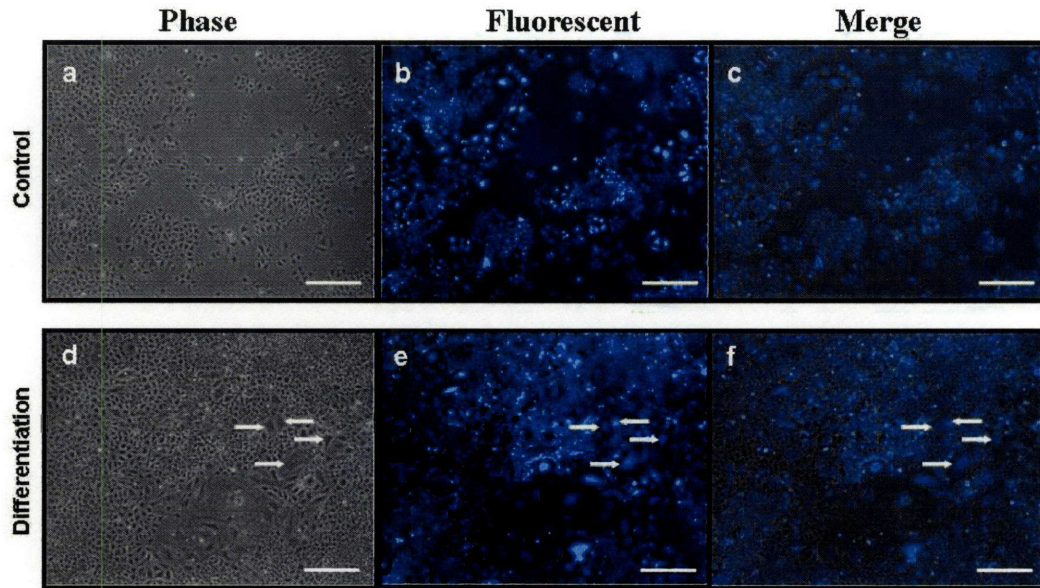
Figure 6.4 | Qualitative comparison of the B3-X CFP-fluorescent cell strain of cultures under undifferentiated and differentiated conditions. B3-X cells were cultured under normal (control) (a-c) and differentiated (d-f; 20 ng/ml epidermal growth factor (EGF) and 0.5 ng/ml transforming growth factor β (TGF-β), in the same culture medium, except that the DFBS was reduced to 1%). culture conditions for 9 days. Shown are phase (a, d), fluorescent (b, e) and merged (c, f) images. Arrows indicate differentiated cells. Scale bar is equivalent to 100 μm.
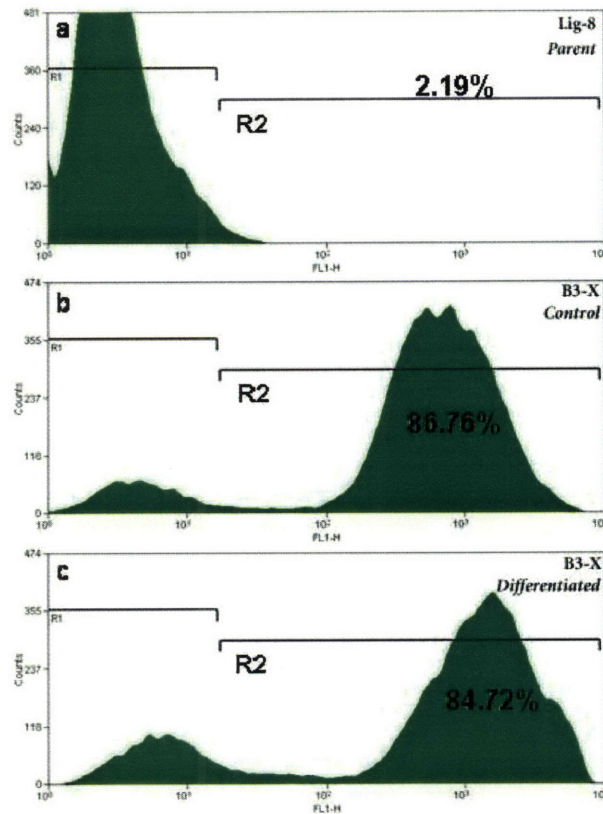
Figure 6.5 | CFP-fluorescence expression of the hepatic adult stem cell (ASC) clone, B3-X, (see also Figure 6.2) is stable after induction of differentiation. Flow cytometry analysis was performed on the non-transfected parent hepatic ASC strain, Lig-8 (a) , and CFP-fluorescent B3-X hepatic ASC cultures, both under undifferentiated(b) and differentiated (c) conditions. Histograms plot the relative numbers of cells as a function of the log-relative CFP fluorescence. The background fluorescence, as defined by non-transfected Lig-8 cells is depicted as the R1 region, and the positive fluorescence is denoted by the R2 region (also see Table 6.2).

138

Bibliographical References

1.   Cody, C., Prasher, D. & Westler, W., et al. Chemical structure of the hexapeptide chromophore of the Aequorea green-fluorescent protein. *Biochemistry* **32(5)**, 1212-8 (1993).

2.   Chalfie, M., Tu, Y. & Euskirchen, G., et al. Green fluorescent protein as a marker for gene expression. *Science* **263(5148)**, 802-5 (1994).

3.   Li, Y. & Horwitz, M. Use of green fluorescent protein in studies of apoptosis of transfected cells. *Biotechniques* **23(6)**, 1026-9 (1997).

4.   Yoon, Y., Pitts, K. & McNiven, M. Studying cytoskeletal dynamics in living cells using green fluorescent protein. *Mol Biotechnol* **21(3)**, 241-250 (2002).

5.   Zeng, Y., Somasundaram, K. & Prabhu, N., et al. Detection and analysis of living, growth-inhibited mammalian cells following transfection. *Biotechniques* **23(1)**, 88-94 (1997).

6.   Wang, S. & Hazelrigg, T. Implications for bcd mRNA localization from spatial distribution of exu protein in Drosophila oogenesis. *Nature* **369(6479)**, 400-03 (1994).

7.   Amsterdam, A., Lin, S. & Hopkins, N. The Aequorea victoria green fluorescent protein can be used as a reporter in live zebrafish embryos. *Dev Biol* **171(1)**, 123-9 (1995).

8.   Peters, K., Rao, P. & Bell, B., et al. Green fluorescent fusion proteins: powerful tools for monitoring protein expression in live zebrafish embryos. *Dev Biol* **171(1)**, 252-7 (1995).

9.   Takada, T., Iida, K. & Awaji, T., et al. Selective production of transgenic mice using green fluorescent protein as a marker. *Nature Biotech* **15** (1997).

10.   Ikawa, M., Kominami, K. & Yoshimura, Y., et al. Green fluorescent protein as a marker in transgenic mice. *Devel. Growth Differ* **37**, 455–459 (1995).

11.   Ikawa, M., Kominami, K. & Yoshimura, Y., et al. A rapid and non-invasive selection of transgenic embryos before implantation using green fluorescent protein (GFP). *FEBS Lett* **375(1-2)**, 125-8 (1995).

12.   Okabe, M., Ikawa, M. & Kominami, K., et al. 'Green mice' as a source of ubiquitous green cells. *FEBS Lett* **407(3)**, 313-9 (1997).

13.   Hakamata, Y., Tahara, K. & Uchida, H., et al. Green Fluorescent Protein-Transgenic Rat: A Tool for Organ Transplantation Research. *Biochemical and Biophysical Research Communications* **286**, 779-785 (2001).

14. Kisseberth, W. C., Brettingen, N. T. & Lohse, J. K., et al. Ubiquitous Expression of Marker Transgenes in Mice and Rats. *Developmental Biology* **214**, 128-138 (1999).

15. Liu, H., Jan, M. & Chou, C., et al. Is green fluorescent protein toxic to the living cells? *Biochem Biophys Res Commun* **260(3)**, 712-7 (1999).

16. Lybarger, L., Dempsey, D. & Franek, K., et al. Rapid generation and flow cytometric analysis of stable GFP-expressing cells. *Cytometry* **25(3)**, 211-20 (1996).

17. Kromenaker, S. & Srienc, F. Stability of producer hybridoma cell lines after cell sorting: a case study. *Biotechnol Prog* **10(3)**, 299-307 (1994).

18. Zeyda, M., Borth, N. & Kunert, R., et al. Optimization of sorting conditions for the selection of stable, high-producing mammalian cell lines. *Biotechnol Prog* **15(5)**, 953-7 (1999).

19. Hong, K., Sherley, J. & Lauffenburger, D. Methylation of episomal plasmids as a barrier to transient gene expression via a synthetic delivery vector. *Biomol Eng* **18(4)**, 185-92 (2001).

20. Tsien, R. The green fluorescent protein. *Annu Rev Biochem* **67**, 509-44 (1998).

21. Heim, R., Prasher, D. & Tsien, R. Wavelength mutations and posttranslational autoxidation of green fluorescent protein. *Proc Natl Acad Sci U S A* **91(26)**, 12501-4 (1994).

22. Lee, H., Crane, G. & Merok, J., et al. Clonal expansion of adult rat hepatic stem cell lines by suppression of asymmetric cell kinetics (SACK). *Biotechnol Bioeng* **83(7)**, 760-71 (2003).

23. Crane, G. & Sherley, J. in preparation. (2004).

24. Sherley, J. Asymmetric cell kinetics genes: the key to expansion of adult stem cells in culture. *ScientificWorldJournal* **2**, 1906-1921 (2002).

25. Semino, C. E., Merok, J. R. & Crane, G. G., et al. Functional differentiation of hepatocyte-like spheroid structures from putative liver progenitor cells in three-dimensional peptide scaffolds. *Differentiation* **71**, 262-270 (2003).

26. Huang, W., Aramburu, J. & Douglas, P. Transgenic expression of green fluorescence protein can cause dilated cardiomyopathy. *Nat Med.* **6**, 482-483 (2000).

27. Devgan, V., Rao, M. R. S. & Seshagiri, P. B. Impact of embryonic expression of enhanced green fluorescent protein on early mouse development. *Biochemical and Biophysical Research Communications* **313**, 1030-1036 (2004).

28. Sanchez, A., Pagan, R. & Alvarez, A., et al. Transforming Growth Factor-[beta] (TGF-[beta]) and EGF Promote Cord-like Structures That Indicate Terminal Differentiation of Fetal Hepatocytes in Primary Culture. *Experimental Cell Research* **242**, 27-37 (1998).

29. Amsellem, S., Pflumio, F. & Bardinet, D., et al. Ex vivo expansion of human hematopoietic stem cells by direct delivery of the HOXB4 homeoprotein. *Nat Med.* **9**, 1423-1427 (2003).

30. Krosl, J., Austin, P. & Beslu, N., et al. In vitro expansion of hematopoietic stem cells by recombinant TAT-HOXB4 protein. *Nat Med.* **9**, 1428-1432 (2003).

31. Uchida, N. & Weissman, I. Searching for hematopoietic stem cells: evidence that Thy-1.110 Lin- Sca-1$^+$ cells are the only stem cells in C57BL/Ka-Thy-1.1 bone marrow. *J. Exp. Med* **175**, 175-184 (1992).

32. Spangrude, G., Heimfeld, S. & Weissman, I. Purification and characterization of mouse hematopoietic stem cells. *Science* **241**, 58-62 (1989).

33. Wagers, A., Sherwood, R. & Christensen, J., et al. Little evidence for developmental plasticity of adult hematopoietic stem cells. *Science* **297(5590)**, 2256-9 (2002).

34. Wagers, A. & Weissman, I. Plasticity of adult stem cells. *Cell* **116**, 639-648 (2004).

35. Camargo, F. D., Chambers, S. M. & Goodell, M. A. Stem cell plasticity: from transdifferentiation to macrophage fusion. *Cell Prolif* **37**, 55-65 (2004).

Chapter 7

Conclusions

Fundamental challenges in the hematopoietic stem cell (HSC) field are impeding the full clinical potential that HSCs possess. Technical barriers include lack of markers expressed exclusively on HSCs, resulting in a lack of specificity in detecting HSCs *ex vivo*; and biological barriers consist of low numbers of HSCs *in vivo*, challenges in mimicking the HSC microenvironment *ex vivo*, and the overlooked HSC kinetics barrier: self-renewal through asymmetric cell kinetics (ACKs). Taken together, these obstacles yield problems in developing strategies to promote the *ex vivo* expansion of HSCs. The main hypothesis for this thesis research was that, in order to expand HSCs *ex vivo*, the fundamental property of all adult stem cells (ASCs), like HSCs, must be overcome: asymmetric cell kinetics. By understanding the critical challenges in the HSC field, this research focused on investigation of a suppression of cell kinetics (SACK) method as a means to promote *ex vivo* expansion of human HSCs.

Previous attempts to expand HSCs *ex vivo* focused on varying cocktails of hematopoietic growth factors (GFs) and cytokines in order to effectively increase HSC numbers. However, this approach, at best, preserved HSC survival, while simultaneously promoting extensive proliferation of hematopoietic progenitor cells (HPCs). Investigations of SACK under these culture conditions resulted in a 1.5-fold reduction in total cell number and 1.6-fold increase in the fraction of the population expressing CD133. This suggested, as proposed, that SACK agents affect the cell kinetics of HSCs in HSC-enriched cell populations. However, no overall increase in SACK-dependent $CD133^+$ cell number was observed. This finding might have indicated lack of sensitivity in detecting SACK-dependent changes in $CD133^+$ HSCs. Consequently, the SACK method was investigated in conditions that allowed for increased sensitivity in detecting SACK-dependent increases in $CD133^+$ HSCs. This was accomplished by culturing $CD34^+$ MPB cells in a GF-starved environment. There was a basis to consider that HSCs were insensitive to GF depletion. On the other hand, HPCs were completely dependent on GFs. Therefore, this consideration allowed for a unique opportunity to selectively enrich for HSCs in culture. For the first time, a 2.5-fold SACK-dependent increase in

CD133$^+$ HSCs was observed, relative to controls. This result suggested that by repressing HPC survival and proliferation, an increase in sensitivity for detecting SACK-dependent effects on CD133$^+$ HSCs could be accomplished. It could also have been the case that repression of HPCs allowed for increased HSC expansion. However, attempts to increase SACK-dependent CD133$^+$ HSC expansion were limited due to poor cell survival, under GF-starved conditions. Accordingly, increased sensitivity in detecting and preserving survival of HSCs was accomplished by balancing the repression of HPC survival and proliferation (by GF starvation) while enhancing survival and expansion of HSCs (with the addition of specific HSC survival factors). From these studies, Flt3 ligand acted as a survival factor (SF) to maintain survival of HSCs, without inducing extensive proliferation of HPCs. Under such conditions, up to a 5.5-fold SACK-dependent increase in CD133$^+$ cells was observed. Therefore, by understanding fundamental obstacles to HSC production, the suppression of asymmetric cell kinetic method promoted a detectable increase in CD133$^+$ cells, predicted to include HSCs.

It could be argued that the SACK-dependent effects observed were not due to HSC expansion, but rather due to SACK-dependent preservation of HSCs. There are several lines of evidence that suggest that HSC expansion occurred. First, in previous studies with ASCs (liver), SACK agents directly promoted shifts to symmetric cell kinetics. This property suggests that SACK effects cell kinetics, not cell survival. Second, an overall increase in total cells was observed. If only HSC preservation was taking place, this would not be expected. Finally, the fraction of cells in the S-phase of the cell cycle after 5 days of culture increases 2- to 4-fold compared to uncultured cells, depending on SACK-supplementation. This increase in cycling S-phase cells suggests that cells are proliferating under *ex vivo* cultured conditions. These three lines of evidence suggest that the SACK-effects observed were due to HSC expansion, not HSC preservation.

In order to exhibit the capacity for self-renewal and the potential to give rise to multilineage differentiation of SACK-dependent cells, both uncultured and cultured CD34$^+$ MPB cells were transplanted into sublethally irradiated non-obese diabetic severe combined immunodeficient (NOD/SCID) mice. SACK-cultured cells from conditions that repress HPC survival and proliferation, while preserving HSC survival and

expansion showed a 4.5-fold increase in engraftment efficiency, as compared to SACK-free cultured cells. This result suggested that by regulating cell kinetics, SACK resulted in increased HSC numbers. This is likely a consequence of promoting shifts in HSCs to symmetric cell kinetics. This is a compelling result as it suggests that SACK-dependent culture expands HSCs *ex vivo*.

However, when compared to uncultured cells at the same culture well equivalence (CWE) dose, an overall 65%-85% reduction in engraftment efficiency was observed. This finding suggested that, although *ex vivo* expansion of CD133$^+$ HSCs under conditions that repress HPC survival and proliferation while preserving HSC survival results in increased sensitivity in detecting HSCs *ex vivo*, it is not the ideal culture condition for increasing engraftment efficiency in *in vivo* transplantations. This finding also raises the possibility that the presence of HPCs may contribute to engraftment potential. HPCs may promote successful HSC homing into the marrow microenvironment from the circulation or may increase the likelihood of the injected cells reaching their final destination. Future experiments will focus on optimizing the *in vivo* engraftment efficiency of SACK-expanded HSCs.

The clinical impact of *ex vivo* expanded HSCs includes enabling umbilical cord blood (UCB) therapy, the realization of the potential of repairing dysregulated genes with gene therapy, and engineering the *ex vivo* production of mature blood cells. The clinical implications of *ex vivo* expanded HSCs are increasing the engraftment efficiency of patients (as a result of low HSCs in transplanted grafts) and decreasing graft-vs.-host-disease (GvHD) related mortality of allogeneic transplants. UCB stem cells represent a unique population of HSCs that can be successfully transplanted into allogeneic patients with low risk of GvHD. However, to realize their full clinical potential, the low numbers of HSCs in UCB must be expanded. A 3-fold *ex vivo* expansion of human HSCs is sufficient to meet current needs in HSC transplants[1]. Gene therapy also depends on expanding HSCs, since in order to incorporate repaired genes into dysregulated HSCs

genome, HSCs must proliferate without differentiating (i.e. expansion). Expanded HSCs could also be used to engineer the production of mature blood cells for therapeutic purposes. The work presented in this thesis dissertation promises to enable the full clinical potential of HSCs.

Bibliographical References

1. Stiff, P. et al. Autologous transplantation of ex vivo expanded bone marrow cells grown from small aliquots after high-dose chemotherapy for breast cancer. *Blood* **95**, 2169-2174 (2000).

Acknowledgements

Boutin, Dr. Minsoo Noh, Joe Moritz, Dr. Janice Lansita, Dr. Gracy Crane, Dr. Josh Merok, Dr. Sean Green, Jennifer Cheng, and Johnathan King.

Dedications

I would like to specifically dedicate the work presented in this dissertation to my family. Specifically I would like to dedicate this work to my mother, Dr. Koli Taghizadeh, for sacrificing so much so that my sisters could have all the opportunities at our hand. Mom, I truly believe that you are an angel and I hope that one day I can pass on the principles and love that you have instilled in me to my children. I love you deeply. Furthermore, I dedicate this dissertation to my two bright, lovely sisters, Nazbeh and Shady Taghizadeh. You guys have supported me during the most difficult time of my life. I would not be where I am were it not for the support that the both of you have shown me. I love you both deeply.

I would also like to dedicate this dissertation to my family in Iran. Specifically, I dedicate this work to my loving grandmother, Zahra Bavili, my aunts, Dr. Simin, Mitra, and Anahita Taghizadeh. You have supported and encouraged us in everyway imaginable. I also dedicate this dissertation to my uncles, Dr. Asad Behkam-Rad, Shahrokh Lotfi, and Dr. Mehrdad Nowrouzi, and my cousins, Dr. Ali Behkam-Rad, Kaveh Behkam-Rad, Sayra Lotfi, Dr. Keyvan Behkam-Rad, Sonya Lotfi, and Melika Nowrouzi. I love you all and thank you for your support and love throughout these years.

I especially would like to dedicate this dissertation to two people who passed on during my graduate career. My grandfather, Hassan Taghizadeh, is a role model to me in everyway possible. He was a man of principle, integrity and honor and he instilled those values in his daughters and grandchildren. You will always be in my heart Agah Jan. My aunt, Shahin Nowrouzi passed away from chronic myelogeneous leukemia, a disease that one day could be completely cured by the work presented in this dissertation. May your love and humanity live forever, Shahin Khanoom.

List of Figures & Tables

Chapter 1

Figure 1.1 | Human Development.

Figure 1.2 | Models for Adult Stem Cell Kinetics (ASCs) in a tissue turnover unit.

Figure 1.3 | Hematopoiesis Lineage Map.

Figure 1.4 | Potential Autonomous Pathways of Cell Division Regulation in HSCs.

Figure 1.5 | Suppression of Asymmetric Cell Kinetics – A Solution to Overcoming the Hematopoietic Stem Cell (HSC) Kinetic Barrier.

Chapter 2

Figure 2.1 | Theoretical Effects of Cytokines of Different Cell Type Specificity on Hematopoietic Stem Cell (HSC) Population Fraction.

Figure 2.2 | Experimental Design of Phase I, Growth Factor (GF) Cocktail Supplemented Studies.

Figure 2.3 | Representative FACS Profiles of Uncultured (Day 0) and Cultured (Day 5) $CD34^+$ Mobilized Peripheral Blood (MPB) Cells in GF Cocktail.

Figure 2.4 | SACK-Dependent Effects on $CD34^+$ Mobilized Peripheral Blood (MPB) Cells Cultured for 5 Days with GF Cocktail Supplementation.

Figure 2.5 | Titration of Hx Concentration for Cell Kinetics Effects on $CD34^+$ Mobilized Peripheral Blood (MPB) Cells Cultured for 5 Days in GF Cocktail Supplementation.

Chapter 3

Figure 3.1 | Experimental Design of Phase II Growth Factor (GF) Starved Studies.

Figure 3.2 | Use of Propidium Iodide (PI) Exclusion to Confirm Live Cell Detection by Bivariate Scatter Profile.

Figure 3.3 | Representative FACS Profiles of Uncultured (Day 0) and Cultured (Day 5) $CD34^+$ Mobilized Peripheral Blood (MPB) Cells in Growth Factor (GF) Starved Conditions.

Chapter 4

Chapter 5

Chapter 6

Abbreviations

SACK – Suppression of Asymmetric Cell Kinetics
ASC – Adult Stem Cell
ESC – Embryonic Stem Cell
ACK – Asymmetric Cell Kinetics
SCK – Symmetric Cell Kinetics
rGNPs – Guanine Ribonucleotides
GT – Generation Time
Hx – Hypoxanthine
Xs – Xanthosine
Xn – Xanthine
XHX – Xanthine, Hypoxanthine, Xanthosine
IMPDH – Inosine-5'-Monophosphate Dehydrogenase
IMP – Inosine Monophosphate
XMP – Xanthosine Monophosphate
HPGM – Hematopoietic Progenitor Growth Medium
GF – Growth Factor
SF – Survival Factor
DLL4 – (Notch) Delta-Like Ligand 4
DMSO – Dimethylsulfoxide
PE – R-Phycoerythrin
FITC – Fluorescein Isothiocyanate
APC – Allophycoerythrin
PFA – Paraformaldehyde
TA – Transit Amplifying
HSC – Hematopoietic Stem Cell
HPC – Hematopoietic Progenitor Cell
BM – Bone Marrow
MPB – Mobilized Peripheral Blood
CMP – Common Myeloid Progenitor
CLP – Common Lymphoid Progenitor
NK – Natural Killer
MPC – Multipotent Progenitor Cell
FACS – Fluorescent Activated Cell Sorting
HSA – Human Serum Albumin
BSA – Bovine Serum Albumin
PBS – Phosphate Buffered Saline
FBS – Fetal Bovine Serum
BMT – Bone Marrow Transplant
UCB – Umbilical Cord Blood
GvHD – Graft-versus-Host-Disease
TGF-β – Transforming Growth Factor-β
EGF – Epidermal Growth Factor
CFU-S – Spleen Colony-Forming Unit

P-Sp – Para-aortic Splanchnopleura
AGM – Aorta-Gonad-Mesonephros
Flt3 L – Fetal Liver Tyrosine Kinase 3 Ligand
SCF – Stem Cell Factor
TPO – Thrombopoietin
LIF – Leukemic Inhibitory Factor
IL-3 – Interleukin-3
IL-6 – Interleukin-6
PI – Propidium Iodide
KSL – c-kit$^+$, Sca-1$^+$, Lin$^-$
BMP-2 – Bone Morphogenetic Protein-2 (BMP-2)
b-FGF – Basic Fibroblast Growth Factor
M-CSF – Macrophage-Colony Stimulating Factor
G-CSF – Granulocyte-Colony Stimulating Factor
GM-CSF – Granulocyte-Macrophage-Colony Stimulating Factor
BMP – Bone Morphogenic Protein
Shh – Sonic Hedgehog
AML – Acute Myelogeneous Leukemia
ADAM – A Disintegrin And Metalloproteinase
SCID – Severe Combined Immunodeficient
NOD/SCID – Non-Obese Diabetic/Severe Combined Immunodeficient
LT – Long-Term
SRC – SCID Repopulating Cell
CWE – Cell Well Equivalents
GFP – Green Fluorescent Protein
YFP – Yellow Fluorescent Protein
CFP – Cyan Fluorescent Protein
DMEM – Dulbecco's Modified Eagle Medium
DFBS – Dialyzed Fetal Bovine Serum

Terese Winslow Medical Illustration 714 South Fairfax Street
Alexandria, Virginia 22314
703.836.9121 Fax 703.836.3715
terese.winslow@mindspring.com

Rouzbeh R. Taghizadeh, Ph.D.
MIT | Biological Engineering Division
Biotechnology Process Engineering Center
Center for Cancer Research
Center for Environmental Health Sciences
Massachusetts Institute of Technology
77 Massachusetts Avenue,
Room 16-771
Cambridge, MA 02139

LICENSE AGREEMENT   May 22, 2006

Copyright rights transferred hereby are limited, non-exclusive, and non-transferable,
one time reproduction rights to original medical illustrations entitled **"Figure 1.1.
Differentiation of Human Tissues and Figure 5.1. Hematopoietic and Stromal
Stem Cell Differentiation"** © 2001 Terese Winslow that originally appeared in the
NIH Stem Cell Report entitled: *"Scientific Progress and Future Research
Directions"*, Kirschstein R and Skirboll LR, Department of Health and Human
Services, June 2001. http://stemcells.nih.gov/info/scireport/

Illustrations may only be used in your Ph.D. thesis (in electronic or hardcopy format)
entitled, "Investigation of a Suppression of Asymmetric Cell Kinetics (SACK)
Approach for ex vivo Expansion of Human Hematopoietic Stem Cells" by
Taghizadeh, Rouzbeh R., M.I.T. Division of Biological Engineering, 2006.
License will expire at the end of the print run of approximately 10 copies.

Ownership of original artwork, copyright, and all rights not specifically transferred
herein remain the exclusive property of the Illustrator. Additional license(s) are
required for ancillary usage(s) and shall require payment of a mutually agreed upon
fee for each subsequent usage subject to all terms. All images are protected by
copyright law and may not be used in any way without prior permission in writing
and payment in full for each such use.

Transparencies, digital files and/or any other media used for the reproduction of
illustration licensed in this Agreement with Rouzbeh R. Taghizadeh, Ph.D. shall not
be sold, transferred or shared with any other party (licensee, web site, affiliate or
other) without the express prior written permission of the Illustrator. The digital file
provided for reprographic purposes, shall be destroyed by licensee after use.
Alterations/derivations of the image herein licensed, except for additions of
typography, are not permitted.

Credit byline, placed adjacent to the illustration(s), shall read as follows:

For Fig. 1.1:
© 2001 Terese Winslow (assisted by Caitlin Duckwall)

For Fig 5.1:
© 2001 Terese Winslow (assisted by Lydia Kibiuk)

The signature of both parties shall evidence acceptance of these terms. This agreement shall remain in force unless canceled by one of the parties in writing. If so canceled, all ownership and reproduction rights shall automatically and exclusively revert to and be vested in the Illustrator.

Consented and agreed to:

	5/22/06
Illustrator, Terese Winslow	Date
	5/22/06
Rouzbeh R. Taghizadeh, Ph.D.	Date

NATURE PUBLISHING GROUP LICENSE
TERMS AND CONDITIONS

May 17, 2006

This is a License Agreement between Rouzbeh R. Taghizadeh ("You") and Nature Publishing Group ("Nature Publishing Group"). The license consists of your order details, the terms and conditions provided by Nature Publishing Group, and the payment terms and conditions.

License Number	1471450159985
License date	May 17, 2006
Licensed content publisher	Nature Publishing Group
Licensed content publication	Nature
Licensed content title	Stem cells, cancer, and cancer stem cells
Licensed content author	Tannishtha Reya, Sean J. Morrison, Michael F. Clarke and Irving L. Weissman
Volume number	
Issue number	
Pages	
Year of publication	2001
Portion used	Figures
Number of figures	1
Requestor type	Student
Type of Use	Thesis/Dissertation
PO Number	
Total	$0.00
Terms and Conditions	

Terms and Conditions for Permissions

Nature Publishing Group hereby grants you a non-exclusive license to reproduce this material for this purpose, **and for no other use**, subject to the conditions below:

1. NPG warrants that it has, to the best of its knowledge, the rights to license reuse of this material. However, you should ensure that the material you are requesting is original to Nature Publishing Group and does not carry the copyright of another entity (as credited in the published version). If the credit line on any part of the material you have requested indicates that it was reprinted or adapted by NPG with permission from another source, then you should also seek permission from that source to reuse the material.

2. Permission granted free of charge for material in print is also usually granted for any electronic version of that work, provided that the material is incidental to the work as a whole and that the electronic version is essentially equivalent to, or substitutes for, the print version.

Where print permission has been granted for a fee, separate permission must be obtained for any additional, electronic re-use (unless, as in the case of a full paper, this has already been accounted for during your initial request in the calculation of a print run).

NB: In all cases, web-based use of full-text articles must be authorized separately through the 'Use on a Web Site' option when requesting permission.

3. Permission granted for a first edition does not apply to second and subsequent editions and for editions in other languages (except for signatories to the STM Permissions Guidelines, or where the first edition permission was granted for free).

4. Nature Publishing Group's permission must be acknowledged next to the figure, table or abstract in print. In electronic form, this acknowledgement must be visible at the same time as the figure/table/abstract, and must be hyperlinked to the journal's homepage.

5. The credit line should read:

    Reprinted by permission from Macmillan Publishers Ltd: [JOURNAL NAME] (reference citation), copyright (year of publication)

    For AOP papers, the credit line should read:

    Reprinted by permission from Macmillan Publishers Ltd: [JOURNAL NAME], advance online publication, day month year (doi: 10.1038/sj.[JOURNAL ACRONYM].XXXXX)

6. Adaptations of single figures do not require NPG approval. However, the adaptation should be credited as follows:

    Adapted by permission from Macmillan Publishers Ltd: [JOURNAL NAME] (reference citation), copyright (year of publication)

7. Translations of up to a whole article do not require NPG approval. The translation should be credited as follows:

    Translated by permission from Macmillan Publishers Ltd: [JOURNAL NAME] (reference citation), copyright (year of publication)

We are certain that all parties will benefit from this agreement and wish you the best in the use of this material. Thank you.